

**Applied Battery Research for Transportation
(B&R No. VT-1102000)**

**Progress Report
for
Third Quarter FY 2013**

**Contributions from
Argonne National Laboratory
Army Research Laboratory
Brookhaven National Laboratory
Jet Propulsion Laboratory
Lawrence Berkeley National Laboratory
National Renewable Energy Laboratory
Oak Ridge National Laboratory
Sandia National Laboratories**

September 2013

Applied Battery Research for Transportation Program Third Quarter Progress Report for FY 2013

This quarterly progress report describes the activities being conducted in support of DOE's Applied Battery Research for Transportation (ABR) Program. This program focuses on helping the industrial developers to overcome barriers for Li-Ion batteries for use in plug-in hybrid electric vehicles (PHEVs). In its goal of developing low-emission high fuel economy light-duty HEVs and PHEVs, the DOE and U.S. DRIVE established requirements for energy storage devices in these applications. The Vehicle Technologies Program at DOE has focused the efforts of this applied battery R&D program on the PHEV application.

Through the U.S. DRIVE Partnership, DOE is currently supporting the development of advanced Li-Ion batteries with industry for HEV, PHEV, and EV applications. The industrial developers have made significant progress in developing such batteries for HEV applications and there are new challenges associated with developing viable battery technologies for the PHEV application, especially when targeting the 40-mile all electric range. In addition to the calendar life, abuse tolerance, and cost challenges that exist for Li-Ion batteries in the HEV application, now the issue of providing sufficient energy within the weight and volume requirements becomes a huge challenge, as does cycle life. Also, the abuse tolerance and cost challenges become even greater. The Applied Battery Research for Transportation program is directed at assisting the industrial developers to identify the major factors responsible for the technical barriers and to find viable cost-effective solutions to them. The goal is to facilitate the development of low-cost cell chemistries that can simultaneously meet the life, performance, abuse tolerance, and cost goals that have been established by the U.S. DRIVE Partnership.

The ABR Program is organized to identify and develop advanced electrochemical couples, and further to efficiently move promising electrochemical couples from the research environment to industrial developers for evaluation. An overview of this process is given in Figure 1. Argonne has joined with other national laboratories, universities, and industry to create an integrated team to accomplish the program goals. There is a significant effort within the program to develop promising advanced electrochemical couples. As these electrochemical couples or others identified from outside the program exhibit reproducible cutting-edge results in small lab cells, the component materials are scaled-up as needed by the Materials Engineering Research Facility (MERF) and prototype cells are built by the Cell Fabrication Facility (CFF). The advanced prototype cells are thoroughly tested, examined, and characterized by a broad spectrum of studies, including utilizing the Electrochemical Analysis and Diagnostic Laboratory (EADL) and the Post-Test Facility (PTF). This information is fed back to the material researchers, and further offered to industrial developers along with prototype cells and scaled materials.

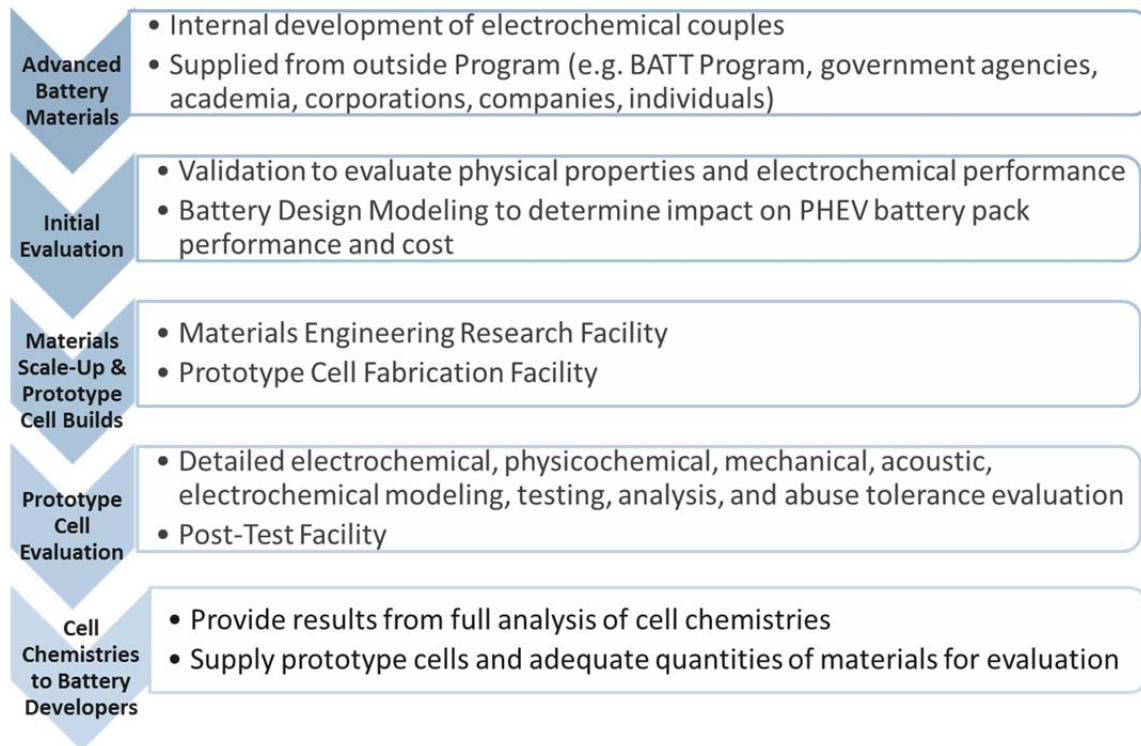


Figure 1. High level view of ABR program.

Initially, the ABR Program was organized into three main technical task areas to address the challenges for PHEVs:

- (1) Battery Cell Materials Development—focuses on research, development, and engineering of advanced materials and cell chemistries that simultaneously address the life, performance, abuse tolerance, and cost issues.
- (2) Calendar & Cycle Life Studies—deals with understanding the factors that limit life in different Li-Ion cell chemistries, which are used as feedback to Task 1. This task also deals with the establishment and operation of in-program cell fabrication capabilities for use in these life studies.
- (3) Abuse Tolerance Studies—deals with understanding the factors that limit the inherent thermal and overcharge abuse tolerance of different Li-ion cell materials and chemistries, as well as developing approaches for enhancing their abuse tolerance.

The ABR Program is currently going through a major reorganization. The broad range of projects is being further integrated into core facility teams and efforts, along with larger electrochemical couples and electrolyte development projects. As part of the restructuring a crosscutting project focused on enabling the Argonne high energy composite layered cathode $x\text{Li}_2\text{MnO}_3 \cdot (1-x)\text{LiMO}_2$ ($M = \text{Ni, Mn, Co}$), also referred to as lithium and manganese rich NMC material (LMR-NMC), for the 40-mile PHEV (PHEV-40) application. This class of materials offers the potential for capacities exceeding

250mAh/g, excellent cycle and calendar life, and outstanding abuse tolerance. However, the material currently possesses a voltage fade issue (and other related issues) that affects its long-term cycle life and needs to be resolved. The voltage fade project results are reported under Task 1 although they cover activities in Task 2 also.

The list of current projects is given in the table, with the individual reports compiled in the Appendix.

Organization	AMR Project ID	AOP Project ID	Title	PI/Contact Point	Page Number
			Task 1: Battery Cell Materials Development		
ANL	ES161	1.2	Voltage Fade in the LMR-NMC Materials	Anthony Burrell	6
ANL	ES167	IV. E.1.1	Process Development and Scale up of Advanced Cathode Materials	Gregory Krumdick	26
ANL	ES168	IV. E.1.2	Process Development and Scale up of Advanced Electrolyte Materials	Gregory Krumdick	30
ARL	ES024		High Voltage Electrolytes for Li-ion Batteries	Kang Xu and Richard Jow	35
JPL	ES026		Electrolytes for Use in High Energy Li-Ion Batteries with Wide Operating Temperature Range	Marshall Smart	39
LBNL	ES029	1.2.2	Scale-up and Testing of Advanced Materials from the BATT Program	Vincent Battaglia	49
ORNL	ES164	18502	Overcoming Processing Cost Barriers of High Performance Lithium Ion Battery Electrodes	David Wood	52
NREL	ES162		Development of Industrially Viable Battery Electrode Coatings	Robert Tenent	60
NREL	ES196	25194	Evaluate ALD Coatings of LGCPI Cathode Materials and Electrodes	Shriram Santhanago palan	63

Organization	AMR Project ID	AOP Project ID	Title	PI/Contact Point	Page Number
			Task 2: Calendar & Cycle Life Studies		
ANL	ES030	1.1	Cell Fabrication Facility Team Production and Research Activities	Andrew Jansen	65
LBL	ES033	1.1.1 and 2.4	Strategies to Enable the Use of High-Voltage Cathodes and Diagnostic Evaluation of ABRT Program Lithium Battery Chemistries	Robert Kostecki	84
BNL	ES034	1.1, 2.4, and 3.3	Life and Abuse Tolerance Diagnostic Studies for High Energy Density PHEV Batteries	Xiao-Qing Yang	87
ORNL	ES165	18502	Roll-to-Roll Electrode Processing NDE and Materials Characterization for Advanced Lithium Secondary Batteries	David Wood	90
			Task 3: Abuse Tolerance Studies		
SNL	ES036	3.2	Abuse Tolerance Improvements	Chris Orendorff	96
LBL	ES037	3.3	Overcharge Protection for PHEV Batteries	Guoying Chen	99

APPENDIX

Individual Project Progress Reports

TASK 1

Battery Cell Materials Development

Project Number: 1.2 (ES161)

Project Title: Voltage Fade in the LMR-NMC Materials

Project PI, Institution: Anthony Burrell, Argonne National Laboratory

Collaborators (include industry): Ali Abouimrane, Daniel Abraham, Mahalingam Balasubramanian, Javier Barenó García-Ontiveros, Ilias Belharouak, Roy Benedek, Ira Bloom, Zonghai Chen, Jason Croy, Dennis Dees, Kevin Gallagher, Hakim Iddir, Brian Ingram, Christopher Johnson, Wenquan Lu, Dean Miller, Yang Ren, Michael Thackeray, Lynn Trahey, and John Vaughey all from Argonne National Laboratory

Project Start/End Dates: March 2012 / September 2014

Objectives: The objective of the work is to enable the Argonne high energy composite layered cathode $x\text{Li}_2\text{MnO}_3 \cdot (1-x)\text{LiMO}_2$ ($M = \text{Ni}, \text{Mn}, \text{Co}$), also referred to as lithium and manganese rich NMC material (LMR-NMC), for the 40-mile PHEV (PHEV-40) application. This class of materials offers the potential for capacities exceeding 250mAh/g, excellent cycle and calendar life, and outstanding abuse tolerance. This material currently possesses a voltage fade issue (and other related issues) that effects its long-term cycle life and this issue needs to be resolved.

Approach: Bring together a diverse technical team that will share data and expertise to “fix” voltage fade in the LMR-NMC cathode materials. This will be a single team effort – not multiple PI’s working independently on the same problem.

- Definition of the problem and limitations of the composite cathode materials.
- Data collection and review of compositional variety available using combinatorial methods.
- Modeling and Theory.
- Fundamental characterization of the composite cathode materials.
- Understand the connections between electrochemistry and structure.
- Synthesis.
- Post treatment/system level fixes.

Milestones:

(a.) Determine if coatings have a positive effect on voltage fade – go/no-go on coatings within this project. **Status Complete**

(b.) Determine the origin of the enhanced capacity in the LMR-NMC materials. **Status, On schedule**

(c.) Determine the effect of synthesis (if any) on voltage fade. **Status, On schedule**

(d.) Synthesize, characterize and optimize the composition of ‘layered-layered-’ and ‘layered-layered-spinel’ electrodes and to determine the causes for, and to counter, the voltage fade phenomenon; **Status, On schedule**

(e.) Using first principles identify strategies for designing high-capacity VF-free cathode materials, and calculate properties of candidate materials that implement these strategies. **Status, On schedule**

(f.) Determine compositions that mitigate voltage fade in the LMR-NMC materials. **Status, On schedule**

Financial data: \$4000K/year

PROGRESS TOWARD MILESTONES

During the past quarter ANL has experienced significant difficulties tanks to the closing of the building that housed all of the ANL battery research. Over this time the research capability of the voltage fade program was severely limited and much of the work in this quarter has focused on data analysis and modeling.

Electrochemical Modeling

LMR-NMC electrode materials are known to exhibit a hysteresis between the charge and discharge voltage curves, even at very slow cycling rates (e.g. C/200). A significant effort is currently being placed on the development of an electrochemical model to account for this hysteresis. Experimental studies on LMR-NMC materials also suggest a link between the hysteresis and the voltage fade phenomenon, thus emphasizing the importance of a valid electrochemical model for this class of materials. A number of different models have been examined with varying degrees of success. The model development described below combines and extends some of the earlier work. As discussed below, this model exhibits characteristics that account qualitatively for many of the observed phenomena, but until the model is rigorously compared and fitted to the experimental data the true utility of the model cannot be determined.

The activated LMR-NMC cathode material is obviously quite complex and made of nanometer scale sized domains. These domains are highly integrated, but appear to have unique electrochemical properties. The cathode material is assumed to be composed of two types of domains, where both domains can be electrochemically active. One domain (designated domain number 1) is considered to be relatively stable to changes in lithium concentration, while the other domain goes through a slow reversible structural transition during cycling. At low lithium concentrations the unstable domain has one lattice structure (designated domain number 2) and at high concentrations another (designated domain number 3). Each of these domains has an associated open circuit voltage (OCV) curve as a function of lithium concentration in that domain (c_{Si} , $i = 1, 2, \text{ or } 3$). Figure 1 has the assumed OCV curve for each of the domains, where x_s is the ratio of the lithium concentration in the specific domain divided by its maximum concentration. The actual OCV curve is inevitably more complicated, but this should be adequate for an initial examination of the model. It is important here that the OCV curves are offset by a significant voltage.

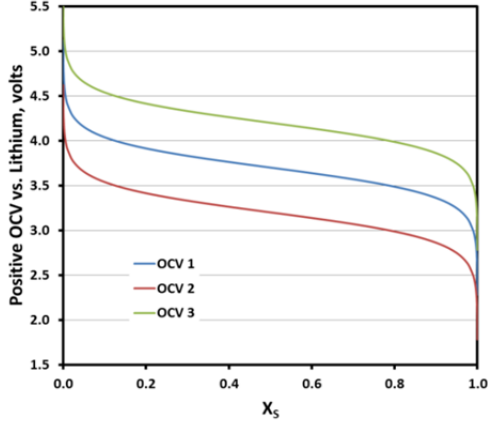


Figure 1. Assumed open circuit voltage curve as a function of relative lithium concentration in domain

Volume-averaged continuum-based diffusion equations are used to describe the transport of lithium through the material. The flux of lithium between two adjacent domains denoted i and j (N_{ij}) is described by an electrochemical potential (μ_{Li}) driven mass transport expression, Equation 1, where k_{ij} is the mass transfer coefficient. The electrochemical potential can be easily associated with the OCV of the domain.

$$N_{ij} = k_{ij} [\mu_{Li}(i) - \mu_{Li}(j)] \quad [1]$$

The transitions from domain 2 to 3 and from domain 3 to 2 are assumed to follow the Avrami phase change expression (see Equation 2), where k is a lithium concentration driven rate constant and ε_{Si} is the volume fraction of domain i .

$$\varepsilon_{Si} = 1 - \exp(-kt^n) \quad [2]$$

By offsetting the individual domain OCV curves and making the structural transitions and lithium transport between domains extremely slow (i.e. very small rate constant and mass transfer coefficient); the electrochemical model exhibits a hysteresis between charge and discharge, even at a $C/200$ rate, as seen in Figure 2. It should be noted that the model simulations presented here are only for the active material (i.e. single particle calculation), although at very slow rates there is little or no difference between the single particle and the full cell. The particle electrochemical model will need to be eventually integrated into the full cell model.

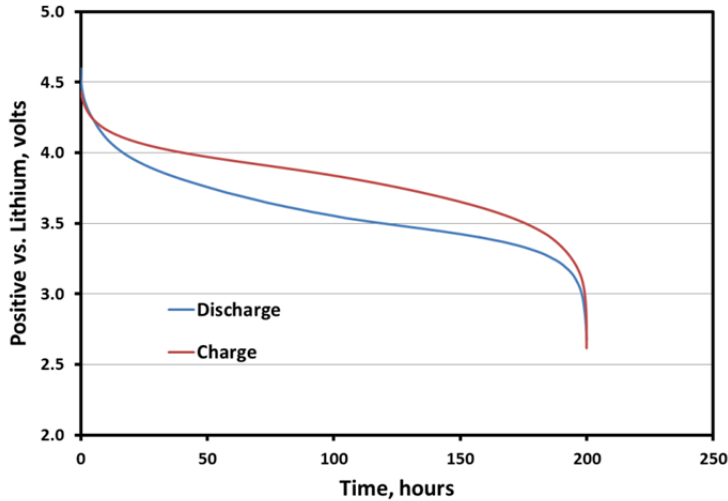


Figure 2. Electrochemical model simulation of active material charge and discharge curves at a $C/200$ rate

The electrochemical model described above will eventually come to equilibrium given enough time. At around a $C/5000$ rate the charge and discharge simulations collapse to a single curve, which indicates that the material takes months to come to a true equilibrium. This raises the question of whether a material with these poor transport characteristics could ever support high discharge/charge rates. To address this, a series of simulations were conducted over a range of C-rates from about $C/5000$ to $C/1$, as shown in Figure 3. One can see that there is a significant loss in total capacity over the range studied, but that the material can support these rates.

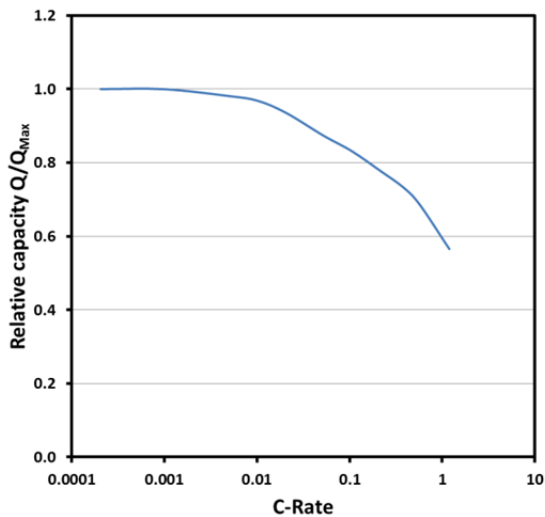


Figure 3. Electrochemical model simulation of active material rate behavior

While there is a long list of studies that need to be conducted to further examine this LMR-NMC electrochemical model, the initial qualitative studies show promise.

To more rigorously examine the proposed electrochemical model a specific LMR-NMC material and electrode has been adopted for study. The extensive database of the baseline HE5050 LMR-NMC ($0.5\text{Li}_2\text{MnO}_3 - 0.5\text{LiNi}_{0.375}\text{Co}_{0.25}\text{Mn}_{0.375}\text{O}_2$) active material and electrode makes it the best option. While there are a wide variety of electrochemical studies on this material, two types of half-cell (i.e. lithium counter electrode) studies are being utilized for fitting the model parameters. The first type is constant current cycling (C/18) and the second type is relatively slow Galvanic Intermittent Titration Technique (GITT) study, both using the standard electrode. In the GITT study a C/18 current is applied for 10 minutes followed by a 100 minute rest, which is then repeated through a complete cycle. The approximately 30 model parameters associated with the LMR-NMC material makes the parameter fitting a challenge. It is anticipated that multiple fitting iterations of the data will be necessary to generate a full concentration dependent parameter set.

As a starting point the constant current cycling data was utilized with the particle model described above to develop a working set of parameters. This data is not particularly sensitive to the transport parameters and was used mainly to fit the OCV curves of the three domains and establish average rate constants for the domain transitions, as well as their range of stability. It was clear from the exercise that a perfect fit of data was not possible without allowing the transition rate and transport parameters to be concentration dependent. However, a reasonably good fit of the data could be obtained with average parameters, as shown in Figure 4.

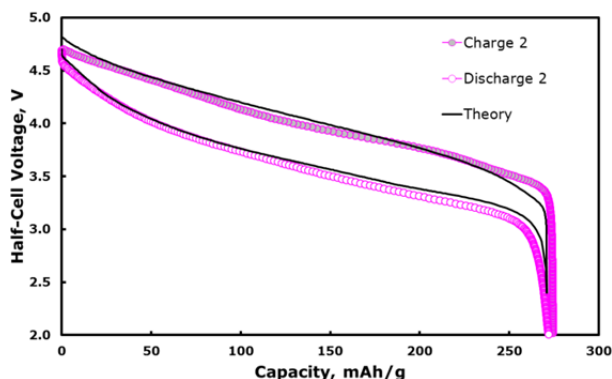


Figure 4. Electrochemical model simulation of HE5050 LMR-NMC standard electrode half-cell charge and discharge curves at a C/18 rate

The complex nature of this material that exhibits the hysteresis between charge and discharge curves can be seen by examining the relative amounts of domains 2 and 3 as the material is cycled (see Figure 5). As indicated above, domain 2 is stable when fully charged and domain 3 is stable when fully discharged. The data fit indicates that the crossover point for this material is around 3.5 volts. The sluggishness of the transition rates cause the material to never be at equilibrium at any reasonable cycling rate. Further, the slow transition rates result in the changes to appear to be out-of-phase with the

cycling. Finally, the differences in the stability ranges and transition rates cause the asymmetry apparent in Figure 5.

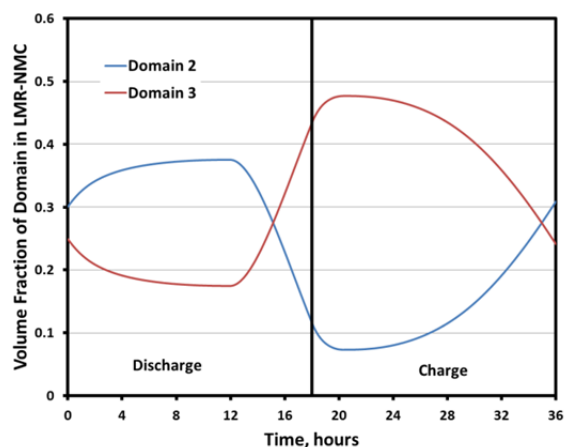


Figure 5. Volume fraction of domains 2 and 3 in HE5050 LMR-NMC active material from electrochemical model simulation of charge and discharge at a C/18 rate

The particle model was integrated into the half-cell electrochemical model to use in fitting the GITT half-cell data. Since there is no actual reference electrode in the cell, an estimate of the lithium electrode interfacial area specific impedance (ASI) is important. This is complicated by the high probability that the lithium electrode impedance is likely not stable throughout the full experiment. Nevertheless, an average lithium electrode ASI was estimated by comparing impedance data on reference electrode cells to the approximately one second ASI of the half-cell. The more accurate the lithium ASI the better the LMR-NMC interfacial ASI can be determined. However, this information can best be determined using reference electrode impedance data on LMR-NMC electrodes (see second quarter report on electrochemical modeling studies in Cell Fabrication Facility Team Production and Research Activities section).

The fitting of GITT data has been initiated using the parameter set from the constant current cycling data. In the initial fitting, the OCV curves and the stability ranges of domains 2 and 3 are not varied. Also, the ratios of the transport parameters and transition rates for each domain are held constant. This reduces the fitted parameters to a reasonable number and these assumptions can be relaxed as the complete parameter set is developed. Even with these assumptions, there is sufficient flexibility to fit the data, as shown in Figure 6 for a single charge pulse and relaxation at about 3.8 volts.

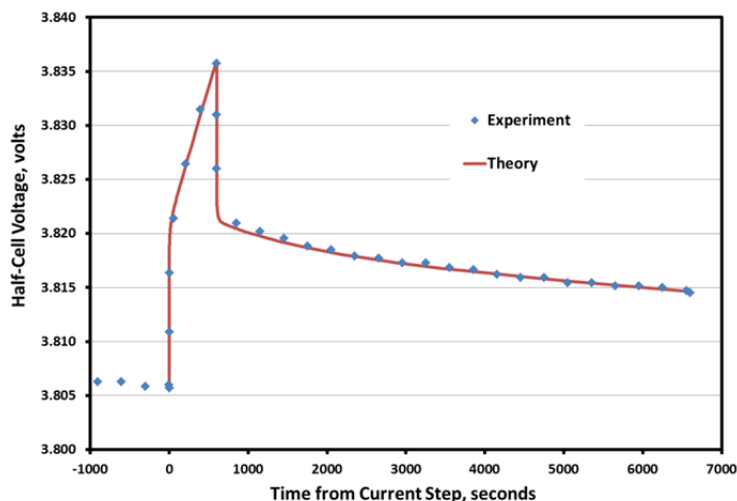


Figure 6. Electrochemical model simulation of HE5050 LMR-NMC standard electrode half-cell GITT experiment (600 second C/18 charge pulse and 6000 second relaxation at about 3.8 volts).

The fitting of the GITT data is continuing. Also, the model will be exercised to examine other studies conducted with the standard HE5050 electrode.

Thermodynamics of LMR-NMC cathode material cycling

Thermodynamically, the voltage of LMR-NMC is directly related to the entropy change of the composite cathode material. Investigation on thermodynamics of composite electrode should shed a light on the root cause of its voltage fade during cycling. In addition, lithium ion diffusion and electronic conductivity of LMR-NCM will be studied to better understand the thermodynamics and kinetics role in voltage fading.

Entropy change is defined as the index of energy dispersal, or a measure of the molecular randomness or disorder of a system, which is directly related to cell potential as given by the function below:

$$\Delta S = nF(dE/dT)_p$$

Entropy change measurement will allow us to probe the root cause of voltage fade for LMR-NMC at macrostate level. In this study, we are examining the voltage variation with changing of temperature at various state of charge.

Eight Li/LMR-NMC cells were divided into two groups. After formation cycles, one group (4 cells) were charged to 4 different state of charge: 10%, 30%, 50%, and 70%. The open circuit voltage of each cell was monitored at various temperatures. Another group of cells were discharged to various state of discharge: 20%, 40, 80%, and 90%. The open circuit voltage of each cell was also monitored at various temperatures. In order to obtain more data points to fill the gap, the 1st group of cells was discharged to various states of discharge and the 2nd groups of cells was charged to various states of charge. Then, the open circuit voltages of all the cells were again tested at various temperatures. The voltage responses as a function of temperature were shown in Figure 7. From this

plot, it was found out the open circuit voltage in general decreases with increasing temperature, vice visa for decreasing temperature. We also noticed that the open circuit voltage was not stable when the cells were tested at highly charged state.

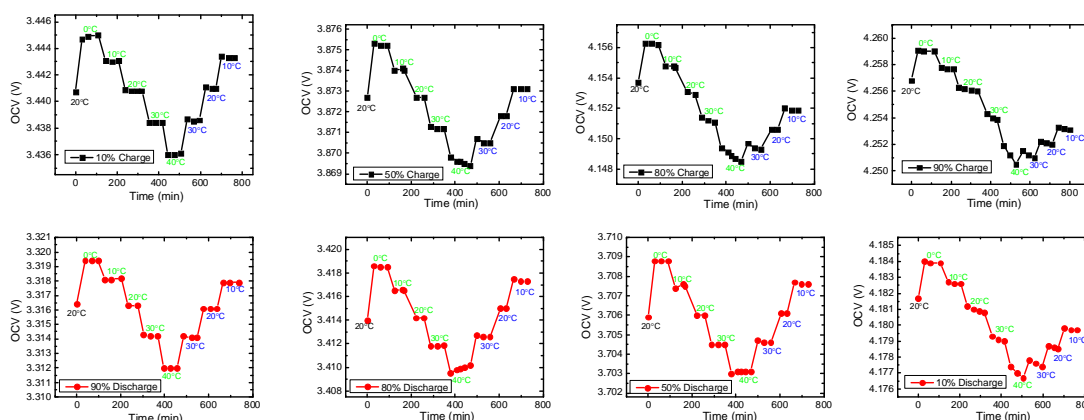


Figure 7. Open circuit voltage variation with temperature at various state of charge

From the voltage variation with changing cell temperature, the dE/dT of LMR-NMC cell at each state of charge can be calculated for both increasing and decreasing temperature experiments, which directly related to the entropy change of LMR-NMC at certain state. The dE/dT values from both increasing and decreasing temperature were averaged and are plotted in Figure. 8. It can be seen from this figure that LMR-NMC becomes less ordered at fully highly charged state with higher dE/dT . The dE/dT results at each state of charge are quick similar to each other regardless of its charge/discharge history.

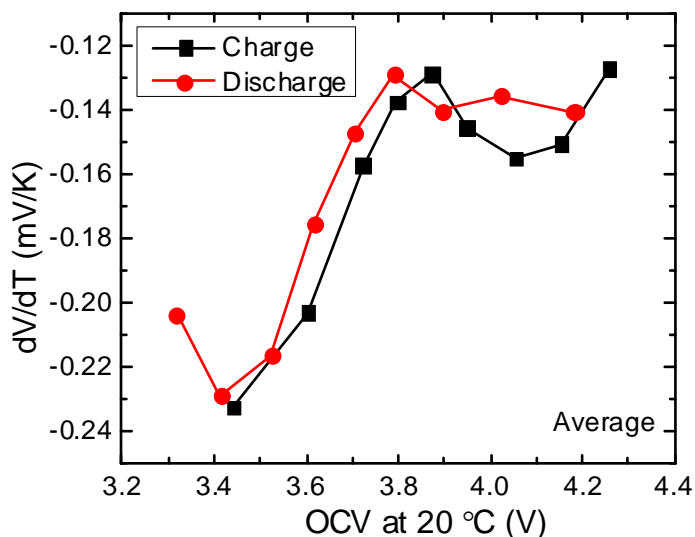


Figure 8 dE/dV of Li/LMR-NMC cell at various state of charge.

Over the next quarter further data will be collected to help elucidate the entropy change associated with cycling.

Structure evolution of LMR-NMC during synthesis and activation

The prevailing theory for the mechanism of voltage fade involves transition atom migration after the activation process that leads the change of local electrochemical environment of lithium-ions in LMR-NMC. Thus, structural study of LMR-NMC is crucial to reveal the mechanism of voltage fade and to develop mitigation technologies.

Figure 9 shows the Monte Carlo simulation of distribution of cations on a 500x500 hexagonal lattice. It is suggested that solid solution can only be formed for materials with small amount (<10%) of excess lithium. Big Li_2MnO_3 domains are highly expected for lithium-manganese-rich transition metal oxides. Figure 9 also suggests that the average domain size of Li_2MnO_3 at the thermodynamically equilibrium state can be fine-tuned by varying the annealing temperature and the interfacial energy, which can be achieved by doping and controlling the synthesizing environment.

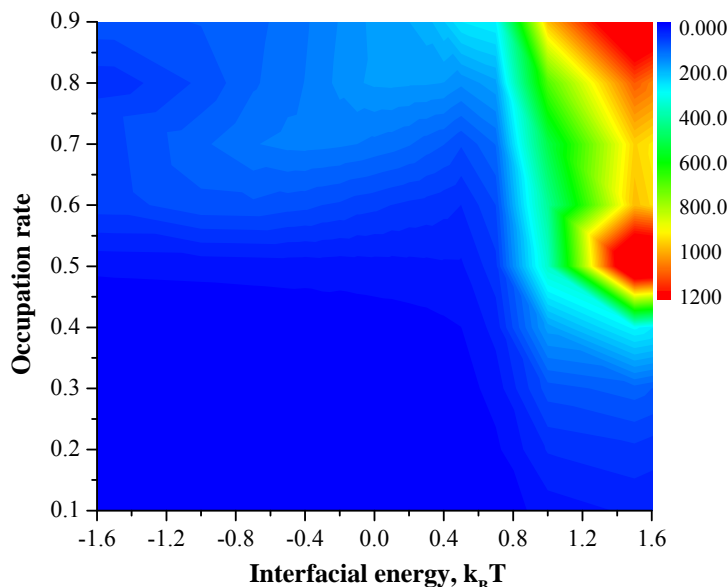


Figure 9 Contour plot of the calculated Li_2MnO_3 domain size as a function of the occupation rate and the interfacial energy.

As a model component for lithium-manganese-rich transition metal oxides, Li_2MnO_3 was characterized with different activation conditions, varying both the exposed temperature and the C rate, and the results are shown in Figure 10. Figure 10a shows that the initial irreversible capacity loss increased linearly with the initial charge capacity, or the degree of activation; the initial capacity loss was accelerated at elevated temperatures and low C rates. If the oxidation of electrolyte is the only contribution, then we can expect a linear relationship between the initial irreversible capacity loss and the charge time (see Figure 10b). However, none of the interpolated lines went through the origin, the intercept values at Y axis increased substantially with the temperature; this indicated that the degradation of delithiated Li_2MnO_3 had a major contribution towards the initial irreversible capacity loss. The capacity measured for the following cycles at C/10 and the room temperature also indicated the degradation of delithiated Li_2MnO_3 as shown in

Figure 10c. Comparing Figures 10a and 10c, we can find that the cells activated at elevated temperatures and low C rates showed both an accelerated irreversible capacity loss (see Figure 10a) and a substantial reversible capacity loss during the followed cycles (see Figure 10c). This confirmed that Li_2MnO_3 degraded at elevated temperatures when deeply delithiated. Figure 10d shows the contour plot of *in situ* HEXRD profiles during the thermal decomposition of delithiated Li_2MnO_3 . It was found that delithiated Li_2MnO_3 started to convert to a M_3O_4 -type spinel structure at about 250°C. This M_3O_4 -type structure was previously found as the intermediate phase for the solid state synthesis of LiMn_2O_4 spinel, which might be related to reported evolution of spinel-type structure after extensive cycling of lithium-manganese-rich transition metal oxides. In addition, the slow degradation of Li_2MnO_3 domains was observed in lithium-ion cells cycled at the room temperature (see Figure 11).

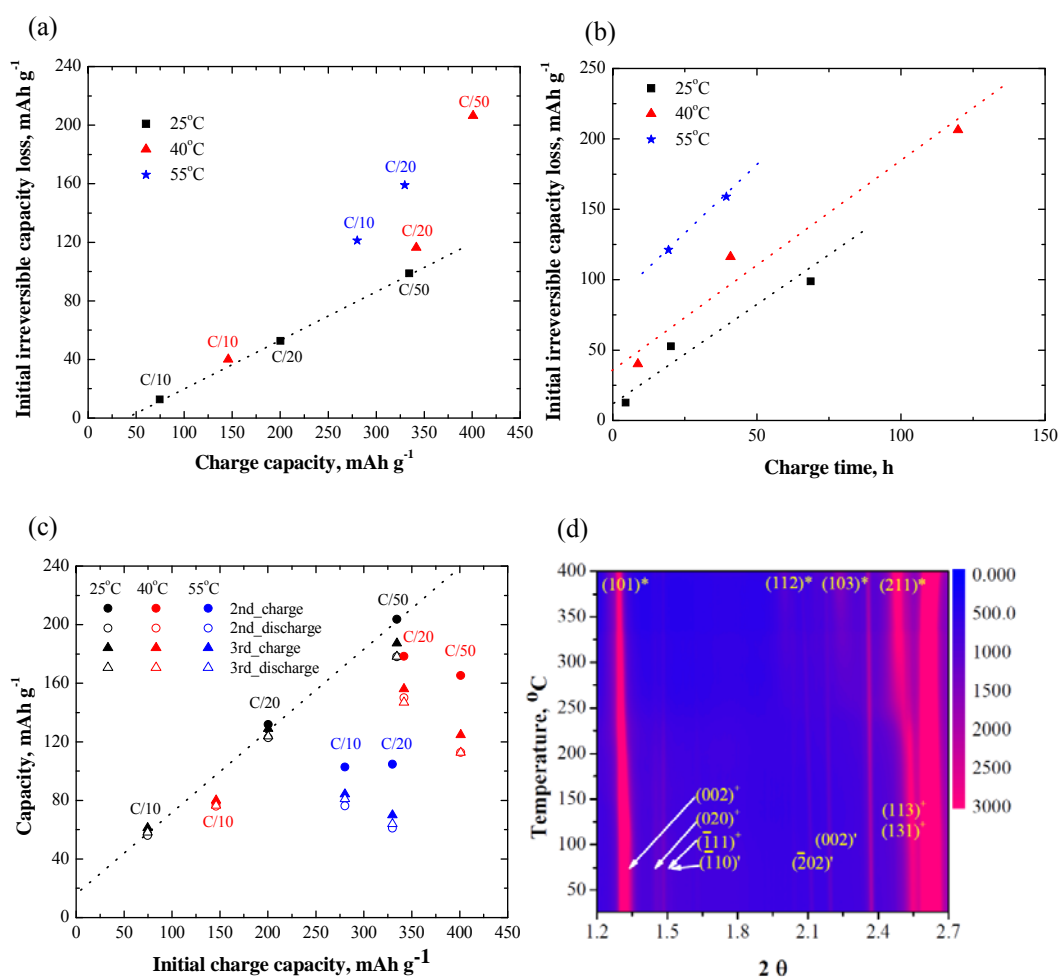


Figure 10 (a) Dependence of the initial irreversible capacity loss on the initial charge capacity of Li_2MnO_3 when electrochemically activated at different conditions. (b) Dependence of the initial irreversible capacity loss on the initial charge time for cells activated at different conditions. (c) Charge/discharge capacity of $\text{Li}/\text{Li}_2\text{MnO}_3$ after the activation cycle. The cells were charge/discharge between 2.0V and 4.6 V using a constant current of C/10. (d) Contour plot of *in situ* high-energy X-ray diffraction profiles of delithiated Li_2MnO_3 during the thermal ramping up to 400 °C. The diffraction peaks for M_3O_4 -type spinel were labeled as $(hkl)^*$, those for delithiated Li_2MnO_3 were labeled as $(hkl)^+$, those for residual Li_2CO_3 were labeled as (hkl) .

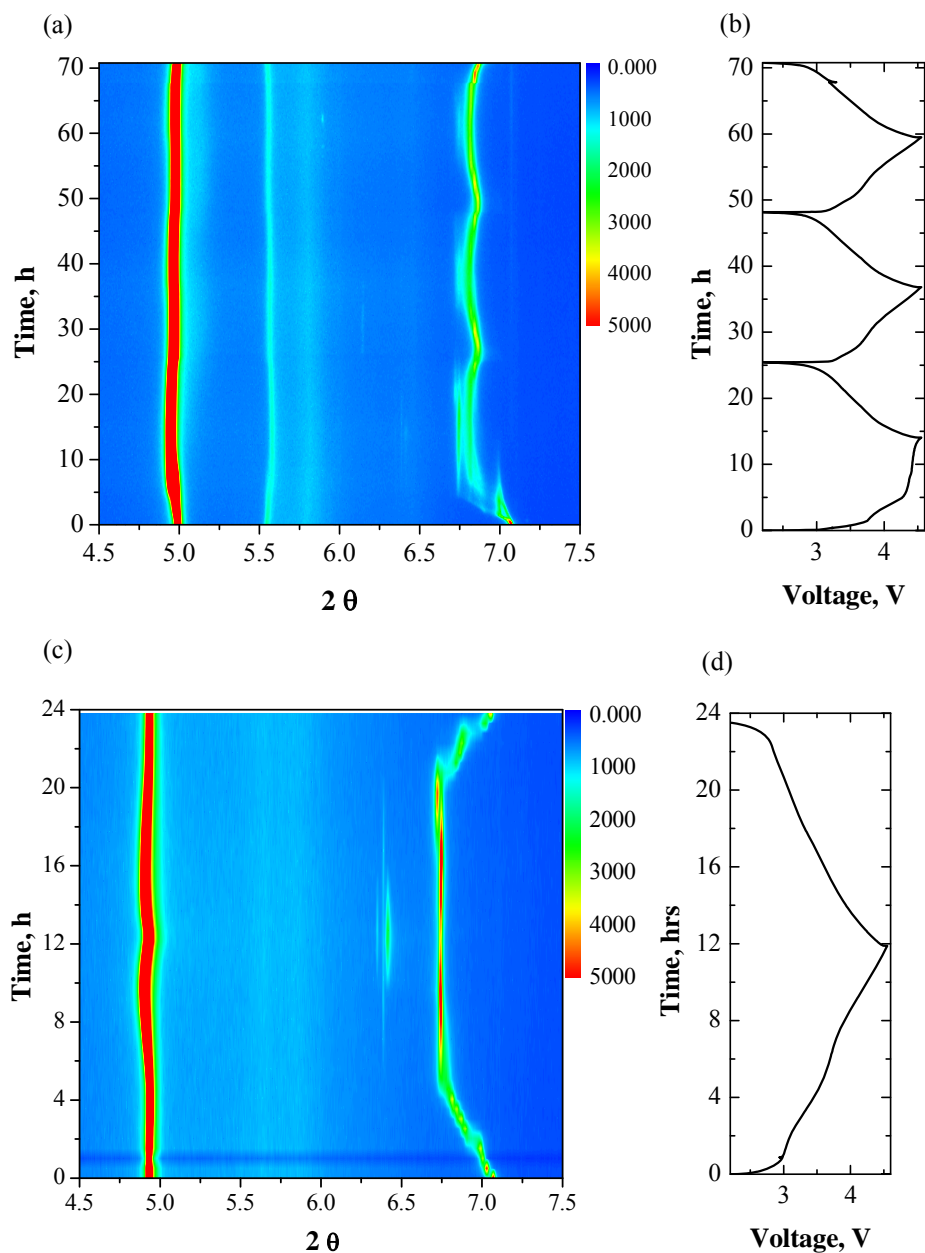


Figure 11 (a) Contour plot of *in situ* high resolution X-ray diffraction patterns and (b) the voltage profile of a graphite/ $\text{Li}_{1.2}\text{Ni}_{0.15}\text{Mn}_{0.55}\text{Co}_{0.1}\text{O}_2$ pouch cell during the initial charge/discharge cycles between 2.2 V and 4.55 V using a constant current of $C/12$ (~ 40 mA); (c) contour plot of *in situ* high resolution X-ray diffraction patterns and (d) the voltage profile of a graphite/ $\text{Li}_{1.2}\text{Ni}_{0.15}\text{Mn}_{0.55}\text{Co}_{0.1}\text{O}_2$ pouch cell that has been continuously charged/discharged between 2.2 V and 4.5 V at room temperature for 100 cycles. The fingerprint peaks for Li_2MnO_3 at 5.6° and 7.6° , respectively, can be clearly seen during the first three cycles, and both of them vanished after 100 cycles. This suggests that the phase transformation of activated Li_2MnO_3 be a slow process, and be related to the continuous voltage fade of lithium-manganese-rich transition metal oxides.

A complement to the XRD work is Solid State NMR, which enables us to probe the environments of both crystalline and non-crystalline samples. NMR is a valuable characterization technique for LIB systems as ^6Li and ^7Li MAS NMR can directly “see” the Li cations, even in amorphous regions of electrochemical systems. We are focusing on characterizing the Li environments and local order present in the cathode materials of interest (Li-rich transition metal oxides), regardless of their crystallinity and phase composition (i.e. composites) and correlating the observations with their electrochemical performance.

By determining of local Li coordination numbers in pristine and activated lithium rich $\text{Li}_{1+x}(\text{MnNi})_{1-x}\text{O}_2$ and $\text{Li}(\text{NiMnCo})\text{O}_2$ cathodes and effect of voltage fade on Li local structure by ^6Li solid state NMR, we can elucidate the changes in the material during cycling.

We have been using solid state NMR techniques for characterization of Li environments and local order present in Li-rich transition metal oxide cathode materials, correlating the lithium local environments observed with the electrochemical performance in association with voltage fade team. With completion of the installation of our new low field magnet and spectrometer setup with high spinning speed capability, we are now able to obtain high resolution ^6Li MAS NMR data on different compositions of pristine and cycled baseline Li rich NM and NMC materials and electrodes before and after activation.

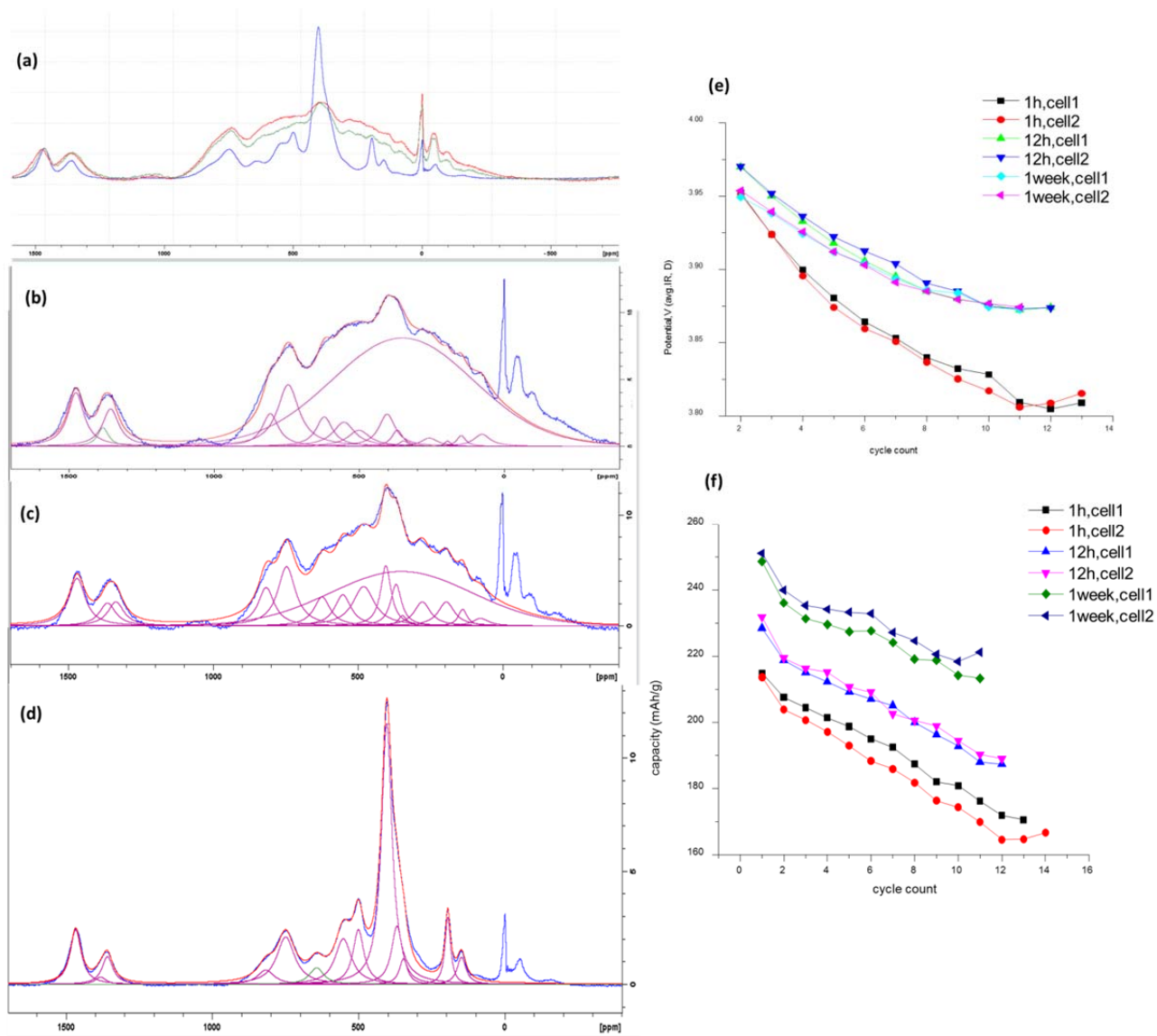


Figure 12. (a) ^6Li MAS NMR of pristine $\text{Li}_{1.5}[\text{Mn}_{0.5}\text{Co}_{0.5}]\text{O}_{2.5}$ compositions synthesized at 850°C for 1hr-quenched (red), 12hr-regular cooled (green), 84hr-regular cooled (blue) (b) deconvoluted spectrum of 1hr-quenched sample (c) deconvoluted spectrum of 12hr-regular cooled sample (d) deconvoluted spectrum of 84hr-regular cooled sample (e) IR corrected average voltage profiles of different synthesis condition electrodes (f) discharge capacity plots of different synthesis condition electrodes. NMR resonances at 0 ppm and at negative shifts are due to diamagnetic Li in LiCoO_2 and spinning sidebands, respectively.

Figure 12 highlights high resolution ^6Li MAS NMR data for the $\text{Li}_{1.5}[\text{Mn}_{0.5}\text{Co}_{0.5}]\text{O}_{2.5}$ composition cathode material. This composition is selected in order to utilize the calculation data from the theory group (Roy Benedek and Hakim Iddir) and to fundamentally study domain size effect on voltage fade (extension of this study for other compositions, both NM and NMC are currently in progress). Two groups of resonances were observed for the Li species present in the lattice; Li in Li layers around 50-1100 ppm region and Li in transition metal layers around 1300-1500 ppm region. The deconvolution of the peaks observed for lithium in Li layers reveals many different

lithium environments indicating different local ordering/ domains and interestingly domain boundaries from Fermi-contact shifts of neighboring Co and Mn. The preliminary assignments for the domain boundary lithiums were confirmed in this study by varying the synthesis conditions (duration) from 1 hr to 84 hrs which is represented by a broad Gaussian resonance centered at 350ppm. This resonance is gradually lost by increasing synthesis duration by allowing the small domains of the composite structure to grow at high temperature. To be specific, the ratio of Li in domain boundaries to the total amount of Li in the sample is 0.68 for 1hr synthesis, 0.42 for 12hr synthesis and near to 0 for 84 hr synthesis. These deconvoluted Li intensities will be used by the theory group to estimate the average domain sizes of the composite materials. The effect of this synthesis parameter and Li occupancy is correlated to electrochemical performance and voltage fade and can be seen in Figure 1e and 1f. The voltage fade rate is found to be minimum for the composites with larger domains/less disorder (1 week synthesis duration) and not surprisingly the electrochemical capacities were maximum for this lattice as well. The electrochemical performance drops and voltage fade rate increases as more and more domain boundary Li are present in the structure and as the domain sizes get smaller (1 and 12 hour synthesis duration).

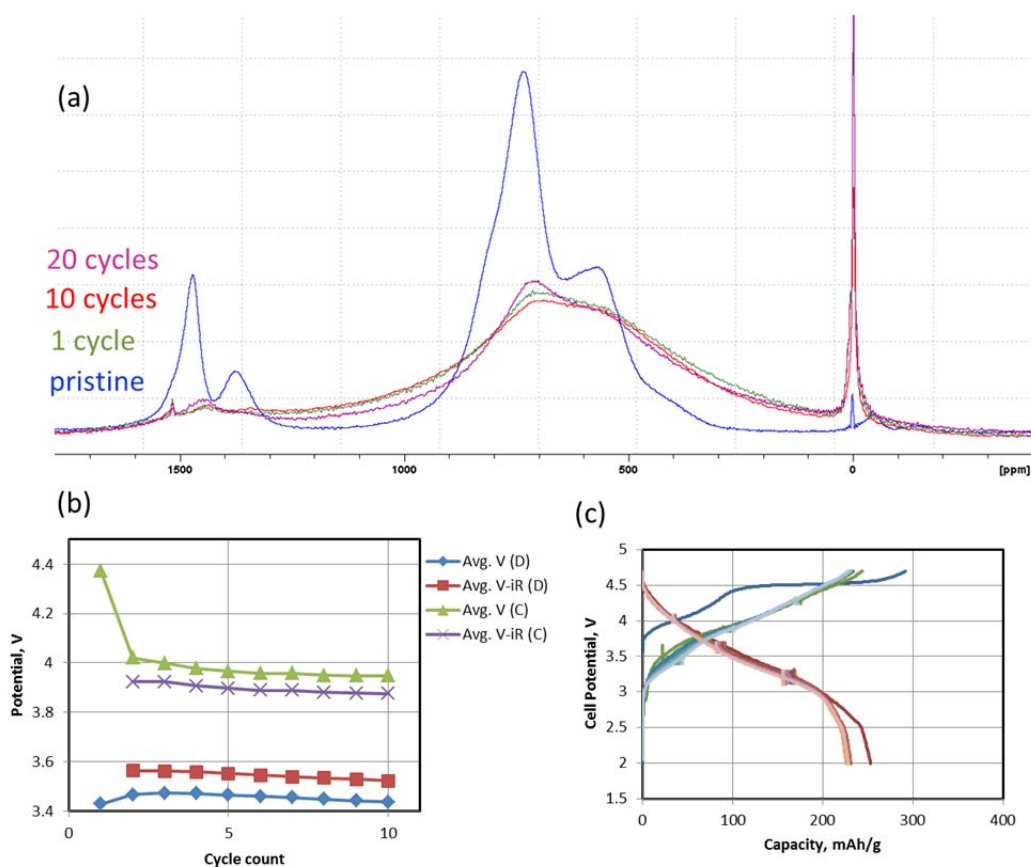


Figure 13. (a) High resolution ^6Li MAS NMR of pristine and voltage fade protocol cycled TODA HE5050 composites ($0.5\text{Li}_2\text{MnO}_3 \cdot 0.5\text{LiNi}_{0.375}\text{Mn}_{0.375}\text{Co}_{0.25}\text{O}_2$ or $\text{Li}_{1.0}[\text{Li}_{0.2}\text{Ni}_{0.15}\text{Mn}_{0.55}\text{Co}_{0.10}]\text{O}_2$), (b) electrochemical voltage fade plot of the 10 cycle electrode and (c) electrochemical profile of the 10 cycle electrode. NMR resonances at 0 ppm and at negative shifts are due to diamagnetic Li in SEI and spinning sidebands, respectively.

We initiated preparation of LRNMC type cathode materials with fully lithium-6 enriched cells (electrolyte, metal and cathode) and perform a quantitative study with high resolution ^6Li MAS NMR spectroscopy on the enriched cycled materials. In Figure 13a, two groups of resonances were observed for the Li species present in the lattice for the pristine material; Li in Li layers around 500-800 ppm region and Li in transition metal layers around 1300-1500 ppm region. The deconvolution of the peaks observed for lithium in Li layers reveals at least five different lithium environments indicating different local ordering/ domains and domain boundaries from Fermi-contact shifts of neighboring Ni, Co and Mn (plot is present in detail in 2nd quarterly report). For the lithium in transition metal layers, two resonances at 1371 and 1475 ppm were observed. Preliminary electrochemical and structural characterization results (see Figure 13a, 13b and 13c) show a direct correlation between the loss of lithium from the transition metal layers post activation, transformation/allocation of available lithium sites in lithium layers (presumably tetrahedral crystallographic positions) and electrochemical voltage fade. In depth analysis of the data is in progress to investigate the effect of lithium site formation in the lithium layers. Electrochemical performance and optimization of enriched cathode materials is in progress to obtain more reliable data and to reduce systematic errors in analysis.

Compositional control

Doping may be a way to retard voltage fade or VF if the dopant can alter the path of structural degradation during the first charge in the parent phase. Our hypotheses contain four criteria: (1) strong bonding with oxygen is required, (2) the oxidation state of the dopant can go higher than 4^+ and is stable (mitigate O_2 loss), (3) the dopant can preferentially substitute for Mn in Li_2MnO_3 domain which will alter the structure or size of the domain, and (4), it should form reversible dumbbell configuration with Li_{tet} during deep charge in order to maintain structural stability. Each dopant tried can fit into one of those classifications. To this end, we are synthesizing compositions that contain various dopants using sol-gel methods that create homogeneous distribution of all cations. The dopants evaluated this past quarter were Ga, V, and Cr. We had evaluated Fe in the last quarterly report but no positive effects were observed.

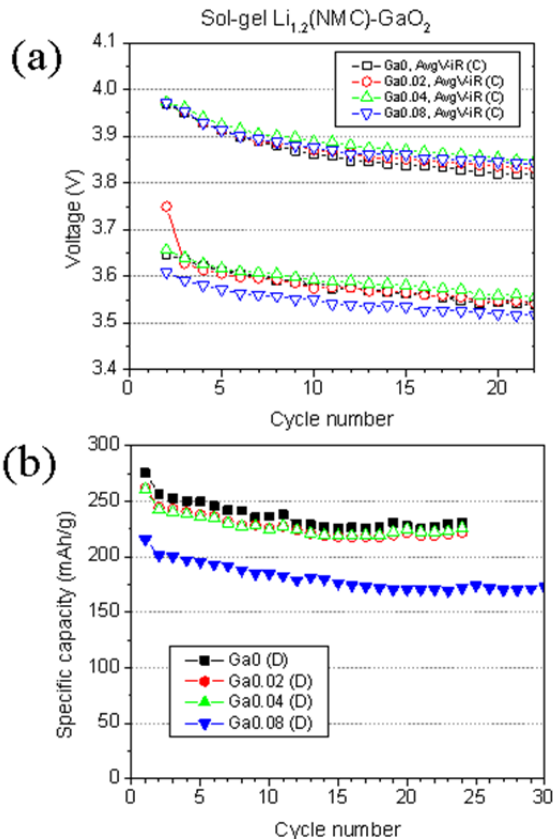


Figure 14. Ga dopant: (a) VF result, and (b) capacity with cycle no.

Typically in the solid state, Gallium (Ga) is known to possess only one oxidation state of three and has been shown to move from O_h to T_d coordination in layered TM oxide phases during cycling. It may immobilize co-bonded cations in the surrounding second-shell T_d coordination sphere of the host phase, and can also act as a pillar effectively co-bonding the Li layer and keeping it intact at high states of charge. As a spectator ion, this could affect the Li_{tet} dumbbell reversibility. Figure 14 shows the data results from coin-cell cycling of the Ga-doped LMR-NMC. As is obvious, there is no beneficial effect having Ga in the structure. The VF still occurs. The capacity remains constant for low values of Ga, which is good sign of consistent electrochemical activity in the phase, however.

Vanadium (V) has a number of stable oxidation states from 2^+ to 5^+ . It also can form a short apical bond with oxygen when it is in the 5^+ oxidation state that will actually distort the coordination sphere. Trivalent oxidation state is normally octahedral. Figure 15 shows the data result from the syntheses of four different dopant levels for $Li_{1.2}Ni_{0.15}Mn_{0.55-x}V_xCo_{0.1}O_2$. As is evident, having V present causes a melting and sintering of the product. The melting is likely due to the formation of a stable lithium vanadium oxide such as LiV_3O_8 in air that creates a flux in the reaction. The product also has poor electrochemical cycling. Future work for doping of V will need to be conducted in inert atmosphere to stabilize the 3^+ V oxidation state. But this problematic for the parent phase, as oxygen likely will be lost from the sample at high firing temperatures.

Chromium (Cr) doping is an interesting strategy to try since there is a possibility that the cation Cr^{6+} may fill available T_d sites in the phase during first charge which in turn may change the mechanism of movement of other cations, like Mn. First, from the XRD patterns we find that single phases can be readily formed, likely with Cr^{3+} . The XRD peaks shift to lower angle with doping, indicating lattice expansion: the Cr cation radii is larger than the averaged sum of Ni^{2+} and Mn^{4+} radii (i.e. $R[\text{Ni}^{+2}_{1/4}\text{Mn}^{+4}_{3/4}] = 0.57\text{\AA}$, $R[\text{Cr}^{3+}] = 0.615\text{\AA}$). Li-Mn ordering peaks become stronger with a low degree of Cr doping ($x = 0.05, 0.1$). Figure 16 shows the data result of cycling the Cr-doped cathodes in the first two cycles. What is interesting is that the first charge (activation) is dramatically altered. As Cr is increased, the plateau is shortened indicative of a change in the degree of oxygen loss in the resultant VF charged material. Cycling of this material continues and more work is needed to understand the role of Cr in the LMR-NMC and its mechanism.

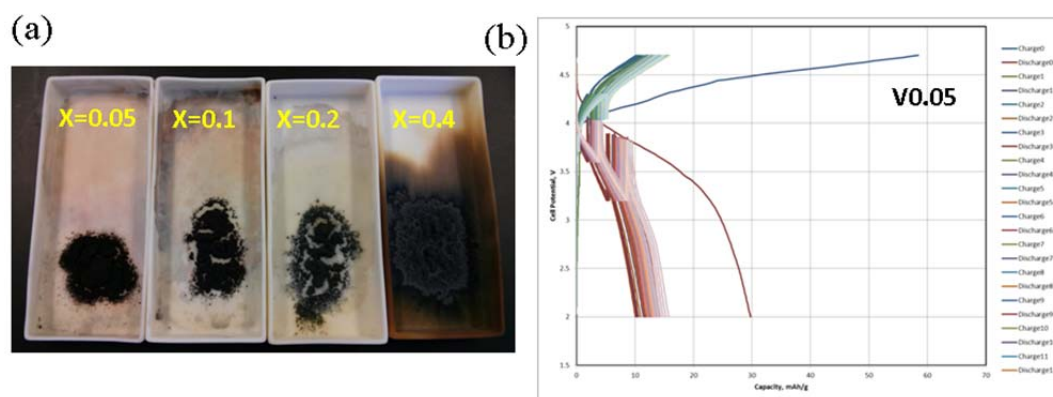


Figure 15. V dopant (a) photo of the products, and (b) coin cell voltage profiles

In the next quarterly we will show the result of Mo doping. In addition, we will try to incorporate Ti and Zr through substitution of Li_2MnO_3 with some Li_2TiO_3 and Li_2ZrO_3 portion of the layered-layered composite.

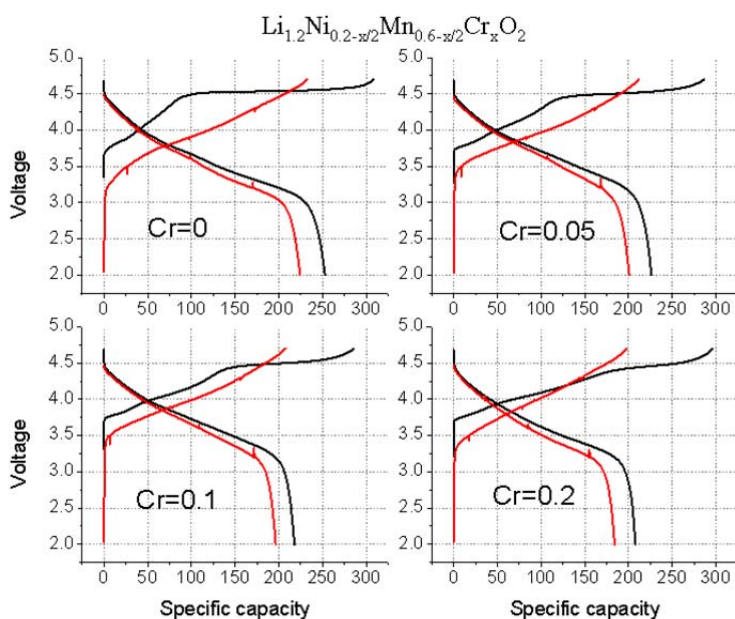


Figure 16. Cr dopant: the first two voltage profiles of the various products.

Structural control

An alternative to the compositional control and doping studies is the development of materials with increasing amounts of a spinel component which may serve to retard the cation mixing characteristic to voltage fade.

The concept of embedding a spinel component in composite $x\text{Li}_2\text{MnO}_3 \cdot (1-x)\text{LiMO}_2$ ($M=\text{Mn}, \text{Ni}, \text{Co}$) ‘layered-layered’ structures is being explored in order to fully realize the advantages of high manganese content cathode materials. The spinel component is embedded by lowering the Li content, thereby driving the composition of the electrode towards a spinel composition. During the past quarter, emphasis was placed on the preparation of $0.5\text{Li}_2\text{MnO}_3 \cdot 0.5\text{LiMn}_{0.375}\text{Ni}_{0.375}\text{Co}_{0.25}\text{O}_2$ electrodes with increasing spinel content synthesized via oxalate precursors to determine the effect on voltage fade. Figure 17 shows the electrochemical results of a reference ‘layered-layered’ $0.5\text{Li}_2\text{MnO}_3 \cdot 0.5\text{LiMn}_{0.375}\text{Ni}_{0.375}\text{Co}_{0.25}\text{O}_2$ electrode, cycled between 2.0 – 4.7 V at 10 mA/g for the first cycle, and at 20 mA/g for subsequent cycles. The left plot shows that the electrode exhibits a steady capacity of $\approx 200 \text{ mAhg}^{-1}$ over 30 cycles. The right plot shows the average voltage for the charge and discharge curves during cycling. Voltage fade is exhibited by the ‘layered-layered’ (0% spinel) electrode over all 30 cycles; the electrode exhibits a voltage fade of 8.8 mV/cycle for cycles 2-10.

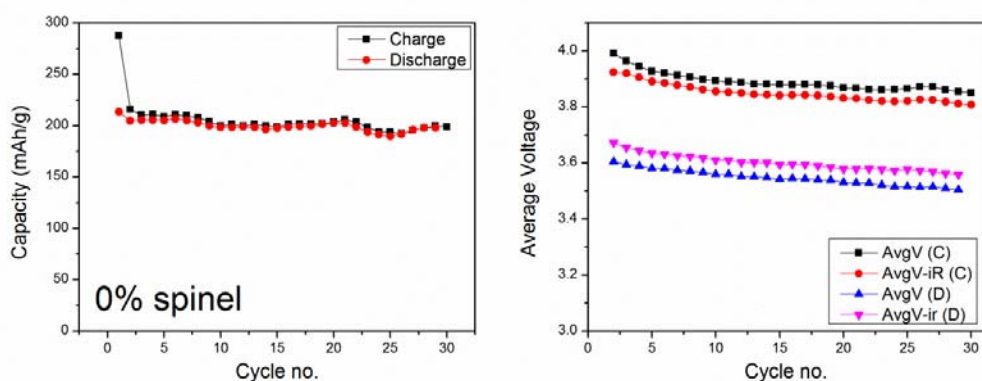


Figure. 17. Left: Capacity plot of a reference, ‘layered-layered’ $0.5\text{Li}_2\text{MnO}_3 \cdot 0.5\text{LiMn}_{0.375}\text{Ni}_{0.375}\text{Co}_{0.25}\text{O}_2$ (0% spinel) electrode composition using an electrochemical protocol for monitoring voltage fade. Right: Plot showing the average voltage of the charge and discharge curves during cycling; both iR-corrected and non-corrected data are shown.

Electrodes with a targeted 6% and 10% spinel content were also synthesized; they have the composite notation $x[0.5\text{Li}_2\text{MnO}_3 \cdot 0.5\text{LiMn}_{0.375}\text{Ni}_{0.375}\text{Co}_{0.25}\text{O}_2] \cdot (1-x)\text{Li}_{0.5}\text{Mn}_{0.55}\text{Ni}_{0.15}\text{Co}_{0.1}\text{O}_2$ with $x=0.94$ and 0.90 , respectively. Note that the spinel component is written with the same transition metal ratios as the precursor, but various cation distributions may occur. Figure 18 shows the electrochemical results for the targeted 10% spinel electrode. The electrode exhibits an improved first-cycle efficiency and a higher capacity ($\approx 225 \text{ mAhg}^{-1}$) relative to the reference ‘layered-layered’ (0% spinel) electrode. The 10% spinel electrode shows voltage fade, similar to the 0% spinel electrode, but at a reduced rate. The 10% spinel electrode reduces the voltage fade to 7 mV/cycle for cycles 2-10, which decreases further on subsequent cycles. Extended electrochemical cycling experiments and variations in electrode composition are being further evaluated.

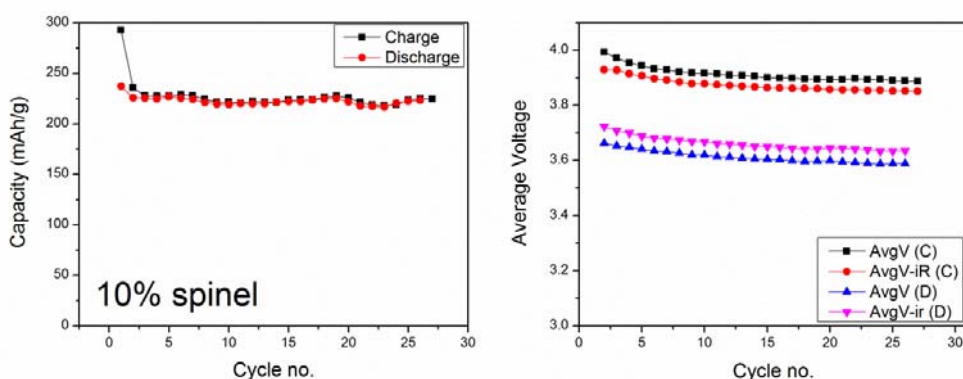


Figure. 18. Left: Capacity plot of a ‘layered-layered-spinel’ composition (10% spinel target) using an electrochemical protocol for monitoring voltage fade. Right: Plot showing the average voltage of the charge and discharge curves during cycling; both iR-corrected and non-corrected data shown.

**Publications, Reports, Intellectual property or patent application filed this quarter.
(Please be rigorous, include internal reports--invention records, etc.)**

Structural and Electrochemical Study of Al₂O₃ and TiO₂ Coated Li_{1.2}Ni_{0.13}Mn_{0.54}Co_{0.13}O₂ Cathode Material Using ALD

Xiaofeng Zhang, Ilias Belharouak, Li Li, Yu Lei, Jeffrey W. Elam, Anmin Nie, Xinqi Chen, Reza S. Yassar and Richard L. Axelbaum *Advanced Energy Materials*, DOI: 10.1002/aenm.201300269

Nanoscale phase separation, cation ordering, and surface oxygen vacancy formation in pristine Li_{1.2}Ni_{0.2}Mn_{0.6}O₂ for Li-ion batteries

Meng Gu, Ilias Belharouak, Arda Genc, Dapeng Wang, Khalil Amine, and Chongmin Wang
Chemistry of Materials, dx.doi.org/10.1021/cm4009392

A Study of High-Voltage LiNi_{0.5}Mn_{1.5}O₄ and High-Capacity Li_{1.5}Ni_{0.25}Mn_{0.75}O_{2.5} Blends

Xiaofeng Zhang, Rui Xu, Li Li, Cun Yu, Yang Ren, and Ilias Belharouak *J. Electrochem. Soc.* **160**(8): A1079-A1083 (2013)

Synthesis of lithium and manganese-rich cathode materials via an oxalate coprecipitation method

Dapeng Wang, Ilias Belharouak, Guangwen Zhou, and Khalil Amine *J. Electrochem. Soc.* **160**(5): A3108-A3112 (2013)

Layered-Layered-Spinel' Cathode Structures for Lithium-ion Batteries D. Kim, G. Sandi, J. R. Croy, K. G. Gallagher, S.-H. Kang, E. Lee, M. D. Slater, C. S. Johnson and M. M. Thackeray, *Composite* ', *J. Electrochem. Soc.* **160**, A31-A38 (2013).

Examining Hysteresis in Composite xLi₂MnO₃•(1-x)LiMO₂ Cathode Structures J. R. Croy, K. G. Gallagher, M. Balasubramanian, Z. Chen, Y. Ren, D. Kim, S.-H. Kang, D. W. Dees, and M. M. Thackeray, *J. Phys. Chem. C.* **117**, 6525-6536 (2013).

Correlating hysteresis and voltage fade in lithium- and manganese-rich layered transition-metal oxide electrodes K. G. Gallagher, J. R. Croy, M. Balasubramanian, M. Bettge, D. P. Abraham, A. K. Burrell, M. M. Thackeray, *Electrochem. Comm.*, **33**, 96–98 (2013).

Comments on Stabilizing Layered Manganese Oxide Electrodes for Li BatteriesD. Kim, J. R. Croy, and M. M. Thackeray, *Electrochem. Comm.* (2013). Submitted.

TASK 1

Battery Cell Materials Development

Project Number: IV.E.1.1 (ES167)

2013 Q3 update

Project Title: Process Development and Scale up of Advanced Cathode Materials

Project PI, Institution: Gregory Krumdick, Argonne National Laboratory

Collaborators (include industry):

Youngho Shin, Argonne National Laboratory

Ozgenur Kahvecioglu Feridun, Argonne National Laboratory

Gerald Jeka, Argonne National Laboratory (analytical)

Mike Kras, Argonne National Laboratory (analytical)

Kumar Bugga, Jet Propulsion Laboratory

Project Start/End Dates: start: 10/1/2012; end: 9/30/2013

Objectives: The objective of this program is to develop scalable processes for manufacturing cathode materials of benefit to the ABR program, synthesize kilogram quantities of each material and provide for industrial evaluation and basic research. Process engineering research is needed to identify and resolve constraints for the scale-up of advanced battery cathode materials, from the bench to pre-pilot scale with the development of cost-effective process technology.

The relevance of this program to the DOE Vehicle Technologies Program is that this program is a key missing link between discovery of advanced battery materials, market evaluation of these materials and high-volume manufacturing. This program provides large quantities of materials with consistent quality, providing standardized material for evaluation by different groups in large format prototype cells and addressing the need for larger amounts of material for basic R&D purposes and industrial needs.

Researchers in the battery materials programs across the DOE complex refer to scale up as synthesis of battery materials in gram quantities, and with time consuming, multiple small-scale runs. There is a need to develop scale up processed for battery materials to the kilogram and tens of kilograms quantities at DOE labs to support the transition of these technologies to industry and well as to provide a standardized material for basic R&D purposes.

Approach: Our approach is to first identify candidate cathode materials of interest to the ABR program participants including materials produced by the carbonate, hydroxide or other processes. A database of materials to scale has been developed and maintained and is used to rate and prioritize candidates for scale up. Candidates are ranked based on electrochemical performance, process complexity and level of interest in the material.

In FY13, we started the scale-up synthesis of JPL hydroxide ($\text{Li}_{1.5}\text{Ni}_{0.16}\text{Mn}_{0.68}\text{Co}_{0.16}\text{O}_{2.5}$) as the 2nd candidate and will generate kilogram quantities of the material for evaluation. We plan to then select and begin the scale-up of the next candidate material in the materials queue.

Schedule and Deliverables: Deliverables will include scaled materials for independent testing, publications and a topical report.

Financial data:

Total project duration: 12 mo.

Staff and M&S: \$1.3M

Progress towards deliverables:

Toda HE5050 as a commercial hydroxide sample was evaluated and compared to JPL pristine and ANL scale-up JPL materials (Table 1). The XRD analysis shows that Toda HE5050, JPL pristine and ANL scale-up JPL materials have the same structure (Figure 1).

ANL scale-up JPL ② cathode material shows better initial capacity than Toda HE5050 and JPL pristine (Figure 2) and the process optimization is being carried out to increase the material tap density.

JPL pristine has a high tap density of about 1.7g/cc. This is primarily due to large particles ($D_{100} = 56\mu\text{m}$) and non-scalable processes used. To maximize the tap density of the scaled material, the hydroxide co-precipitation process is under optimization. We are evaluating the effect of pH during co-precipitation, ratio of NH_4OH to transition metals and other parameters on tap density. We will complete a systematic statistical approach on the co-precipitation process to get optimal pH and NH_4OH ratio to maximize tap density. In addition, post treatment processes will also be optimized to produce kilogram quantity of cathode materials which is equal or better than JPL pristine material.

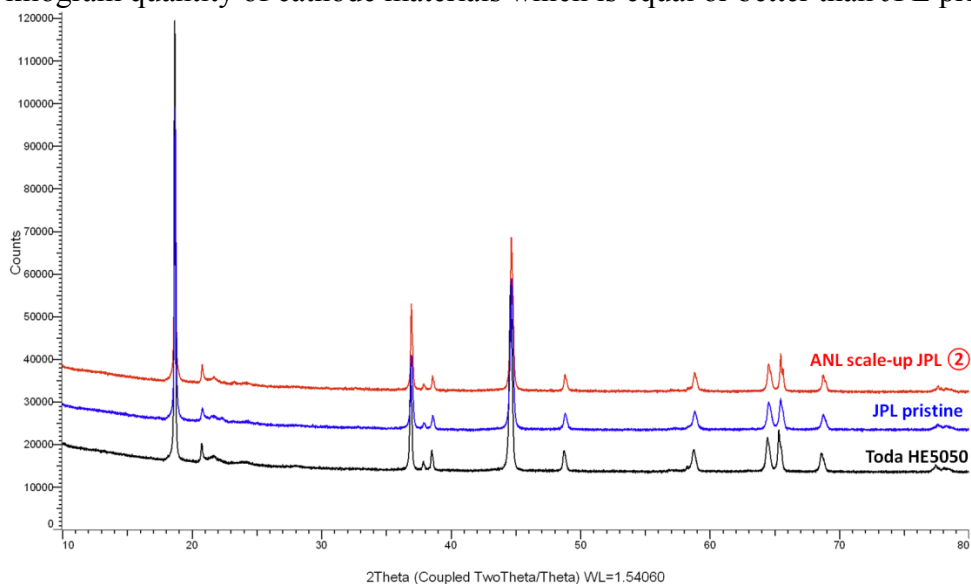
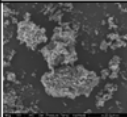
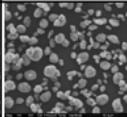
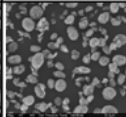
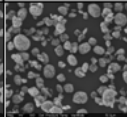
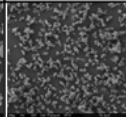
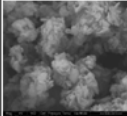
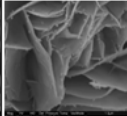
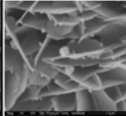
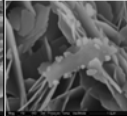
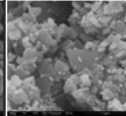
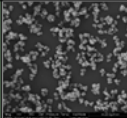
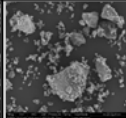
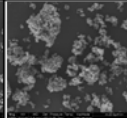
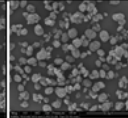
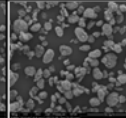
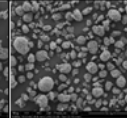
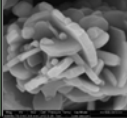
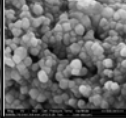
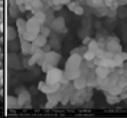
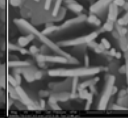
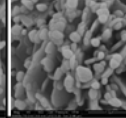
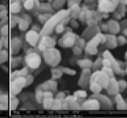


Figure 1. XRD comparison between Toda HE5050, JPL pristine and ANL scale-up JPL ②.

Table 1. Summary of scale-up progress of JPL material using hydroxide co-precipitation.

Scale-up of JPL material ($\text{Li}_{1.5}\text{Ni}_{0.1625}\text{Mn}_{0.675}\text{Co}_{0.1625}\text{O}_{2.5}$)

● Comparison and summary of scale-up progress using hydroxide process

Manufacturer		Toda HE5050	JPL pristine	ANL scale-up JPL ①	ANL scale-up JPL ②	ANL scale-up JPL ③	ANL scale-up JPL ④	ANL scale-up JPL ⑤
Scale		Commercial	Bench	Pre-pilot preliminary	Pre-pilot under optimization			
P r e c u r s o r	pH during co-precipitation	x	x	12.13	9.92	10.35	10.65	12.03
	Ratio of NH_4OH to MSO_4	x	x	0.2	0.6	1.0	1.4	1.0
	SEM x1,000	x	x					
	SEM x50,000							
Tap density [g/cc]	x	x	0.5	0.4	0.5	0.5	0.7	
C a t h o d e	D ₁₀ /D ₅₀ /D ₉₀ /D ₁₀₀ [μm]	3.1/5.3/ 9.2/18.0	1.2/11.1/ 29.3/56.0	1.3/6.9/ 22.1/45.0	2.7/9.9/ 15.1/25.0	5.2/10.7/ 16.1/28.0	5.7/10.6/ 16.1/28.0	on-going
	SEM x1,000							on-going
	SEM x50,000							
	Tap density [g/cc]	1.0	1.7	0.7	0.7	0.7	0.8	1.04
	ICP analysis	Li 1.52 Ni 0.16 Mn 0.71 Co 0.13 Oy	Li 1.61 Ni 0.16 Mn 0.71 Co 0.13 Oy	Li 1.50 Ni 0.16 Mn 0.67 Co 0.17 Oy	Li 1.56 Ni 0.12 Mn 0.71 Co 0.17 Oy	Li 1.66 Ni 0.10 Mn 0.72 Co 0.18 Oy	Li 1.63 Ni 0.08 Mn 0.74 Co 0.18 Oy	Li x Ni 0.16 Mn 0.67 Co 0.17 Oy
	Initial capacity [mAh/g]	244.6 (4.75-2.4 V)	226.5 (4.75-2.4 V)	238.1 (4.75-2.4 V)	263.6 (4.7-2.0 V)	on-going	on-going	on-going

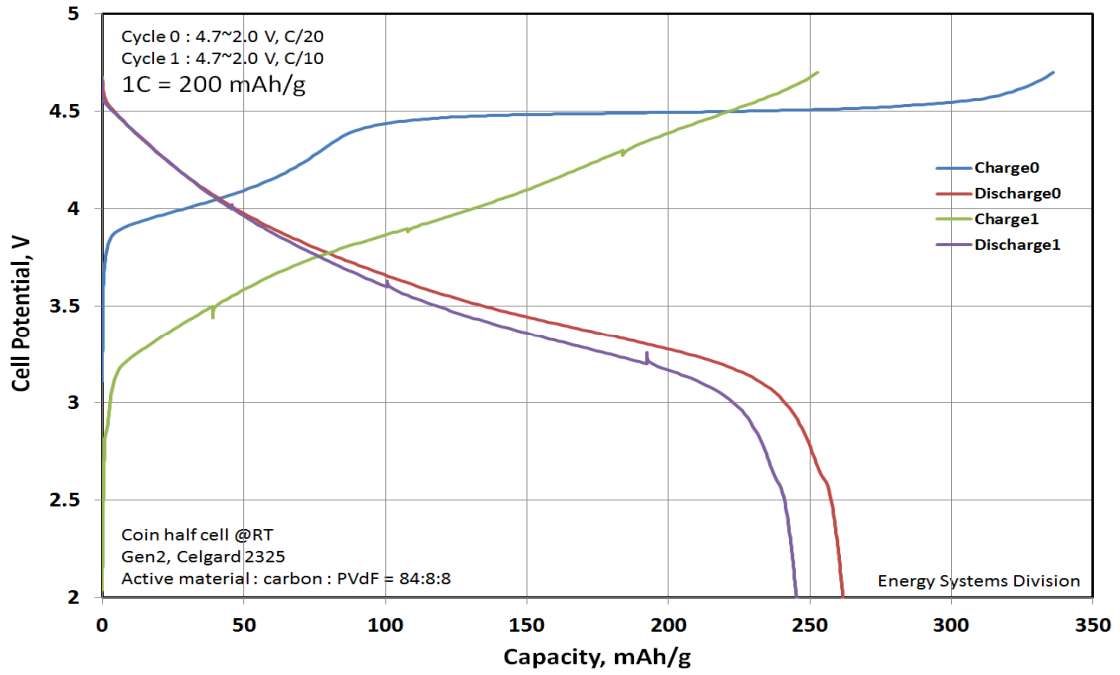


Figure 2. Plot of cell voltage vs. capacity for ANL scale-up JPL ②.

TASK 1

Battery Cell Materials Development

Project Number: IV.E.1.2 (ES168)

2013 Q3 update

Project Title: Process Development and Scale up of Advanced Electrolyte Materials

Project PI, Institution: Gregory Krumdick, Argonne National Laboratory

Collaborators (include industry):

Krzysztof Pupek, Argonne National Laboratory

Trevor Dzwiniel, Argonne National Laboratory

Wenquan Lu, Argonne National Laboratory

Daniel Scherson, Case Western University

Gao Liu, Lawrence Berkeley National Laboratory

Project Start/End Dates: start: 10/1/2012; end: 9/30/2013

Objectives: The objective of this task is to conduct process engineering research for the scale-up of next generation electrolyte solvents and additive materials. Advanced electrolyte materials are being developed to improve battery safety and to stabilize the interface of lithium ion batteries by forming a very stable passivation film at the carbon anode. Stabilizing the interface has proven to be key in significantly improving the cycle and calendar life of lithium ion batteries for HEV and PHEV applications. Scaling up the process involves modification of the bench-scale procedure and selection of the optimized chemical route that allows for the semi-continuous production of materials, development of a process engineering flow diagram, design of a mini-scale system layout, construction of the experimental system and experimental validation of the optimized process. Electrolyte materials will be produced at the kilogram scale and will be analyzed to confirm material properties and for quality assurance. The electrochemical properties of the material will be validated to confirm a performance match to the original materials. Synthesized materials will then be made available to industry for evaluation or to researchers for experimentation.

Approach: A formal approach for the scale-up of electrolyte materials has been defined. This approach starts with the initial discovery of a new electrolyte material and an initial electrochemical evaluation. This determines if the material is to be added to the inventory spreadsheet, ranked and prioritized. At this point, the scale-up process begins with the initial feasibility study, proof of concept testing, 1st stage scale-up and 2nd scale-up. Go/No go decisions are located after feasibility determination and electrochemical validation testing. Scaled materials distributed to industry or to collaborating researchers are tracked in a materials distribution spreadsheet which includes intended use and results obtained.

Schedule and Deliverables: The schedule of electrolyte materials to scale is determined by the prioritized ranking of the scale-up spreadsheet. Materials currently being scaled are reflected in the project milestones. Deliverables will include scaled materials for evaluation or experimentation and a technology transfer package of information on each material scaled. We expect to complete the scale-up of 3-5 electrolyte materials in FY13.

Financial data:

Total project duration: 12 mo.
Staff and M&S: \$1.2 M

Progress towards deliverables: Work on the scale-up of the electrolyte additive lithium perfluoro-*tert*-butoxide (LiPFTB) for the Army Research Lab has been completed. The synthesis was scaled up to 1.2 kg of the material. The material is available for sampling.

Work on the Argonne redox shuttle ANL-RS5 was completed. The process was found to be not scalable due to several factors (extremely flammable solvents, pyrophoric chemicals, large amounts of peroxides, chlorinated solvents, limited supply of raw materials and large amounts of waste generated). An alternate route to the molecule was investigated and several analogs were prepared. ANL-RS51 is a new shuttle that has a very similar structure to ANL-RS5 and is expected to be an acceptable substitute. It has been prepared on a 100g scale *via a scalable process*. Both synthesized RS5 and RS51 are waiting for final electrochemical testing. No second process scale-up (kilogram batch) is currently planned for these compounds.

Work on the Case Western University FRION material is underway. A second process scale-up will be determined based on results of the 100g electrochemical testing.

Work on the LBL conductive polymer is scheduled to start September 2013 and continue into FY14. A second process scale-up will be determined based on results of the 100g electrochemical testing.

Since the start of the electrolyte materials scale-up program, 11 materials have been scaled, over 24,000 g of battery grade materials was produced, 47 samples have been provided to industry and various national labs for evaluation and experimentation (total 7,300 g, 4 samples in FY11, 25 samples in FY12 and 18 samples in FY13).

Table 1 – Electrolyte Materials FY13 Milestones

MILESTONE	DATE	STATUS	COMMENTS
ANL-1NM2			
Assess scalability of disclosed process	7/20/12	Completed	
WP&C documentation approved	8/1/12	Completed	
Develop and validate scalable process	8/20/12	Completed	

chemistry (10g scale)			
First process scale-up (100g bench scale)	9/17/12	Completed	
Second process scale-up (1000g pilot scale)	10/09/12	Completed	9,715g produced in single batch
ANL- RS21			
Assess scalability of disclosed process	9/28/12	Completed	
WP&C documentation approved	9/28/12	Completed	
Develop and validate scalable process chemistry (10g scale)	10/30/12	Completed	
First process scale-up (100g bench scale)	11/30/12	Completed	
Second process scale-up (1000g pilot scale)	01/10/13	Completed	2,320 g produced in single batch
ARL-LiPFTB			
Assess scalability of disclosed process	11/21/12	Completed	
WP&C documentation approved	9/28/12	Completed	Covered under existing WP&C document
Develop and validate scalable process chemistry (10g scale)	12/21/12	Completed 2/14/2013	This task took longer than anticipated due to an issue with the target material, which will be detailed in the FY13-Q2 report
First process scale-up (100g bench scale)	2/28/13	Completed	Date revised due to material issue
Second process scale-up (1000g pilot scale)	3/15/13	Completed 3/3/2013	Date revised due to material issue. 1.2 kg of the material was produced, >99%
ANL- RS5			
Assess scalability of disclosed process	9/28/12	Completed	
WP&C documentation approved	9/28/12	Completed	Covered under existing WP&C document
Develop and validate scalable process chemistry (10g scale)	7/31/13	Completed	
First process scale-up (100g bench scale)	8/30/13	On Schedule	
ANL- RS51			
Assess scalability of disclosed process	N/A	N/A	
WP&C documentation approved	9/28/12	Completed	Covered under existing WP&C document
Develop and validate scalable process chemistry (10g scale)	7/31/13	Completed	

First process scale-up (100g bench scale)	8/16/31	Completed	155g crude, 94g purified in one batch.
CWU-FRION			
Assess scalability of disclosed process	5/21/13	Completed	
WP&C documentation approved	9/28/12	Completed	Covered under existing WP&C document
Develop and validate scalable process chemistry (10g scale)	7/9/13	Completed	
First process scale-up (100g bench scale)	9/30/13	Pending	Pending final discussion with CWU PI
LBL-311 PFPFOFOMB			
Assess scalability of disclosed process	9/13/13	Pending	
WP&C documentation approved	9/28/12	Completed	Covered under existing WP&C document
Develop and validate scalable process chemistry (10g scale)	9/30/13	Pending	
First process scale-up (100g bench scale)	10/31/13	Pending	

		<h1>ANL-RS51</h1>	
Description	(2,5-dimethoxy-1,4-phenylene)bis(diethylphosphine oxide)		
CAS	N/A		
Formula	$C_{16}H_{28}O_8P_2$		
FW	346.34		
LOT #	TD5-149		
Purity	99.2%		
Quantity	96 g		
Manufactured	8/22/2013		
Other	N/A		



Analysis	Method	Results	Analysis By:
HPLC	Agilent Eclipse Plus C18, 3.5 um, 4.6x100, UV 225, water/ACN gradient	99.16% ¹	T. Dzwiniel
GC/MSD	Agilent 7890A/5975C Triple-Axis		
	Agilent HP-5MS, 0.25 um, 30m x 0.250 mm, 45 to 300 deg, 30 deg/min	>99.9% ¹ M ⁺ = 346	T. Dzwiniel
Melting Point	Automatic, range method (Buchi M-565)	238-241°C	T. Dzwiniel
NMR	Bruker 500 MHz, CDCl ₃ solution.	Consistent with Structure	T. Dzwiniel

¹ By area integration.

Table 2 – Spec sheet on ANL-RS51

TASK 1

Battery Cell Materials Development

Project Number: ES024

Project Title: High Voltage Electrolytes for Li-ion Batteries

Project PI, Institution: Arthur Cresce, Kang Xu, Jan Allen, Oleg Borodin, Samuel Delp, Joshua Allen, T. Richard Jow, U.S. Army Research Laboratory

Collaborators (include industry): K. Gaskell (U. of Maryland); K. Amine, D. Dees, G. Krumdick (ANL); X. Yu and X. Yang (LBNL)

Project Start/End Dates: June 2011 / May 2014

Objectives: Develop high voltage electrolytes that enable the operation of 5 V Li Ion Chemistry. With a 5-V high voltage electrode materials and a capacity similar to that of the state-of-the-art cathode, the energy density will be increased more than 25% than that of the state-of-the-art Li-ion batteries for HEV/PHEV. Our other objective is to understand the surface chemistry at the high voltage cathode and electrolyte interface through surface characterization and computational effort. With better understanding, better electrolyte components and cathode materials can be developed.

Approach: Three approaches were taken.

1. Design and Synthesis of New Additives

- a. Rationale of electron deficient center
- b. Synthesis, purification and structural characterization by NMR and FTIR

2. Electrochemical Evaluation

- a. CC and CC-CV cycling in half and full cells at various temperatures
- b. Impedance analysis

3. Characterize Interfacial Chemistry at the Electrode/electrolyte Interface

- a. Use high resolution XPS, NMR and AFM

4. Computational Evaluation

- a. Understand oxidative stability of solvents/electrolytes
- b. Understand reactive pathways of additives and electrolytes
- c. Understand how electron-deficiency would impact on the oxidation stability of additives

Milestones:

- (a) Continued testing of new additives (June 2013)
- (b) Postmortem diagnostic studies: surface characterization and SEI chemistry (Oct 2013)
- (c) Erratum and re-characterization of additive structure (Dec 2012)
- (d) Test and evaluate electrolytes with additives in LNMO/graphite, doped-LCP/graphite and other cell couples (Dec 2013)

Financial data: \$250,000/year

PROGRESS TOWARD MILESTONES

(a) Additives Design and Synthesis Rationale (Arthur Cresce, Kang Xu)

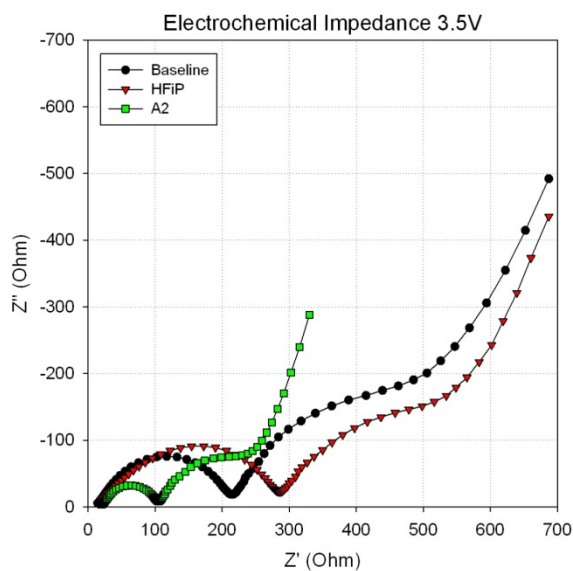
It has been realized in the past reports that fluorinated alkyl groups may play the main role of passivating the oxidizing sites on cathode. Starting this quarter, syntheses were conducted to make a few favored rationally designed structures that can deliver the effective ingredient of the additives onto cathode surface, especially the $\text{Ni}^{2+}/\text{Ni}^{4+}$ sites.

Four such compounds were already synthesized, and structural characterization electrochemical testing is under way.

(b) Impact of Additives on Cycling of LNMO/A12 at 55 °C (Samuel Delp, Jan Allen, Richard Jow)

The cycling of LNMO at 55 °C remains challenging. The LNMO/A12 full cells were tested at at 25 °C and 55 °C to study the effectiveness of various additives including HFiP, VC and A2 on capacity retention. Both LNMO ($\text{LiNi}_{0.5}\text{Mn}_{1.5}\text{O}_4$) and A12 (graphite) were provided by ANL. The baseline electrolyte is 1.2 M LiPF_6 in EC:EMC (3:7).

The effectiveness of the additives such as HFiP and VC in retaining capacity at 55 °C was not as good as A2. In addition to the cell capacity retention improvement as reported in the last quarterly report, the impedance of the cells in the baseline electrolyte containing A2 additive exhibits the most stable and low impedance at 55 °C compared to those in baseline electrolytes containing HFiP or no additive at all as shown in the figure below.



(c) Cycling of Substituted Lithium Cobalt Phosphate (LCP) High Voltage Cathode (Jan Allen, Joshua Allen, Samuel Delp, Richard Jow)

Further improvements in rate, capacity retention and coulombic efficiency for LCP based high voltage cathode were achieved through additional substitutions in the LCP based cathodes.

(d) Modeling the SEI-Electrolyte Interface (Oleg Borodin, Richard Jow)

The 272-ns simulations of the $\text{Li}_2\text{EDC} \mid \text{EC}:\text{DMC}(3:7) \text{LiPF}_6$ (solvent:Li=10 in electrolyte) interface were performed at ARL at 393 K, more than 80 Li^+ transfers from electrolyte to SEI and from SEI to electrolyte occurred during the course simulations. A snapshot of the simulated system is shown in the figure below. The smectic-like ordered Li_2EDC was used in these simulations.

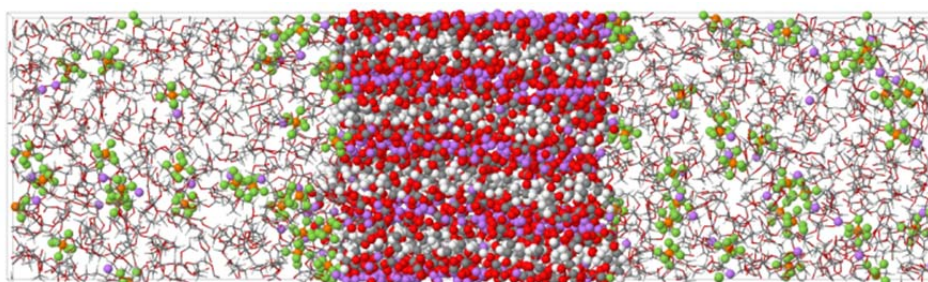


Figure . A simulation snapshot showing ordered Li_2EDC in contact with the electrolyte. Solvent molecules are shown as wireframe, while Li_2EDC and LiPF_6 are highlighted using a ball and stick model.

Many-body polarizable force field APPLE&P was used in simulations. Examination of the SEI-electrolyte interface revealed an enrichment of EC and PF_6^- at the SEI surface and depletion of DMC compared to bulk electrolyte concentrations. The EC and DMC molecules in the interfacial layer next to SEI preferentially oriented with carbonyl groups towards the SEI surface. The process of the Li^+ desolvation from electrolyte was examined with more than 80 of desolvation events occurring at the simulation timescale 300 ns for Li_2EDC -electrolyte at 393 K. During the initial desolvation step a Li^+ cation showed a preference to shed DMC in a significantly faster rate than losing EC of PF_6^- . The rate of the Li^+ desolvation reaction was estimated from these preliminary simulations. Using the Li^+ desolvation rates at 393 K and 500 K we obtain an estimate for the activation energy for the Li^+ desolvation process of 52 kJ/mol assuming the Arrhenius process. The activation energy for the desolvation reaction is lower than the activation energy for the Li^+ conduction in Li_2EDC (64 kJ/mol, Borodin et al. 2013) likely due to plasticizing effect of electrolyte on the dynamics of the interfacial SEI layer. The activation energy is, however, similar to the previously experimentally determined activation energy for the Li^+ desolvation from the EC:DMC-based electrolytes into lithiated spinel titanate ($\text{Li}_4\text{Ti}_5\text{O}_{12}$) of 50-52 kJ/mol, but lower than the previously reported activation energy for the desolvation into SEI covered graphite of 60-70 kJ/mol.^{1,2}

1. Xu, K.; von Cresce, A.; Lee, U., Differentiating Contributions to "Ion Transfer" Barrier from Interphasial Resistance and Li⁺ Desolvation at Electrolyte/Graphite Interface. *Langmuir* 2010, 26, 11538-11543.
2. Ogumi, Z., Interfacial Reactions of Lithium-Ion Batteries. *Electrochemistry* 2010, 78, 319-324.

Publications

- (1) "Oxidative Stability and Initial Decomposition Reactions of Carbonate, Sulfone and Alkyl Phosphate-Based Electrolytes", O. Borodin, W. Behl, and T. R. Jow, *J. Phys. Chem. C*, 2013, 117, 8661-8682.
- (2) "Quantum Chemistry Study of the Oxidation-Induced Decomposition of Tetramethylene Sulfone (TMS) Dimer and TMS/BF₄", Borodin, O.; Jow, T. R., *ECS Transactions* 2013, 50, 391-398.
- (3) "Molecular dynamics simulations and experimental study of lithium ion transport in dilithium ethylene dicarbonate", O. Borodin, G. Zhuang, P. Ross, and K. Xu. *J. Phys. Chem.*, 2013, 117, 7433-7444.
- (4) "Architecturing Hierarchical Function Layers on Self-Assembled Viral Templates as 3D Nano-Electrode Arrays for Integrated Li ion Microbatteries", Y. Liu, W. Zhang, Y. Zhu, Y. Luo, A. Brown, J. N. Culver, K. Xu, C. A. Lundgren, Y. Wang, and C. S. Wang, *Nano Lett.*, 2013, 13, 293.
- (5) "3D Sn nanoforest template on viral scaffolds as high capacity anodes for Na ion chemistry", Yihang Liu, Yunhua Xu, Yujie Zhu, Adam Brown, James N. Culver, Cynthia A. Lundgren, Kang Xu, and Chunsheng Wang, in press at *ACS Nano*.
- (6) "Understanding Li⁺-carbonate interaction with ¹⁷O-NMR", X. Bogle, S. Greenbaum, A. Cresce, and K. Xu, *J. Phys. Chem. Lett.*, 2013, 4, 1664-1668. to be submitted
- (7) "Direct Observation of SEI Formation on Graphitic Electrodes", A. v. Cresce, D. Baker, S. Russell, and K. Xu, to be submitted September 2013.

Presentations

- (1) "Additive Impacts on the Electrochemical Behavior of High Voltage Li-ion Batteries", S. A. Delp, T. R. Jow, 223rd *ECS Meeting*, May 12-16, 2013, Toronto, ON, Canada.
- (2) "Interphases on graphitic anodes in Li-ion battery", S. Russell, D. Baker, A. Cresce, K. Xu, *Pac-Rim American Ceramic Society Meeting* (June 5, 2013)
- (3) "Effect of electrolyte additives on SEI properties in Li-ion batteries as analyzed by in-situ AFM", A. Cresce, D. Baker, S. Russell, K. Xu, *American Chemical Society meeting* (Sept. 28, 2013).

TASK 1

Battery Cell Materials Development

Project Number: ES026

Project Title: Electrolytes for Use in High Energy Li-Ion Batteries with Wide Operating Temperature Range

Project PI, Institution: Marshall Smart, Jet Propulsion Laboratory, California Institute of Technology

Collaborators (include industry): (1) University of Rhode Island (Prof. Brett Lucht) (Analysis of harvested electrodes, on-going collaborator), (2) Argonne Nat. Lab (Khalil Amine) (Source of electrodes, on-going collaborator), (3) LBNL (John Kerr, Li Yang) (Evaluation of novel salts), (4) Loker Hydrocarbon Institute, USC (Prof. Surya Prakash) (Fluorinated Solvents and novel salts), (5) A123 Systems, Inc. (Electrolyte development, previous collaborator), (6) Quallion, LCC. (Electrolyte development, on-going collaborator), (7) Yardney Technical Products (Electrolyte development, on-going collaborator), (8) Saft America, Inc. (Collaborator, industrial partner under NASA program), (9) NREL (Smith/Pesaran)(Supporting NREL in model development by supplying data), (10) Sandia National Laboratory (Safety testing of low flammability electrolyte and supplier of electrode materials), (11) Hunter College (Prof. Greenbaum) (Ex-situ NMR measurements), and (12) North Carolina State University (Prof. Wesley Henderson) (Evaluation of novel salts).

Project Start/End Dates: Start Date: Oct 1, 2009, Projected End Date: September 30, 2014

Objectives:

- Develop a number of advanced Li-ion battery electrolytes with improved performance over a wide range of temperatures (-30 to +60°C) and demonstrate long-life characteristics (5,000 cycles over 10-yr life span).
- Improve the high voltage stability of these candidate electrolyte systems to enable operation up to 5V with high specific energy cathode materials.
- Define the performance limitations at low and high temperature extremes, as well as, identify life limiting processes.
- Demonstrate the performance of advanced electrolytes in large capacity prototype cells.

Approach: The development of electrolytes that enable operation over a wide temperature range, while still providing the desired life characteristics and resilience to high temperature (and voltage) remains a technical challenge. To meet the proposed objectives, the electrolyte development will include the following general approaches: (1) optimization of carbonate solvent blends, (2) use of low viscosity, low melting ester-based co-solvents, (3) use of fluorinated esters and fluorinated carbonates as co-solvents, (4) use of novel “SEI promoting”

and thermal stabilizing additives, (5) use of alternate lithium based salts (with USC, LBNL, and NCSU). Many of these approaches will be used in conjunction in multi-component electrolyte formulations (i.e., such as the use of low viscosity solvents and novel additives and salts), which will be targeted at improved operating temperature ranges while still providing good life characteristics.

The candidate electrolytes are characterized using a number of approaches, including performing ionic conductivity and cyclic voltammetry measurements, and evaluating the performance characteristics in experimental ~ 200-400 mAh three-electrode cells. In addition to evaluating candidate electrolytes in spirally-wound experimental cells, studies will be performed in coin cells, most notably in conjunction with high voltage cathode materials. Cells will be fabricated using a number of electrode couples: (a) MCMB/LiNi_{0.8}Co_{0.2}O₂, (b) graphite/LiNi_{0.8}Co_{0.15}Al_{0.05}O₂, (c) graphite/LiNi_{1/3}Co_{1/3}Mn_{1/3}O₂, (d) Li₄Ti₅O₁₂ (LTO)/LiNi_{0.5}Mn_{1.5}O₂ (LMNO), and (e) graphite/LiNiCoMnO₂ (lithium excess, layered-layered composite). Other chemistries can be evaluated depending upon availability from collaborators. In addition to performing charge/discharge characterization over a wide range of temperatures and rates on these cells, a number of electrochemical characterization techniques will be employed, including: (1) Electrochemical Impedance Spectroscopy (EIS), (2) DC linear (micro) polarization, and (3) Tafel polarization measurements. The electrochemical evaluation in proven three-electrode test cells enables electrochemical characterization of each electrode (and interface) individually and the identification of performance limiting mechanisms for each electrode and for the cell. Electrodes are easily harvested from these test cells and samples will be delivered to collaborators (i.e., URI and Hunter College).

Performance testing of prototype cells containing candidate advanced electrolytes will be performed and evaluated under a number of conditions, i.e., assessment of wide operating temperature capability and life characteristics. JPL has on-going collaborations with several battery vendors and also has the capabilities to perform extensive testing. Typical prototype cell designs that will be considered include (i) Yardney 7 Ah prismatic cells, (ii) Quallion prismatic cells (0.250Ah size and 12 Ah size), and (iii) A123 2.2 Ah cylindrical cells. Cells will be procured and/or obtained through on-going collaborations

Milestones:

Month/Year	Milestone
Sept. 2013	Milestone A: Prepare and characterize experimental laboratory cells containing advanced electrolytes, designed to operate over a wide temperature range in high-voltage systems (i.e., LiNiMnCoO ₂), and identify performance-limiting characteristics. (Sept. 13)
Sept. 2013	Milestone B: Demonstrate improved performance of experimental and prototype cells with next generation electrolytes over a wide temperature range (-30° to +60°C) compared with baseline electrolytes. (Sept. 13)

Financial data:

Total project funding:

- 875K total (~ 175K/year)
- Contractor share = 0K

Funding received:

- FY'10 = 175K (Start Date = Oct 1, 2009)
- FY'11 = 175K
- FY'12 = 170K
- FY'13 = 170K

Accomplishments and Progress toward Milestones:

In the last quarter, we have focused upon developing wide operating temperature range electrolytes for the graphite/high voltage NMC system (i.e., Conoco graphite anodes and NMC cathodes (HE5050) supplied by Argonne National Labs), in support of the FY'13 Milestone A. Primarily, we continue to investigate methyl butyrate-based formulations containing various additives, which were studied in both coin cells as well as larger experimental three-electrode cells equipped with lithium reference electrodes. The approach of incorporating electrolyte additives is to improve the high voltage stability, high temperature resilience, and in some cases improve the low temperature performance due to improved lithium kinetics at the interfaces. A number of electrolyte additives have been investigated, including (i) LiBOB, (ii) lithium difluoro(oxalato)borate (LiDFOB), (iii) lithium tetrafluoroborate (LiBF₄), (iv) lithium 4,5-dicyano-2-(trifluoromethyl) imidazole (LiTDI), (v) vinylene carbonate (VC), and (vi) lithium oxalate. The LiDFOB and LiTDI were synthesized and provided by Prof. Wesley Henderson's group at North Carolina State University (NCSSU). In the previous quarter, we described some of the results that were obtained with the three-electrode cells which were subjected to electrochemical measurements at a number of temperatures (23°, 0°, -20°, -30°, and -40°C), including Electrochemical Impedance Spectroscopy (EIS), Tafel polarization, and linear micro-polarization measurements. In particular, at -20°C the most favorable kinetics at the anode was observed with the cells containing lithium oxalate and VC. Whereas, the most facile kinetics observed at the cathode was observed with the cell containing LiBOB as an additive, suggesting that it participates beneficially in the formation of the cathode electrolyte interface (CEI). However, although LiBOB was observed to produce desirable kinetics at the cathode, it was seen to be detrimental to the anode kinetics resulting in high polarization resistance. After completing the electrochemical characterization of these cells, they were subjected to discharge characterization over a wide range of temperature, which will be reported on next quarter.

To complement the three-electrode cell study, a number of methyl butyrate based electrolytes were evaluated in coin cells consisting of graphite anodes (Conoco A12 graphite) and Li₂MnO₃-LiMO₂ (M=Mn, Co, Ni) cathodes (also referred to as Toda HE 5050 LiNiMnCoO₂). The electrolytes investigated include: (1) 1.20M LiPF₆ in EC+EMC+MB (20:20:60 v/v %) + 0.10M LiBF₄, (2) 1.20M LiPF₆ in EC+EMC+MB (20:20:60 v/v %) + 0.10M LiDFOB, (3) 1.20M LiPF₆ in EC+EMC+MB (20:20:60 v/v %) + 0.10M LiBOB, (4) 1.20M LiPF₆ in EC+EMC+MB (20:20:60 v/v %) + 0.10M LiTDI,

and (5) 1.20M LiPF₆ in EC+EMC+MB (20:20:60 v/v %) + 2% DBPC (where DBPC= di-*t*-butyl pyrocarbonate). These electrolytes were compared with the DOE-ABR baseline electrolyte (i.e., 1.20M LiPF₆ in EC+EMC (30:70 v/v %)). Good performance characteristics were observed after completing the five formation cycles with most of the methyl butyrate-based electrolytes containing the various electrolyte additives, as judged from the coulombic efficiency on the first cycle (being an indication of the inherent stability and the electrode film forming process) and the cumulative irreversible capacity losses. In summary, the following trend was observed in terms of cumulative irreversible capacity loss: baseline \approx LiBOB < LiDFOB < LiBF₄ < LiTDI < DBPC, where lower irreversible capacity loss generally is associated with desirable film formation on the electrode surfaces.

After performing the formation cycling, some of the cells were subjected to systematic discharge rate characterization testing over a wide temperature range. The first tests consisted of both charging and discharging the cells at the desired temperatures, after equilibrating at the temperature for the desired amount of time. The results of these studies are summarized in Table 1. As illustrated, significant low temperature rate capability was observed for the cell containing the 1.20M LiPF₆ in EC+EMC+MB (20:20:60 v/v %) + 0.10M LiDFOB electrolyte, with over a four-fold improvement in the capacity delivered at high rate (1.0C rate) at low temperature (-20°C) compared with the baseline electrolyte. Improved performance was also observed for the formulations containing LiBOB and LiBF₄.

In addition to evaluating the discharge rate capability where the cells were charged at the respective temperature, discharge performance testing of the cells was also performed in which the cells were charged at room temperature prior to low temperature discharge at different rates (up to 2C rates). As illustrated in Table 2, similar trends were observed with the cell containing the 1.20M LiPF₆ in EC+EMC+MB (20:20:60 v/v %) + 0.10M LiDFOB electrolyte providing the best low temperature performance, which is assumed to be due to the desirable cathode film formation process associated with the use of the LiDFOB additive. Work is on-going to investigate the benefit of this electrolyte at lower temperatures and higher discharge rates. It should be noted that the electrolytes containing the LiBF₄ and LiBOB displayed similar performance, being somewhat poorer than LiDFOB but both outperforming the baseline solution. As shown in Fig. 1, the cell containing the MB-based electrolyte with LiDFOB delivered approximately twice the capacity compared with the baseline electrolyte when discharged at a C/10 rate at -20°C, and roughly four times the capacity at a C/2 rate at -20°C. The MB-based electrolyte with LiDFOB was also observed to result in improved rate capability at more moderate temperatures, such as 0°C, as illustrated in Fig. 2. Work is also on-going to further evaluate the low temperature performance characteristics of electrolytes containing the LiTDI and DBPC additives, which were not included in the testing described above. In addition, future work will also be focused upon characterizing the high temperature stability and cycle life performance of these electrolytes in the high voltage system.

Table 1: Summary of the discharge characteristics of Carbon-LiNiMnCoO₂ cells containing various electrolytes over a wide temperature range (-20 to +20°C).

		MB01			MB03			MB05			MB07		
Electrolyte Type 		1.2M LiPF ₆ in EC+EMC (30:70 vol%)			1.2M LiPF ₆ + 0.10M LiBOB in EC+EMC+MB (20:20:60 vol%)			1.2M LiPF ₆ + 0.10M LiDFOB in EC+EMC+MB (20:20:60 vol%)			1.2M LiPF ₆ + 0.10M LiBF ₄ in EC+EMC+MB (20:20:60 vol%)		
Temperature	Discharge Rate	Capacity (Ah)	Cathode Capacity (mAh/g)	Percent (%)	Capacity (Ah)	Cathode Capacity (mAh/g)	Percent (%)	Capacity (Ah)	Cathode Capacity (mAh/g)	Percent (%)	Capacity (Ah)	Cathode Capacity (mAh/g)	Percent (%)
20°C	c/20	0.00314	250.03	100.00	0.00312	248.72	100.00	0.00318	249.75	100.00	0.00299	233.62	100.00
	c/10	0.00301	239.61	95.83	0.00302	240.89	96.85	0.00306	240.59	96.33	0.00290	226.70	97.04
	c/5	0.00280	222.76	89.09	0.00286	227.50	91.47	0.00287	225.70	90.37	0.00275	214.57	91.85
	c/2	0.00244	193.96	77.57	0.00252	200.57	80.64	0.00253	198.77	79.59	0.00232	180.99	77.47
	1.0C	0.00211	168.30	67.31	0.00222	176.57	70.99	0.00222	174.60	69.91	0.00189	147.42	63.10
0°C	c/20	0.00257	204.92	81.96	0.00260	207.01	83.23	0.00267	209.53	83.89	0.00252	196.98	84.32
	c/10	0.00223	177.30	70.91	0.00227	180.41	72.53	0.00235	184.78	73.98	0.00222	173.41	74.23
	c/5	0.00197	157.06	62.82	0.00202	161.21	64.81	0.00210	165.35	66.21	0.00195	152.40	65.24
	c/2	0.00164	130.60	52.23	0.00171	135.97	54.67	0.00178	140.00	56.05	0.00162	126.16	54.00
	1.0C	0.00135	107.44	42.97	0.00144	114.84	46.17	0.00154	120.93	48.42	0.00135	105.23	45.04
-10°C	c/20	0.00200	159.13	63.64	0.00202	160.81	64.66	0.00220	172.89	69.22	0.00207	161.32	69.05
	c/10	0.00177	140.84	56.33	0.00180	143.70	57.77	0.00197	155.02	62.07	0.00186	145.12	62.12
	c/5	0.00155	123.25	49.29	0.00157	125.08	50.29	0.00177	139.03	55.67	0.00168	130.98	56.07
	c/2	0.00115	91.47	36.58	0.00127	100.97	40.60	0.00149	116.77	46.75	0.00141	109.67	46.94
	1.0C	0.00066	52.47	20.98	0.00095	75.32	30.28	0.00125	98.01	39.24	0.00111	86.35	36.96
-20°C	c/20	0.00151	120.57	48.22	0.00152	121.39	48.81	0.00171	134.51	53.86	0.00163	127.49	54.57
	c/10	0.00132	105.21	42.08	0.00137	109.31	43.95	0.00156	122.25	48.95	0.00147	115.05	49.25
	c/5	0.00099	78.72	31.48	0.00117	93.27	37.50	0.00137	107.50	43.04	0.00128	99.79	42.72
	c/2	0.00052	41.40	16.56	0.00080	64.00	25.73	0.00109	85.96	34.42	0.00096	74.92	32.07
	1.0C	0.00018	14.59	5.84	0.00039	31.43	12.64	0.00082	64.33	25.76	0.00059	45.93	19.66

Table 2: Summary of the discharge characteristics of graphite-LiNiMnCoO₂ cells containing various electrolytes over a wide temperature range (-20 to +20°C). Cells were charged at room temperature prior to discharge.

		MB01			MB03			MB05			MB07		
Electrolyte Type		1.2M LiPF ₆ in EC+EMC (30:70 vol%)			1.2M LiPF ₆ + 0.10M LiBOB in EC+EMC+MB (20:20:60 vol%)			1.2M LiPF ₆ + 0.10M LiDFOB in EC+EMC+MB (20:20:60 vol%)			1.2M LiPF ₆ + 0.10M LiBF ₄ in EC+EMC+MB (20:20:60 vol%)		
Temperature	Discharge Rate	Capacity (Ah)	Cathode Capacity (mAh/g)	Percent (%)	Capacity (Ah)	Cathode Capacity (mAh/g)	Percent (%)	Capacity (Ah)	Cathode Capacity (mAh/g)	Percent (%)	Capacity (Ah)	Cathode Capacity (mAh/g)	Percent (%)
20°C	C/20	0.00314	250.03	100.00	0.00312	248.72	100.00	0.00318	249.75	100.00	0.00299	233.62	100.00
	C/10	0.00301	239.61	95.83	0.00302	240.89	96.85	0.00306	240.59	96.33	0.00290	226.70	97.04
	C/5	0.00280	222.76	89.09	0.00286	227.50	91.47	0.00287	225.70	90.37	0.00275	214.57	91.85
	C/2	0.00244	193.96	77.57	0.00252	200.57	80.64	0.00253	198.77	79.59	0.00232	180.99	77.47
	1.0C	0.00211	168.30	67.31	0.00222	176.57	70.99	0.00222	174.60	69.91	0.00189	147.42	63.10
+10°C	C/20	0.00261	208.24	83.28	0.00284	225.88	90.82	0.00293	229.89	92.05	0.00220	171.91	73.59
	C/10	0.00242	193.05	77.21	0.00267	212.26	85.34	0.00282	221.35	88.63	0.00210	163.53	70.00
	C/5	0.00227	180.89	72.34	0.00246	196.11	78.85	0.00257	201.61	80.73	0.00208	162.51	69.56
	C/2	0.00131	104.65	41.86	0.00203	161.36	64.87	0.00214	168.17	67.34	0.00188	146.45	62.69
	1.0C	0.00058	46.33	18.53	0.00165	131.08	52.70	0.00180	141.47	56.64	0.00145	113.12	48.42
0°C	1.5C	0.00031	24.52	9.81	0.00135	107.36	43.16	0.00158	124.09	49.69	0.00108	84.36	36.11
	2.0C	0.00028	22.39	8.96	0.00101	80.05	32.18	0.00139	109.34	43.78	0.00065	50.60	21.66
	C/20	0.00249	198.18	79.26	0.00264	210.19	84.51	0.00280	219.72	87.97	0.00238	185.99	79.61
	C/10	0.00226	180.18	72.06	0.00234	186.35	74.92	0.00249	195.41	78.24	0.00222	173.06	74.08
	C/5	0.00198	157.94	63.17	0.00208	165.81	66.67	0.00220	172.70	69.15	0.00203	158.14	67.69
-10°C	C/2	0.00117	92.81	37.12	0.00172	136.69	54.96	0.00183	143.86	57.60	0.00163	126.91	54.32
	1.0C	0.00033	26.41	10.56	0.00135	107.20	43.10	0.00153	120.10	48.09	0.00123	96.22	41.19
	1.5C	0.00024	18.86	7.54	0.00102	81.38	32.72	0.00131	102.76	41.14	0.00082	63.93	27.36
	2.0C	0.00018	14.60	5.84	0.00059	47.11	18.94	0.00109	85.48	34.23	0.00033	25.40	10.87
	C/20	0.00216	171.82	68.72	0.00222	177.17	71.23	0.00235	184.47	73.86	0.00221	172.59	73.88
-20°C	C/10	0.00165	131.39	52.55	0.00200	159.25	64.03	0.00211	166.02	66.48	0.00200	155.75	66.67
	C/5	0.00101	80.73	32.29	0.00174	138.24	55.58	0.00183	144.16	57.72	0.00167	130.59	55.90
	C/2	0.00042	33.27	13.31									
	1.0C	0.00022	17.85	7.14	0.00090	71.89	28.90	0.00123	96.62	38.68	0.00091	71.37	30.55
	1.5C	0.00016	12.61	5.04	0.00053	42.29	17.00	0.00099	77.56	31.05	0.00044	34.51	14.77
-20°C	2.0C	0.00008	6.26	2.51	0.00021	16.82	6.76	0.00058	45.91	18.38	0.00013	9.80	4.19
	C/20	0.00134	106.80	42.71	0.00181	144.03	57.91	0.00197	154.48	61.85	0.00185	144.29	61.77
	C/10	0.00089	70.75	28.30	0.00157	125.13	50.31	0.00175	137.13	54.91	0.00159	124.12	53.13
	C/5	0.00064	50.99	20.40	0.00132	105.03	42.23	0.00153	119.99	48.04	0.00134	104.63	44.79
	C/2	0.00036	28.86	11.54	0.00094	75.09	30.19	0.00123	96.86	38.78	0.00099	77.32	33.10
-20°C	1.0C	0.00027	21.16	8.46	0.00059	47.20	18.98	0.00097	76.45	30.61	0.00061	47.66	20.40
	1.5C	0.00008	5.98	2.39	0.00021	16.65	6.69	0.00055	43.13	17.27	0.00021	16.01	6.85
	2.0C	0.00002	1.30	0.52	0.00006	4.77	1.92	0.00017	13.74	5.50	0.00004	2.97	1.27

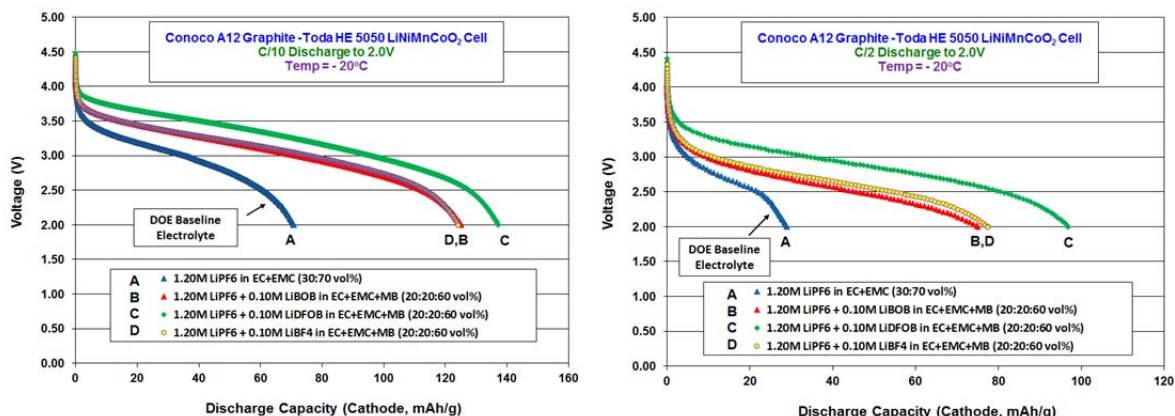


Figure 1: Discharge capacity (expressed in terms of cathode specific capacity) of Conoco Graphite-LiNiMnCoO₂ cells containing methyl butyrate-based electrolytes at -20°C using a C/10 discharge rate (1A) and a C/2 discharge rate (1B). (Cells were charged at room temperature prior to low temperature discharging).

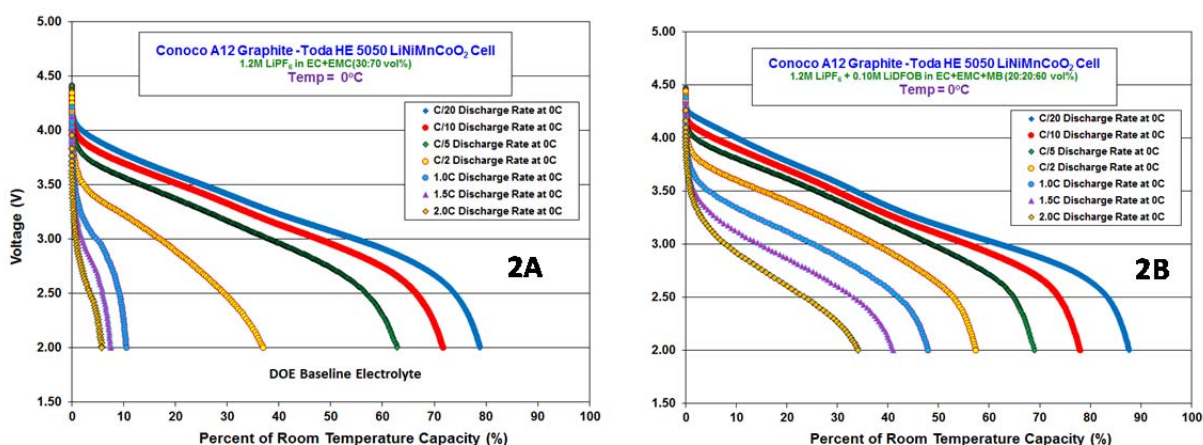


Figure 2: Discharge capacity (expressed in terms of percentage of the room temperature capacity) at various rates of Conoco Graphite-LiNiMnCoO₂ cells containing a baseline all carbonate-based electrolyte (2A) and a methyl butyrate-based electrolyte containing LiDFOB (2B) at 0°C. (Cells were charged at room temperature prior to low temperature discharging).

In work focused toward the FY'13 Milestone B, we continue to characterize the performance of prototype cells (0.25Ah MCMB/LiNiCoAlO₂ cells manufactured by Quallion, LCC) that possess methyl propionate-based electrolytes that we have developed under this program. The electrolytes investigated consist of methyl propionate with varying amount of mono-fluoroethylene carbonate (FEC) (i.e., 4, 10, and 20%), with the primary intent of improving the high temperature resilience. In one permutation, we have entirely replaced ethylene carbonate (EC) with FEC. We have also continued the study of using LiBOB as an additive to methyl propionate-based electrolytes, based upon previous results obtained from three-electrode cell data in which the cathode kinetics was

significantly improved. As recently reported, we have demonstrated that a number of these cells can support high rate discharge (i.e., 10C to 20C rates) at low temperature (-20°C to -40°C). As noted, the MP-based electrolytes displayed dramatically improved power capability compared with the DoE baseline all carbonate electrolyte. For example, a cell containing the electrolyte with methyl propionate and LiBOB displayed very high power capability at -20°C, being able to provide over 60 Wh/kg at a 20C discharge rate. We continue to evaluate the cycle life characteristics of these cells over a wide temperature range, including 100% DOD cycling at 20°C, 40°C, and 50°C, as well as variable temperature cycling between temperature extremes (i.e., -20° and +40°C). As illustrated in Fig. 3, we continue to observe excellent performance with the cells when subjected to 100% DOD cycle life testing at 20°C, with over 2,500 cycles completed to-date on some of the cells. A trend of lower capacity fade is observed with increasing FEC content in the electrolyte, although high FEC content was observed to lead to somewhat lower initial capacity. As illustrated in Fig. 3B, the cell containing LiPF₆ in FEC+EMC+MP was observed to deliver > 91% of the initial capacity after completing 2,550 cycles, outperforming the baseline. In addition, excellent retention of the watt-hour efficiency was observed with the cell containing LiPF₆ in FEC+EMC+MP when subjected to cycling at +20°C, suggesting minimal impedance growth. In terms of the capacity fade observed, the cell containing the electrolyte with 10% FEC and 10% EC also outperforms the all carbonate baseline. Although the electrolyte with LiBOB resulted in cells with the best low temperature discharge rate capability, the cycle life performance was inferior to that of the baseline and the cells containing FEC in high proportion.

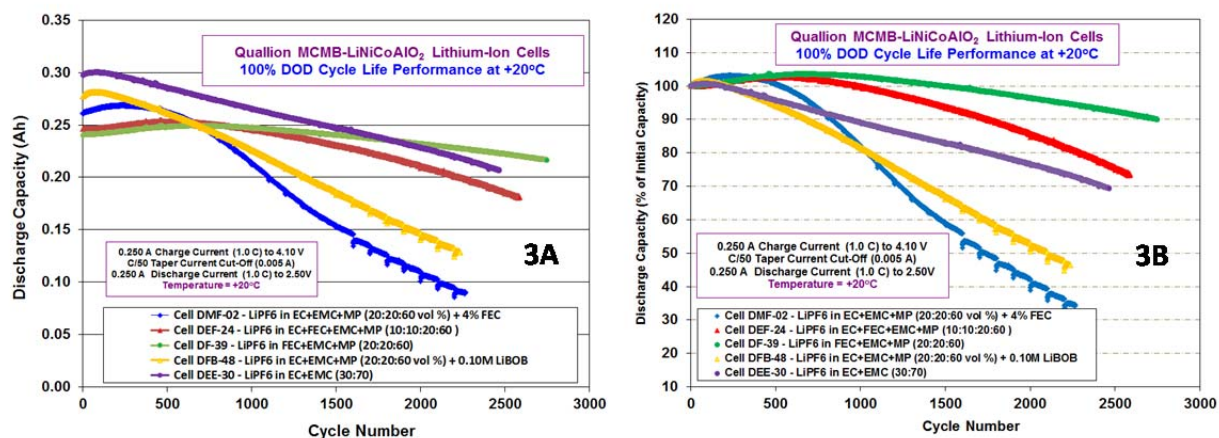


Figure 3: Cycle life performance 0.25Ah MCMB-LiNiCoAlO₂ cells (Quallion, LCC) containing methyl propionate-based electrolytes at 20°C using C rate charge and discharge.

We also continue to evaluate the large capacity 12 Ah cells (MCMB Carbon/LiNiCoAlO₂) manufactured by Quallion, LCC that possess JPL methyl propionate (MP)-based wide operating temperature range electrolytes. We are currently evaluating their life characteristics and the degree to which the low temperature capability degrades with time. These cells contain electrolytes that have been previously shown to have excellent low temperature capabilities, namely (i) 1.20M LiPF₆ in

EC+EMC+MP (20:20:60 v/v %) and (ii) 1.20M LiPF₆ in EC+EMC+MP (20:20:60 v/v %) + 4% FEC. In addition to JPL developed electrolytes, the group of cells contain a Quallion developed wide operating temperature range electrolyte and the DOE baseline electrolyte (i.e., 1.2M LiPF₆ in EC+EMC (30:70 v/v %)). The cycle life testing consists of partial depth of discharge cycling (approximately 50% DOD), where one cycle is performed each day using a variable load profile with low to moderate rates. After completing increments of 100 cycles (i.e., 100 days of testing), the cells have been re-characterized to determine the capacity, impedance, and low temperature discharge rate capability. The cells will complete 400 cycles shortly, representing 400 days of life testing. Upon completion, we will re-characterize the cells at low temperature (down to -50°C), which will be reported on next period. In summary, the best capacity retention observed was with the cell containing the methyl propionate-based electrolyte that contains FEC as an additive (4%), slightly outperforming the baseline electrolytes, suggesting that the additive has produced a desirable, protective SEI layer. In addition, good retention of low temperature capability has been observed thus far at -40° and -50°C, when evaluated at 2C and C/5 rates, after completing the cycling testing, with the cells containing the methyl propionate-based cells delivering the highest capacity.

We also have continued the evaluation of the life characteristics of a number of A123 cells that possess methyl butyrate-based electrolytes that have been previously investigated and reported under this program (i.e., specifically 1.20M LiPF₆ in EC+EMC+MB (20:20:60 vol %) + 4% FEC and 1.20M LiPF₆ in EC+EMC+MB (20:20:60 vol %) + 2% VC). Excellent cycle life has been obtained with these cells, which contain wide operating temperature range electrolytes, and they have completed over 9,200 cycles to-date (on test for over 3 years) and have displayed comparable performance to the baseline electrolyte (with over 78.7% of the initial capacity being displayed). As previously reported, these cells (i) have exhibited excellent rate capability over a wide temperature range (down to -60°C), (ii) were demonstrated to have dramatically improved power capability compared with the baseline (at -30 and -40°C), and (iii) have been shown to have good cycle life performance up to +60°C. We also continue to evaluate commercial-of-the-shelf (COTS) A123 cells which are being subjected to partial depth of discharge (DOD) cycling, ranging from 30% to 60% DOD, as reported last quarter. This testing was originally initiated under a NASA-IPP program in collaboration with A123 Systems, Inc. Under the current program, we have continued the testing and have provided data to NREL in support of their in-house modeling program.

Publications:

1. M. C. Smart, M. R. Tomcsi, L. D. Whitcanack, B. V. Ratnakumar, M. Nagata, and V. Visco, "The Use of Methyl Propionate-Based Electrolytes with Additives to Improve the Low Temperature Performance of LiNiCoAlO₂-Based Li-Ion Cells, 224th Meeting of the Electrochemical Society, San Francisco, October 2013.

2. F. C. Krause, C. Hwang, B. V. Ratnakumar, M. C. Smart, D. W. McOwen and W. A. Henderson, "The Use of Methyl Butyrate-Based Electrolytes with Additives to Enable the Operation of Li-Ion Cells with High Voltage Cathodes over a Wide Temperature Range", 224th Meeting of the Electrochemical Society, San Francisco, October 2013.
3. M. C. Smart, B. V. Ratnakumar, and L. D. Whitcanack, "Development of Low Temperature Electrolytes for Lithium-Ion Batteries", Advanced Automotive Batteries Conference, Pasadena, CA, February 5, 2013.
4. M. C. Smart, C. Hwang, F. C. Krause, J. Soler, W. C. West, B. V. Ratnakumar, and K. Amine, "Wide Operating Temperature Range Electrolytes for High Voltage and High Specific Energy Li-Ion Cells", ECS Transactions, accepted.
5. M. Jun, K. Smith, E. Wood, and M. C. Smart, "Battery Capacity Estimation of Low-Earth Orbit Satellite Application", *International Journal of Prognostics and Health Management*, ISSN2153-2648, 2012 009.

The work described here was carried out at the Jet Propulsion Laboratory, California Institute of Technology, under contract with the National Aeronautics and Space Administration (NASA).

TASK 1

Battery Cell Materials Development

Project Number: 1.2.2 (ES029)

Project Title: Scale-up and Testing of Advanced Materials from the BATT Program

Lead PI and Institution: Vince Battaglia, Lawrence Berkeley National Laboratory

Barrier: Cost is too high (energy density needs to be increased); life is short of 15 year target.

Specific Objectives: (i) Identify materials in the BATT Program that are ready for enhanced screening diagnostics, (ii) provide feedback on cell performance attributes to BATT researchers so that they may improve their materials, and (iii) provide information to the ABR Program about materials that provide significant improvements over the baseline chemistry, ABR₁.

General Approach: Work with BATT PIs in deciding what materials are ready for scale-up and enhanced testing and diagnostic evaluation in full cells. Once materials are identified, decide on the best approach for increasing the quantity of the material to approximately 10 g (1 ml if it is electrolyte). Prepare laminates of the material and test in coin cells against Li. Based on initial test results, decide on best vehicle application for the material, design the electrodes for that application, and perform long-term cycling tests. Provide comparisons to ABR Program baseline materials and cells.

Current Status as of October 1, 2012: Five Ni-spinel materials, including three from MIT and UT, were tested for rate capability to the same cut-off voltages in half- and full-cells. All but one of the materials consisted of cations in a disordered state. The one ordered material showed the lowest rate capability when tested against Li metal. When the materials were tested against graphite, the cells displayed worse rate performance than against Li. Four electrolytes were tested in graphite/Ni-spinel cells. The electrolyte with FEC showed the best rate capability. Electrolytes from CWRU and URI were tested in graphite/NCM cells. All of the electrolytes showed improved cycling performance when compared with 1 M LiPF₆ in EC:DEC 1:2.

Expected Improvement by September 30, 2013: Will have identified at least five more BATT Program materials that should or should not undergo further testing. There will be an emphasis on electrolytes and anodes as these projects have been running for four and three years, respectively. Results of this analysis will help guide BATT PIs and BATT management with regard to their approach to future RFPs

Schedule and Deliverables: Attend review meetings and present interim results on the scale-up of BATT Program materials (November 2011, February 2012, August 2012) and in Quarterly Reports.

Milestone:

Battery design, performance, and cycling characteristics of multiple materials from the BATT Program and for the $\text{LiNi}_{1/2}\text{Mn}_{3/2}\text{O}_4$ system will be reported on at the DOE Annual Merit Review (May 2012).

PLAN TO ACHIEVE DELIVERABLES

At the 2013 DOE AMR, discussions were held with representatives from NEI, the supplier of the baseline material used in the BATT, High-voltage, Ni-spinel Focus Group. They agreed to send us their latest material and promptly did so. This quarter the results of the preliminary analysis of this latest material are reported.

The physical characterization of this material included SEM, particle size analysis, and a measure of its surface area *via* the BET method. The SEM not only revealed that the particles are on the order of a few microns in diameter and consist of stacked crystal planes, but also provided no indication that these particles consist of smaller primary particles. The particle size analysis indicated a fairly tight particle size distribution: $d_{10} = 4.2$ microns and $d_{90} = 11.8$ microns. The mean particle size was measured at 6.6 microns with a standard deviation of 3.5 microns. The surface area was measured at $0.45 \text{ m}^2/\text{g}$, which is consistent with a particle diameter of 3.0 microns. It is typically found that the BET-derived diameter is approximately 1/3 the size as indicated by the PSA measurement, and this characteristic is attributed to a rough particle surface.

A cell of relatively low capacity, approximately $0.65 \text{ mAh}/\text{cm}^2$, was constructed for electro-chemical characterization. The initial tests indicated that the material has a first-cycle coulombic efficiency of 94.1 % and a discharge capacity of $133 \text{ mAh}/\text{g}$ between 4.9 and 3.5 V. Of this capacity, 88.5 % was accessible above 4.3 V.

This low specific-area capacity density cell demonstrated high rate performance as expected. A modified Peukert plot of cell discharge capability for three different loadings is provided in Fig 1. It is clear that a C/2 discharge rate is within the capability of all three of these electrodes where mass transfer limitations are not a factor.

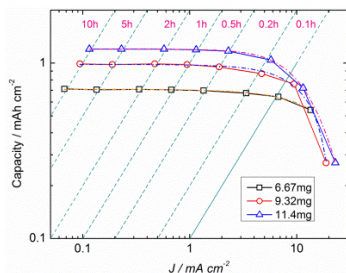


Figure 3. Capacity versus current for three loadings.

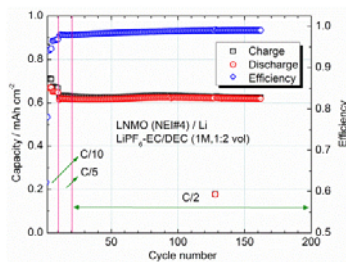


Figure 2. Capacity and efficiency versus cycle

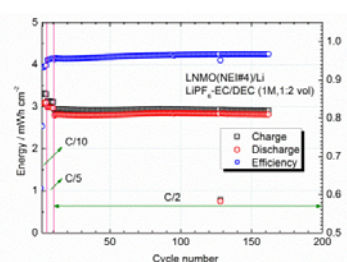


Figure 1. Energy and efficiency versus cycle number.

The half-cell capacity between 3.5 and 4.95 V *versus* cycle number is provided in Fig 2. With a large operational voltage range, one may not expect much capacity fade, and for this reason the energy of the cell *versus* cycle number is also provided (Fig 3.) These data include the impedance rise of both the cathode and lithium counter electrode. Since these data show very little energy decline, it is clear that there is very little impedance rise in this cell over 150 cycles. All data were acquired from a cell with a standard electrolyte of 1 M LiPF₆ in EC:DEC, 1:2. As indicated previously, the problem with this chemistry is not its high-voltage instability but the effects this chemistry has on graphitic anodes. Those data will be provided in the next quarterly.

TASK 1

Battery Cell Materials Development

Project Number: CPS Project 18502, CPS Agreement 23060, ORNL FWP CEVT110 (ES164)

Project Title: Overcoming Processing Cost Barriers of High Performance Lithium Ion Battery Electrodes

Project PI, Institution: David Wood, Oak Ridge National Laboratory

Collaborators by Category:

- National Laboratories: Argonne National Laboratory, Sandia National Laboratories
- Battery Manufacturers: Dow Kokam, A123 Systems, Navitas Systems
- Material Suppliers: ConocoPhillips, Phostech Lithium, TODA America, Timcal, JSR Micro, Solvay Specialty Polymers, Arkema
- Equipment Manufacturer: Frontier Industrial Technology

Project Start/End Dates: 10/1/11 to 9/30/14

Objectives: Electrode suspensions for lithium ion batteries are currently formulated using expensive polyvinylidene fluoride (PVDF) binder and toxic, flammable n-methylpyrrolidone (NMP) solvent. It is desirable to replace these components with water and water-soluble binders, but methods of mass production of these suspensions are currently underdeveloped. The major problems with aqueous electrode dispersions are: 1) agglomeration of active phase particles and conductive carbon additive; 2) poor wetting of the dispersion to the current collector substrate; and 3) cracking of the electrode coating during drying. NMP based processing also has the inherent disadvantages of high solvent cost and the requirement that the solvent be recovered or recycled. Initial projections of the minimum cost savings associated with changing to water and water-soluble binder are 70-75%, or a reduction from \$0.210/Ah to \$0.055/Ah. The objective of this project is to transform lithium ion battery electrode manufacturing with the reduction or elimination of costly, toxic organic-solvents.

Approach: Fabrication of composite electrodes via organic (baseline) and aqueous suspensions will be completed. A focus will be placed on the effect of processing parameters and agglomerate size on the aqueous route cell performance and microstructure of the composite electrode. Several active anode graphite and cathode (NMC, LiFePO₄, etc.) materials will be selected with various water-soluble binders. The conductive carbon additive will be held constant. Rheological (viscosity) and colloidal (zeta potential) properties of the suspensions with and without dispersant will be measured with a focus on minimization of agglomerate size. These measurements will show the effects of agglomerate size and mixing methodology on suspension rheology and help determine the stability (i.e. ion exchange processes across the surfaces of various crystal structures) of active materials in the presence of water. Composite

electrodes will be made by tape casting and slot-die coating, and the drying kinetics of the electrodes will be measured by monitoring the weight loss as a function of time and temperature. Solvent transport during drying will also be monitored as a method to control electrode morphology, porosity, and tortuosity. Electrode microstructure and surface chemistry will be characterized and correlated with cell performance. Electrochemical performance of electrode coatings made from the various suspensions will be supplied to ORNL's strategic industrial partners for external validation in large cell formats.

Improved cell performance with reduced processing and raw material cost will be demonstrated using pilot-scale coatings. At ORNL coin cells will be tested and evaluated for irreversible capacity loss, AC impedance, capacity vs. charge and discharge rates, and long-term behavior through at least 500 charge-discharge cycles. Half cells, coin cells, and pouch cells will be constructed and evaluated. The coin cells will be used for screening and coarse evaluation of different suspension chemistries and coating methodologies. A fine tuning of these research areas will be completed using ORNL pouch cells and large format cells with ORNL's industrial partners. Electrode coatings will be produced on the ORNL slot-die coater and supplied in roll form to the industrial partners for assembly into large format cells.

Electrode morphology will be characterized by scanning electron microscopy (SEM) and TEM. The bulk structure and surface of the active materials will be characterized using XRD and XPS, respectively.

FY13 Milestones:

- 1) Complete half-cell, full coin cell, and pouch cell round robin testing with ANL and SNL with CP A10/A12 and Toda NCM 523 electrochemical couple for NMP/PVDF based dispersion chemistry (Complete).
- 2) Match full coin cell performance through 100 cycles (0.2C/-0.2C) of aqueous suspension and water-soluble binder to NMP/PVDF based suspensions for CP A10/A12 and Toda NCM 523 electrochemical couple (June 2013 – delayed to August 2013).
- 3) Match pouch cell (≥ 3 Ah capacity) performance through 100 cycles (0.2C/-0.2C) of aqueous suspension and water-soluble binder to NMP/PVDF based suspensions for CP A10/A12 and Toda NCM 523 electrochemical couple (September 2013).

Financial data: \$300k/year (FY12-FY13)

PROGRESS TOWARD MILESTONES

Summary of work in the past quarter related to milestones (1)-(3)

1. Assembled and tested 1.3-Ah pouch cells with VTO Applied Battery Research (ABR) baseline TODA NMC 532 cathode and ConocoPhillips (CP) A12 graphite anode:

CP A12 anode (A12/super P Li carbon/Kureha 9300 PVDF=92/2/6 wt fraction) and NMC 532 (NCM 523/Denka carbon black/Solvay 5130 PVDF=90/5/5 wt fraction) were

fabricated at the ORNL Battery Manufacturing Facility (BMF). The areal weights of NMC 532 and A12 electrodes were 11.49 mg/cm^2 and 7.12 mg/cm^2 , respectively. The active areas of the single-sided cathode and anode were 47.3 cm^2 and 50.1 cm^2 , respectively. Assuming capacities for NMC 532 and A12 to be 160 mAh/g and 320 mAh/g , respectively, the electrode balance was 1.34 N/P. The separator used was Celgard 2325, and the electrolyte was 1.2 M LiPF_6 in EC/DEC (3/7 wt).

Figure 1 shows an example of a NMC/A12 pouch cell and pouch cell holder. The holder's purpose is to apply compression to the batteries during testing, which is critical for good cell performance. The 1.3-Ah pouch cell demonstrated a normal voltage profile, as shown in Figure 2. Formation cycling was performed at C/20 for 3 cycles, followed by repeated C/10 discharging for capacity fade, which is shown in Figure 3 (test is still ongoing). The cell demonstrates outstanding Coulombic efficiency ($>99\%$) and remains at $>95\%$ capacity through 50 cycles.

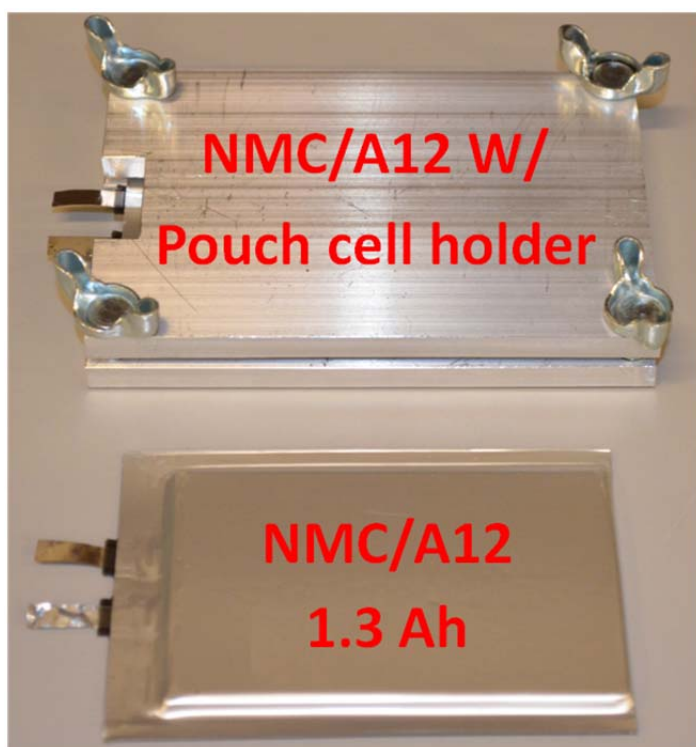


Figure 1. 1.3 Ah-NMC/A12 pouch cell.

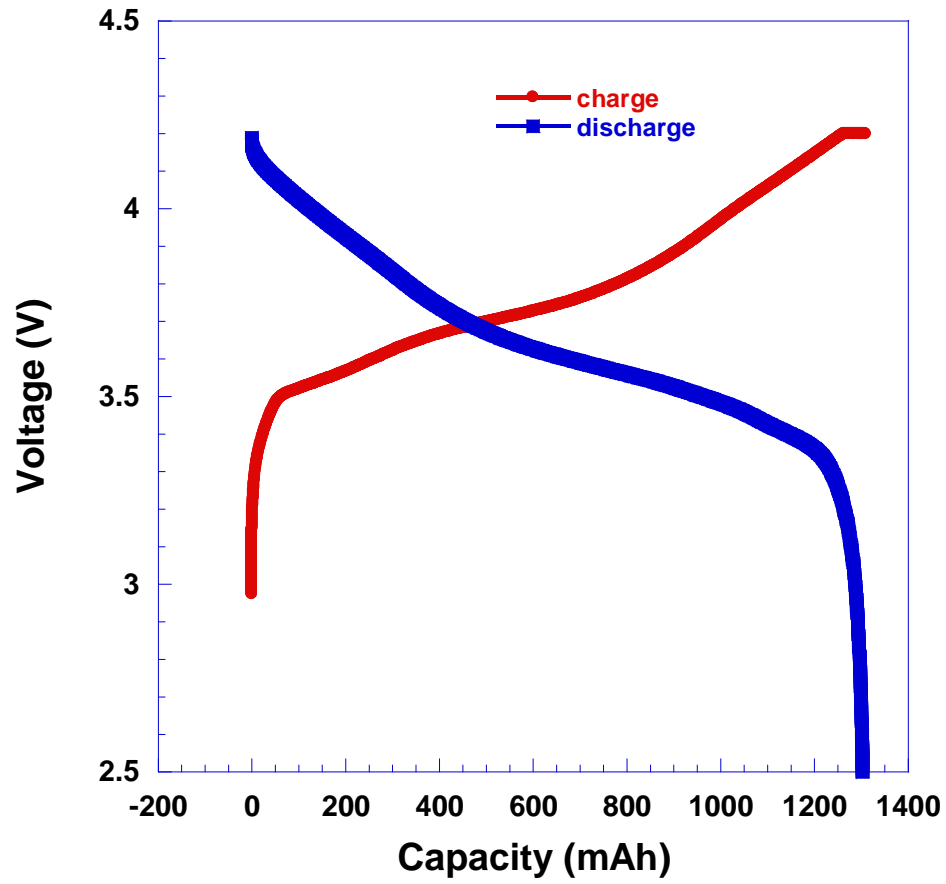


Figure 2. Voltage profile of the 1.3 Ah-pouch cell.

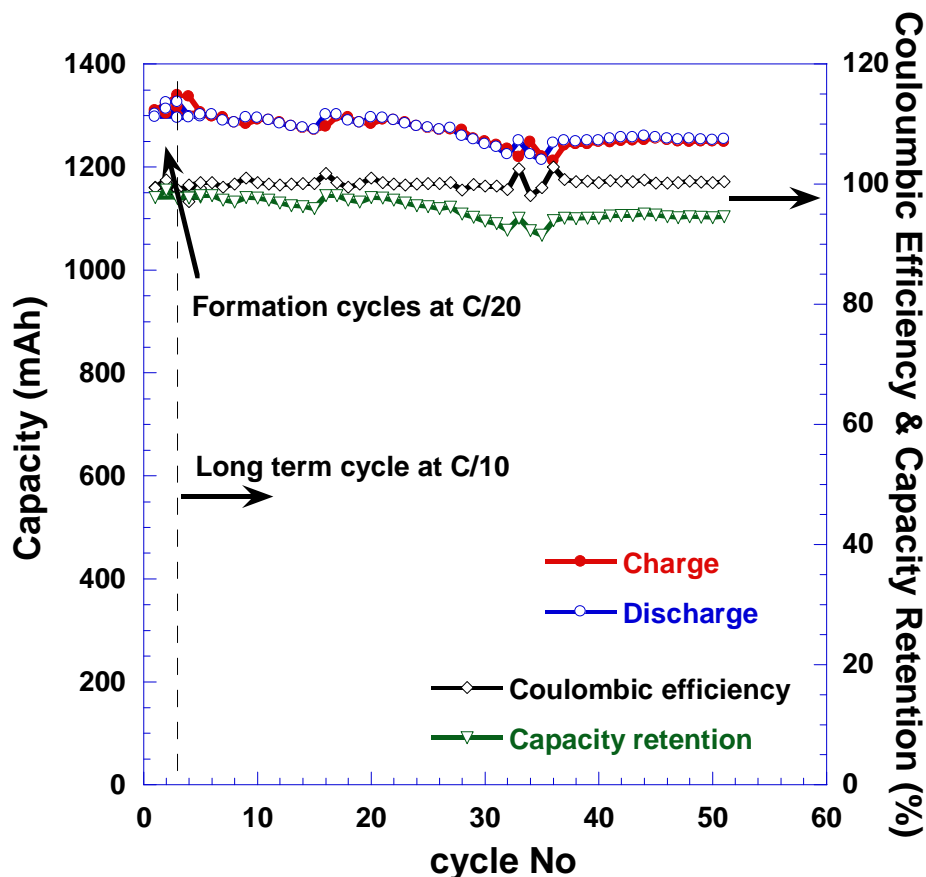


Figure 3. Cycling performance of 1.3 Ah-pouch cell.

2. Drying study on NMC 532 cathodes via water-based processing:

How to efficiently remove residual water from electrodes has been a persisting problem for electrode manufacturers with respect to aqueous electrode processing. ORNL and its industrial partner have demonstrated extremely low capacity fade with large-format pouch cells with LiFePO_4 over 1000 high-rate charge-discharge cycles when water was removed to below 500 ppm before cell assembly. It was demonstrated in the previous quarterly report that water content in a NMC 532 cathode, which was fabricated through water-based processing and pre-dried in seven convective-air zones up to 90°C immediately following the coating step, was 170 ppm when the NMC 532 cathode was further dried at 90°C for 2 hours under 68 kPa abs (secondary drying). Furthermore, residual moisture content in NMC 532 cathodes was evaluated under various drying temperatures and correlated to cell performance using Karl Fischer titration. The cathodes were dried at 80°C , 100°C , 110°C , and 120°C for 2 h without vacuum. The NMC 532 cathode was composed of NMC 532/Denka carbon black/TRD202A/carboxymethyl cellulose (90/5/4/1 wt fraction). As shown in Figure 4, the water content dropped from 625 ppm to 45 ppm when the temperature was increased from room temperature to 120°C .

The NMC 532 cathodes dried under various temperatures were assembled into half coin cells with lithium metal as the counter electrode. Three cells were assembled and tested under each condition. The C-rate was calculated based on $1C = 160 \text{ mA}$. Five charge-discharge cycles were acquired at each C-rate. Figure 5 shows the average rate performance of these cells at various drying temperatures. The capacities of NMC 532 dried at $\sim 25\text{-}110^\circ\text{C}$ were comparable and within the performance error bars, which means the effect of residual moisture on the NMC 532 cathode is similar. However, the NMC 532 dried at 120°C exhibited superior rate performance, especially at $<10C$. The rate performance was even higher than that from NMC 532 via NMP processing with secondary drying at 90°C . Thus, NMC 532 cathodes should be dried under at least 120°C for 2 h without vacuum to mitigate the detrimental effect of residual moisture on cell performance.

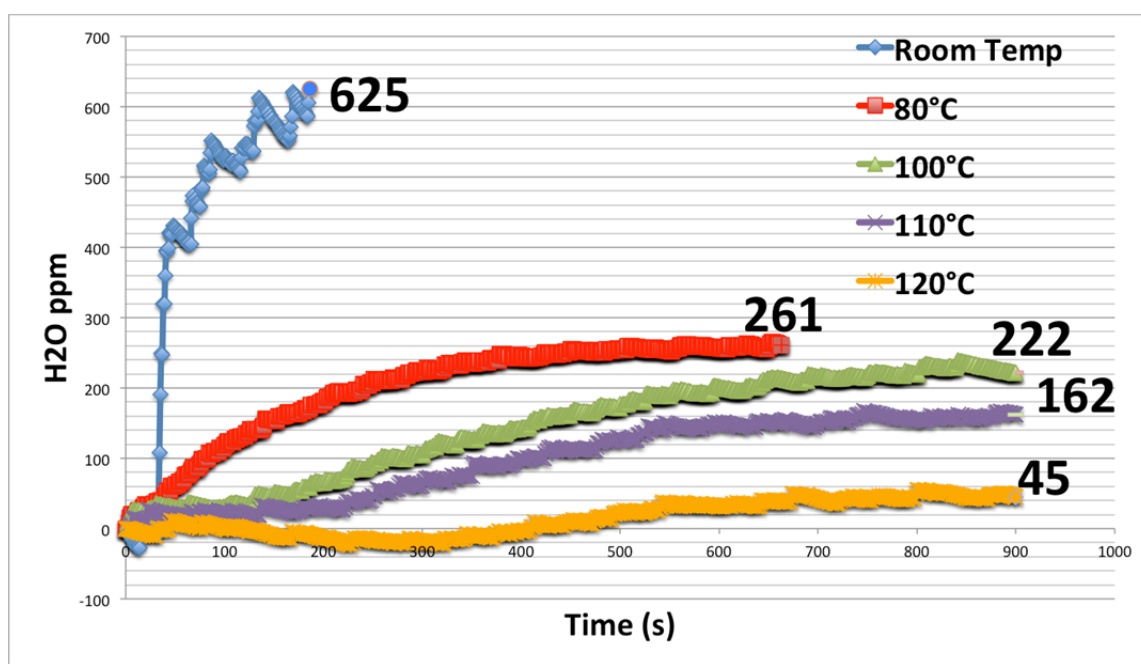
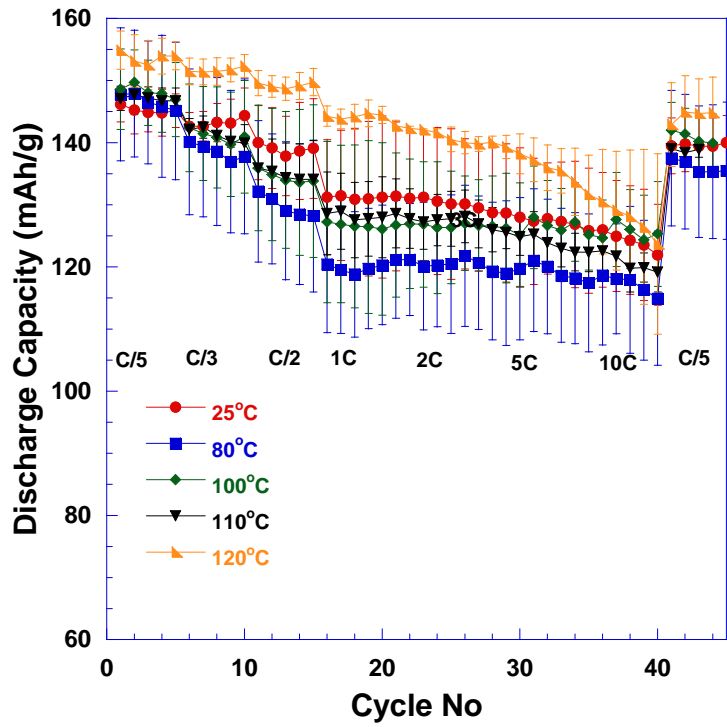


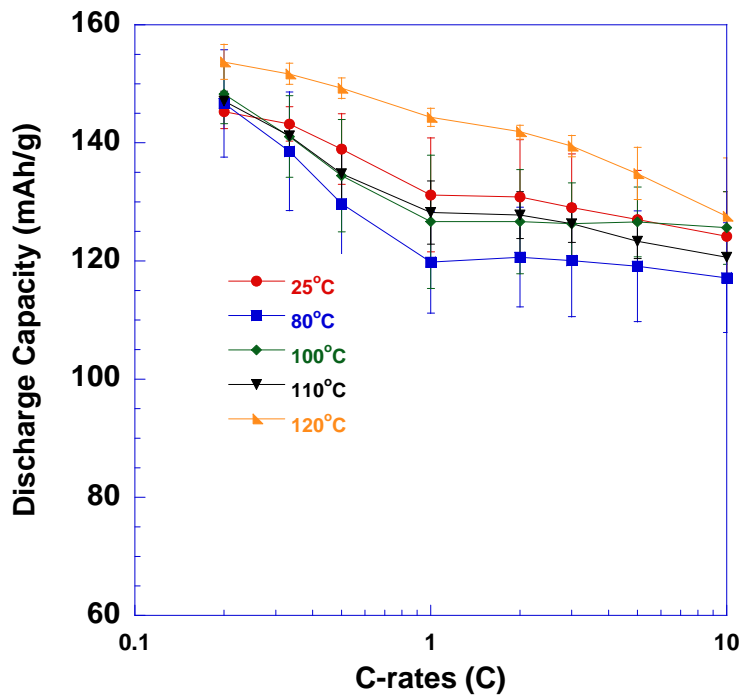
Figure 4. Residual water content of NMC 532 cathode after water-based electrode processing (measured by Karl Fischer titration).

3. Future work:

NMC 532 cathodes will be fabricated with various water soluble binders using the ORNL slot-die coater and aqueous processing. Full cells with NMC 532 cathodes made from water-based processing and A12 anode from both NMP-based and water-based processing will be tested and the performance matched to NMC 532/A12 full cells made from NMP-based processing. Pouch cells sized to 3 Ah will be assembled and tested to demonstrate pilot-scale proof-of-concept for the aqueous electrode processing methodology.



(a)



(b)

Figure 5. Comparison of NMC 532 cathode rate performance under various drying temperatures: a) average discharge capacity of 3 cells at each cycle and b) average discharge capacity of 3 cells and 5 cycles each as a function of C-rate.

Publications, Reports, Intellectual Property or Patent Application filed this quarter.

1. J. Li, B. Armstrong, J. Kiggans, C. Daniel, and D. Wood, "Optimal Polyethyleneimine Concentration and Mixing Sequence for LiFePO₄ Aqueous Nanoparticle Dispersions", *Journal of Colloids and Interface Science*, **405**, 118-124 (2013).
2. Claus Daniel, Debasish Mohanty, **Jianlin Li**, and David Wood, "Cathode materials review" submitted to *AIP Advances*.
3. Andrew Henry, **Jianlin Li**, Debasish Mohanty, David Wood, and Claus Daniel "Drying study on lithium-ion battery cathode", Volkswagen distinguished scholars program 2013 final poster presentation, Oak Ridge, TN, August 8, 2013.
4. Blake Griffey, **Jianlin Li**, and Claus Daniel "Effect of various binder materials on LiNi_{0.5}Mn_{0.3}Co_{0.2}O₂ (NMC532) cathode performance", Volkswagen distinguished scholars program 2013 final poster presentation, Oak Ridge, TN, August 8, 2013.
5. Michael Neil Brown and **Jianlin Li**, "Investigating of water soluble conducting binders for enhancing the lithium-ion battery cathode performance", Volkswagen distinguished scholars program 2013 final poster presentation, Oak Ridge, TN, August 8, 2013.

TASK 1

Battery Cell Materials Development

Project Number: ES162

Project Title: Development of Industrially Viable Battery Electrode Coatings

Project PI, Institution: Robert Tenent (PI), NREL

Collaborators (include industry): Chunmei Ban (NREL), Steven George and Robert Hall (University of Colorado, Boulder), Chris Orendorff (Sandia National Laboratory), Bryant Polzin (Argonne National Laboratory), Claus Daniel, David Wood and Jianlin Li (ORNL)

Project Start/End Dates:

Objectives: (1) Demonstration of Al₂O₃-based Atomic Layer Deposition coatings for improved cycling durability and abuse tolerance using standard electrode materials currently employed within the ABR program. (2) Design of an in-line atmospheric pressure atomic layer deposition (AP-ALD) system to demonstrate a process that may easily and inexpensively be integrated into the existing industrial Li-ion electrode fabrication lines.

Approach: Previously obtained results indicate that atomic layer deposition (ALD) can be used to form thin and conformal coatings on electrode materials that lead to both increased cycling lifetime, especially at high-rate, as well as abuse tolerance (e.g. stable cycling at high temperature and/or high voltage). This project will initially focus on using existing deposition capabilities to demonstrate an Al₂O₃-based ALD protective coating process for materials that are already commercially available at large-scale or are under advanced study within the VTP-EERE programs. This will include both anode and cathode materials in order to facilitate full cell testing and abuse studies. Initially, testing will be performed at the coin cell level to establish a stable baseline for comparison to existing data. In a later phase of the project larger format electrodes will be coated for testing in both pouch and 18650 cells. Coatings will be demonstrated on electrode materials produced at NREL as well as from outside parties. Finally, testing will be conducted both at NREL as well as within collaborating laboratories via a “round robin” process to ensure quality of data and the development of robust and transferrable processes.

In addition to small-scale exploratory research on various possible coating/electrode combinations, design work will be conducted for the development of a deposition system that will allow in-line coating at atmospheric pressure using an “ALD-like” process. The ultimate goal is to demonstrate a process that can be inexpensively integrated into existing industrial Li-ion battery electrode fabrication lines.

Milestones:

- a) Continued supply of ABR collaborators with alumina ALD coated electrodes and materials
Due: On-Going
Status: In Progress

- b) Design and initiate construction of a deposition system capable of in-line AP-ALD on commercially relevant substrate sizes.
Due: September 2013
Status: On-Schedule

Financial data: Current Funding \$150K/year (project currently ending)

PROGRESS TOWARD MILESTONES (1 page)

(a) Summary of work in the past quarter related to milestone (a).

No new samples were prepared and sent to other ABR laboratories during this quarter. Earlier efforts focused on supplying ALD coatings to Argonne NL as a portion of the voltage fade project effort. Several samples were coated with a variety of thicknesses of aluminum oxide via ALD and tested at NREL using the Argonne voltage fade protocol. This data was supplied to Argonne as well as information required to publish a joint paper focused on the potential impact of surface coatings on the voltage fade phenomenon. There was unanimous agreement across all of the laboratories that while surface coatings can impact capacity fade issues, there is no appreciable effect on voltage fade for the HE5050 material due to surface coatings. NREL has previously supplied ALD coated NMC111 and graphite samples to Sandia NL for safety analysis and has recently received coated samples of NMC523 from Oak Ridge. There have been discussions on coating more samples for Sandia and ORNL, however it is unclear if that work will continue at this time.

(b) Summary of work in the past quarter related to milestone (b)

The NREL/CU team completed a refined design for an inline ALD reactor using what has been termed a “digital modular” approach. The new reactor is based on a rotating drum design in which a foil would be mounted on an internal drum that would rotate inside a second drum structure with slitted sides that would enable the mating of a variety of gas introduction and exhaust modules to enable in-line deposition. This new design allows a high degree of flexibility in terms of placement and configuration of gas introduction and purging manifolds. This enables a wide range of configurations and deposition parameters to be varied in a highly controlled fashion to enable Design of Experiment methods to be used for optimization. A key concern for the validity of the in-line ALD process is demonstration of the ability to uniformly coat highly porous substrates using an in-line process at substrate translation rates compatible with current battery manufacturing. This new system has been specifically designed to explore this experimental space.

New parts were designed and specifications defined for components of the new reactor design in conjunction with machine shop staff at CU-Boulder. Parts are currently being produced at that facility and supplied to the CU (George group) laboratories for assembly. Assembly of the reactor unit is on-going currently as parts are made available from the machine shop.

Publications, Reports, Intellectual property or patent application filed this quarter. (Please be rigorous, include internal reports--invention records, etc.)

Robert Tenent presented work to date as well as the initial “digital modular” design at the EERE VTO Annual Merit Review.

NREL PI's contributed along with fellow ABR PIs at Argonne and Oak Ridge to a manuscript entitled “Effect of Interface Modifications on Voltage Fade in $0.5\text{Li}_2\text{MnO}_3 \cdot 0.5\text{LiNi}_{0.375}\text{Mn}_{0.375}\text{Co}_{0.25}\text{O}_2$ Cathode Materials which is currently under review.

TASK 1

Battery Cell Materials Development

Project Number: 25194 (IV.B.2.5) (ES196)

Project Title: Evaluate ALD Coatings of LGCPI Cathode Materials and Electrodes

Project PI, Institution:

Shriram Santhanagopalan, National Renewable Energy Laboratory, Golden CO 80401

Collaborators (include industry):

Mohamed Alamgir, LG Chem Power Inc., Troy MI
Karen Buechler, David King, ALD Nanosolutions, Broomfield CO

Project Start/End Dates: June 2012 – June 2013

Objectives:

The objectives of this work are two-fold: i) to evaluate the scalability of the process to coat LG Chem Power Inc. (LGCPI) cathodes with alumina, using the Atomic Layer Deposition (ALD) technique, and ii) to demonstrate improvements in rate capability and life of ALDcoated LGCPI electrodes.

Approach:

LGCPI and NREL have collaborated to demonstrate the scalability of the ALD coating process over the last 12 months, and the benefits of ALD coatings for long term cycling and calendar life are being quantified.

- NREL received samples of baseline material to be coated from LGCPI.
- NREL carried out ALD coating of the samples with help from a subcontractor - ALD Nanosolutions.
- NREL fabricated cells from those samples for quick screening and feedback to ALD Nanosolutions.
- LGCPI evaluated cycling performance using large format pouch cells.

Milestones: Project deliverables and decision points. Milestones should clearly show progress towards your project objectives, including overcoming issues, and should clearly support achieving a significant improvement in cell energy density, safety, and/or cost. If your material or couple has known issues, please address some or all of them in your milestones.

- (a) Receipt and characterization of baseline material and electrodes, July 2012, Complete
- (b) ALD coating and characterization of baseline cathode powder, Sept. 2012, Complete
- (c) ALD coating of baseline electrodes, Dec. 2012, Complete
- (d) Pouch cell fabrication and long term evaluation, June 2013: Complete

Financial data: 110k (2012), 50k Sub-contract to ALD Nanosolutions
\$0 (2013)

Progress Towards Milestones:

The previous reports summarized the ALD coating of the Mn-rich material from LGCPI. Screening of the ALD parameters and some initial cell data were shown. The work during this quarter focused on pouch cell fabrication and long term testing at LGCPI.

ALD Nanosolutions had previously conducted a design of experiments study varying the number of ALD layers on this material. Pouch cells were fabricated from the batch that demonstrated the least drop in cell voltage (corresponding to minimal increase in cell impedance) while maintaining the improvements exhibited by the ALD coated material over the baseline.

The results for the cells fabricated using the baseline versus ALD coated material are shown at two different temperatures – there is a significant improvement in the cell performance. In particular, at 45°C the number of cycles before the cell reaches the same level of degradation for end-of-life (70% of initial capacity) is more than three times that for the baseline.

Future work, pending support, will include optimizing the coating process for the electrodes based on the sheet-electrode coating results from this quarter, and improvements to the recipe to build the cathodes from the ALD coated powders.

Publications, Reports, Intellectual Property or Patent Application filed this quarter:

None

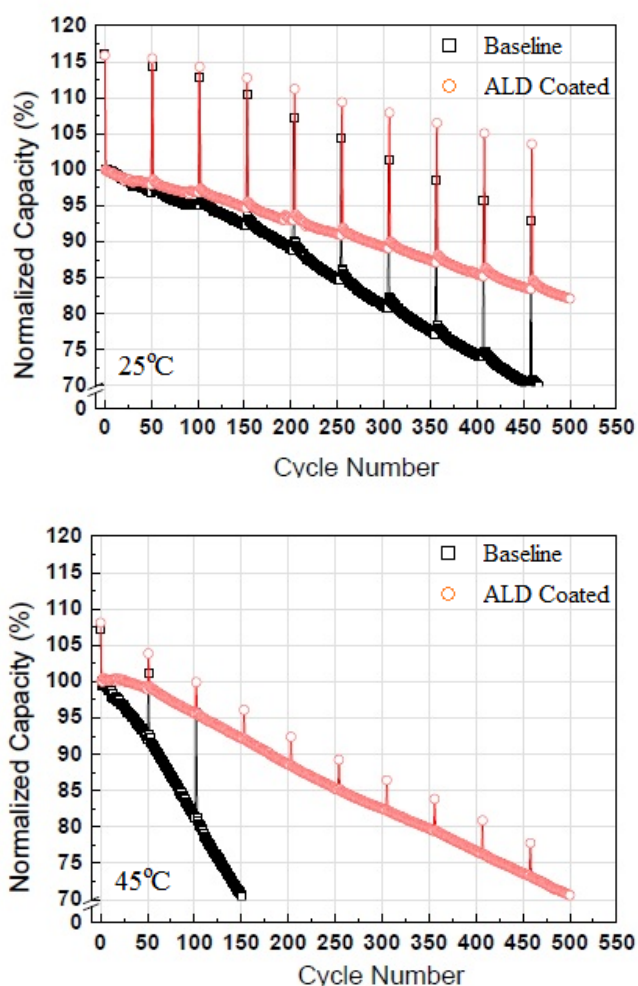


Figure 1. Cycling performance of ALD Coated cathodes tested at LGCPI

TASK 2

Calendar & Cycle Life Studies

Project Number: 1.1 (ES030)

Project Title: Cell Fabrication Facility Team Production and Research Activities

Project PI, Institution: Andrew N. Jansen, Argonne National Laboratory

Collaborators (include industry): Dennis W. Dees, Daniel P. Abraham, Kevin G. Gallagher, Wenquan Lu, Bryant J. Polzin, Stephen E. Trask, Nancy L. Dietz-Rago, Javier Barena, Qingliu Wu, Martin Bettge, Ye Zhu, Joseph J. Kubal, and Paul A. Nelson (Argonne National Laboratory)

Prof. Jai Prakash (Illinois Institute of Technology)

Prof. Ivan Petrov (University of Illinois)

Prof. Alex Wei (Purdue University)

Yan Li (University of Rochester)

Toda Kogyo

Phillips 66

JSR Micro

Zeon Chemicals

Materials Engineering Research Facility (MERF)

Post-Test Facility (PTF)

Electrochemical Analysis and Diagnostic Laboratory (EADL)

Project Start/End Dates: October 2012 / September 2014

Objectives: The overarching objective of this core-funded effort is to design, fabricate, and characterize high-quality prototype cells of at least 200-mAh capacity to enable a realistic and consistent evaluation of candidate chemistries in a time-effective manner. In order to achieve this main objective, it was necessary to divide this effort into interlinked sections designed to support the activities of the Cell Fabrication Facility (CFF). As with the CFF, each of these support sections (Materials Validation, Modeling, and Diagnostics) are designated specific goals and responsibilities. It is not the aim of this task to become a small battery manufacturer, but instead to become a laboratory research facility with cell production capabilities that adequately evaluate the merits and limitations of mid-to-long term lithium-ion chemistries in a close-to-realistic industrial format.

Approach: As new cell chemistries and systems progress, they may reach the point where they are considered for further development in larger prototype cells. When this happens, a limited quantity of these materials, along with their preliminary data, are transferred from the inventor or originator to the Materials Validation support section, where they will be evaluated to determine if they warrant production in prototype cells by

the CFF. The source of these materials (anodes, cathodes, electrolytes, additives, separators, and binders) may originate from the ABR and BATT Programs, as well as from other domestic and foreign organizations such as universities, national labs, and industrial vendors. Electrochemical couples with high power and energy density will be given extra priority.

Coin cells (2032 size) will be used for materials validation purposes with initial studies performed at room temperature or 30°C. After formation cycles, the coin cells will go through hybrid pulse power characterization (HPPC) testing, rate capability testing, and limited cycle life testing. Accelerated aging studies will also be performed at 45°C to 55°C for promising materials to give a preliminary indication of life. Where appropriate, the thermal abuse response will be studied using a differential scanning calorimeter. The key areas to monitor are the materials' influence on capacity, energy, power, and cycle/calendar life. The Materials Validation results will be used by the other support efforts, and if needed, by the Materials Engineering Research Facility (MERF) and the Post-Test Facility (PTF).

Once the materials' performance has been validated, promising cell chemistries will be recommended for further development by the CFF. Using the recommendations and results obtained by the Materials Validation, the CFF will initiate a prototype cell build that will include the generation of single-sided electrodes for the Diagnostics support effort. Diagnostics examines the new cell chemistries in detail using advanced electrochemical and analytical techniques, including the employment of micro-reference electrode cells. This information lays the foundation for the electrochemical Modeling support effort focused on correlating the electrochemical and analytical studies, in order to identify performance limitations and aging mechanisms. The Modeling effort supports the CFF through the development and utilization of efficient simulation and design tools for advanced lithium-ion battery technologies. These modeling tools cover a broad range of applications, from correlating analytical diagnostic results with electrochemical performance in small test cells to predicting the performance and cost of full size PHEV battery packs based on limited results.

If the results from Diagnostics still look promising, the CFF will begin fabrication of full cell builds using double-sided electrodes. The CFF at Argonne has the capability to make two prototype cell formats in their 45 m² dry room: pouch cells (xx3450 format, with capacity around 0.4 Ah) and 18650 cells. Pouch cells are anticipated to be easier to assemble, but they may suffer from bulging if gases are evolved during cell aging and cycling. 18650s, which are rigid containers, may be used if the pouch cell format is deemed unreliable due to gassing, or if higher capacity cells are needed (greater than 1 Ah). Central to this effort is a pilot-scale coating machine that operates with slurry sizes that range from 20 grams to a few kilograms. This is a key feature of the CFF that enables a professional evaluation of small quantities of novel materials. If needed, the MERF is available for scaling up materials for these prototype cell builds.

The main emphasis of the CFF will be to fabricate electrodes and prototype cells for calendar and cycle life studies. These cells will undergo rigorous electrochemical

evaluation and aging studies under the combined effort of the CFF and Argonne's Electrochemical Analysis and Diagnostic Laboratory (EADL). The Diagnostics effort will use advanced electrochemical and physicochemical diagnostic tools and techniques to identify factors that determine cell performance and performance degradation (capacity fade, impedance rise) on storage and on extensive deep-discharge cycling. The results of these tests are used to formulate data-driven recommendations to improve the electrochemical performance/life of materials and electrodes that will be incorporated in pouch- and 18650- type PHEV cells assembled in the CFF. After testing, the cells will be destructively examined by the Post-Test Facility that will interface with the Diagnostics effort to elucidate failure mechanisms in end-of-life cycled cells from CFF – the information generated will enable the design of cell chemistries that meet the performance, life and safety targets of PHEV cells. The CFF & Support effort will collect and share all results with other members of the ABR Program and to the materials origin. This information is then used to further improve the new chemistry, as well as future electrode and cell builds. The CFF may also provide this information and prototype cells to battery developers for their evaluation.

The general approach taken in the Modeling effort is twofold. First, spreadsheet based simulations are employed that determine the impedance behavior, available capacity, and thermal effects for general and specific cell, battery module, and battery pack designs. The design model calculates power and energy, weight and volume of materials and components, as well as their thermal performance. The model is also capable of performing simulations on multiple battery designs for comparison and optimization. The battery design model also includes a module that calculates battery costs by combining materials and components costs with manufacturing expenses based on a plant design.

The second part of the Modeling effort utilizes an electrochemical model that accurately describes all the pertinent physicochemical phenomena in the cell under study. Continuum based transport equations using concentrated solution theory describe the movement of salt in the electrolyte. Volume-averaging of the transport equations accounts for the composite electrode geometry. Electrode kinetics, thermodynamics, electronic migration, and diffusion of lithium in the active material particles are also included. Phase change in the active materials and detailed transport through the solid electrolyte interphase or SEI can also be included. Two versions of the electrochemical model have been developed (i.e. AC and DC) to describe the full range of electrochemical tests conducted on the advanced lithium-ion battery technologies.

Milestones:

- (a.) Obtain viable supplier of battery grade silicon powder, March, 2013 (Delayed)
- (b.) Assess influence of LiDFOB, LiBOB, and HFIP electrolyte additives for HE5050 cathode, May, 2013 (Delayed)
- (c.) Evaluate MERF cathodes ($\text{Li}_{1.25}\text{Ni}_{0.3}\text{Mn}_{0.62}\text{O}_2$) based on hydroxide and carbonate precursors, July, 2013 (Delayed)

- (d.) Add silicon-graphite, LiFePO₄, LiCoO₂, and hard carbon to electrode library,
July, 2013 (Delayed)
- (e.) Fabricate pouch cells based on silicon-graphite anodes and LMR-NMC cathodes,
August, 2013 (Delayed)
- (f.) Validate performance of advanced battery materials,
September, 2013 (On schedule)
- (g.) Determine sources of impedance rise and capacity fade during extensive cycling of
cells containing various electrochemical couples, September, 2013 (On schedule)
- (h.) Recommend solutions that can improve the life of high energy LMR-NCM electrodes
and cells by 30% at 30°C and 15% at 55°C, September, 2013 (On schedule)
- (i.) Enhance battery design and cost model concentrating on designs for advanced
lithium-ion electrochemical couples, September, 2013 (On schedule)
- (j.) Advance development of electrochemical models focusing on the impedance of
LMR-NMC positive electrodes, September, 2013 (On schedule)

Financial data: \$2500K / FY13 (subcontracted \$30K to Purdue University, \$70K to Illinois Institute of Technology, and \$30K to University of Rochester)

PROGRESS TOWARD MILESTONES

(a) Summary of work in the past quarter related to milestone (a).

Limited studies continued with the silicon powder obtained from Nanostructured and Amorphous Materials Incorporated (NanoAmor). This material is a 130 nm silicon powder (spherical with some nanowires mixed in). While additional validation needs to be performed, this appears to be the best candidate to date to use for silicon anodes for pouch cells; it cycles better than most other silicon powders cycled thus far, and sizable quantities of this material can be obtained at reasonable prices without any limitations on its distribution and data reporting.

One observation made when using the NanoAmor silicon powder is that the particles tend to agglomerate during the mixing process for small batches of slurry. The inhomogeneous properties of these laminates will most likely affect long term cycling when placed in full cells. This issue most likely draws from the low amount of shear put upon these particles from either using a mortar and pestle, or the commonly used Thinky mixer. Future work involves creating a procedure that will maximize dispersion of these silicon particles with use of different mixers available along with trying a variety of solvents to improve dispersion.

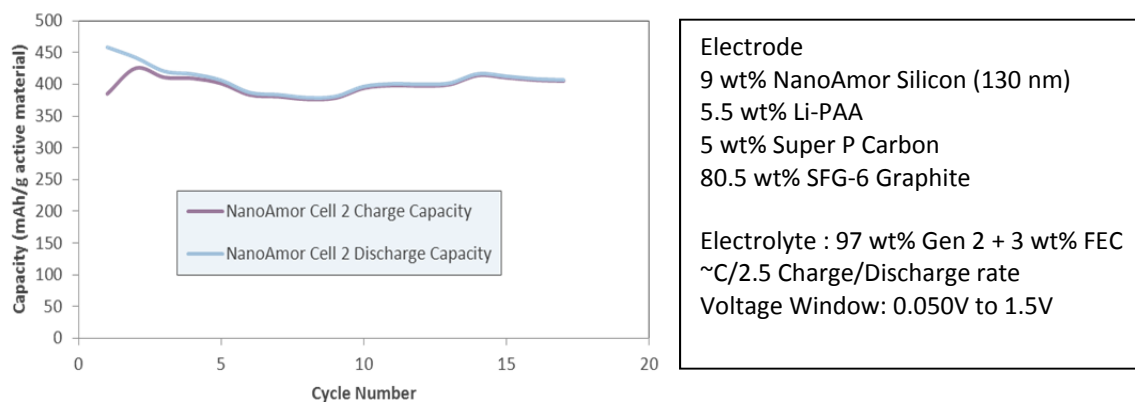


Figure 1. Coin cell data for an anode made using the NanoAmor silicon powder. These cells were able to maintain capacities of over 400 mAh/g at a C/2.5 rate.

In addition to testing commercial silicon materials obtained thus far, collaborations are ongoing with companies to make improved silicon/graphite composite electrodes. A second sample of silicon was received from Electrochemical Materials (EM), who has put their proprietary organic coating on the silicon that allows it to cycle when using PVDF as a binder in a silicon/graphite composite electrode. Their improved coating also allows the particles to be coated in aqueous systems. A multitude of electrodes have been made with this new batch of powders, altering both the binder and the graphite. Currently, two different graphite powders are being used in conjunction with the EM powder. The first is the standard A12 (high power graphite) along with the less dense but more exfoliated SFG-6. A12 has been shown to underperform when mixed with silicon in aqueous systems, which is believed to be caused by improper binding to the graphite. However, since this silicon material can be made using PVDF (a binder which works well with the A12 graphite), this relationship needs to be further examined. In addition to testing PVDF, CMC (carboxyl methyl cellulose) is being tested as well per recommendation of EM.

A silicon graphene electrode from XG sciences was received and tested. The electrode consists of 70% Si/graphene active material, 20% graphene, and 10% PAA binder. The total loading, including graphene and binder, is about 1.15 g/cm². 1.2 M LiPF₆ in EC/EMC with additional 10% FEC additive was used as the electrolyte. The Li/Si-C half cell was initially tested between 10mV and 1V with C/10 rate at 30°C. The test results of two formation cycles are shown in Figure 2 below. The reversible specific capacity was determined to be over 2400 mAh/g from the weight of silicon graphene composite. The first cycle irreversible capacity loss was 17%. Rate performance tests were also conducted on the Li/Si-C half cell. The lithiation rate was fixed to C/5 rate and the delithiation rate varied from C/5 to 2C. Surprisingly, the silicon graphene composite electrode demonstrated excellent rate performance: no capacity drop was observed at even the 2C rate.

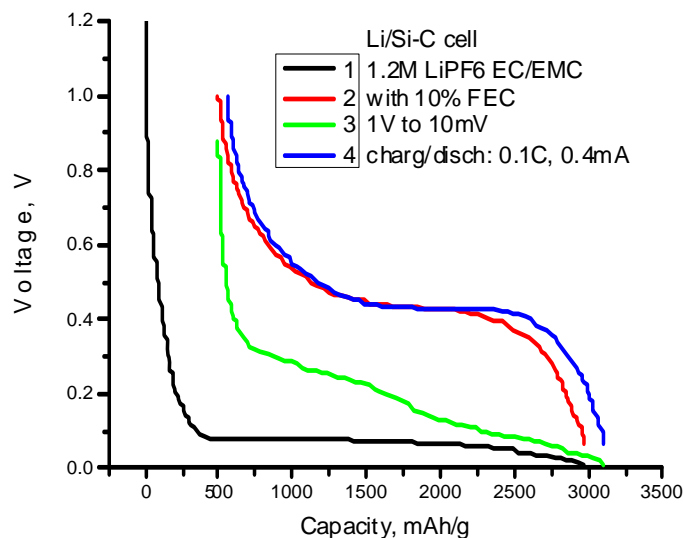


Figure 2. Voltage profile of Li/Si-C half cell during formation cycles.

(b) Summary of work in the past quarter related to milestone (b)

In previous quarterly reports, an issue was identified with additives behaving differently between pouch cells and coin cells. It is believed that the more elaborate formation process used for pouch cells is inadvertently causing the additives to be activated prematurely (and completely) at the negative electrode. This was in part due to the tap charge used to prevent copper corrosion in the pouch cells. In order to understand what effect the tap charge and 24h rest has on additive performance, a study was begun using coin cells. Initial tests are underway using the A12/HE5050 electrode couple in coin cells that are formed using the pouch cell formation process. A baseline set of data is being established that accounts for the effect of different electrode size configurations (matched 9/16" anode and cathode, or 14 mm cathode and 9/16" (14.3 mm) anode), as well as the ratio of electrolyte/additive to electrode area. Once it is established that the pouch cell conditions and performance can be replicated in coin cells, studies will begin with the targeted additives incorporated in the coin cell electrolyte. The formation process will then be adjusted to maximize the performance of the coin cells in a manner that will be later deployable in a pouch cell environment. After the formation and additive performance is optimized, the process will be confirmed in a pouch cell build.

(c) Summary of work in the past quarter related to milestone (c)

No significant activities on this milestone due to building shutdown.

(d) Summary of work in the past quarter related to milestone (d)

Materials are constantly being sought that are of interest to the battery R&D community. If warranted, several of these materials are then added to the electrode

library. The latest material that is ready to be made into electrodes is LiCoO_2 . The Materials Validation process has been completed on this material and an electrode has been designed for inclusion in the Electrode Library. Additional materials that are currently going through the Materials Validation process are as follows: Hanwah LFP, Toda 4V Spinel, Phillips 66 G8 graphite, Toda NCM 424, Toda HE5050 (5/13 10kg batch), Kureha Hard Carbon (J and S(F) grades) and MCMB (G-15) graphite. The electrochemical performance data on these materials will be used to design electrodes that will match those in the Electrode Library.

The electrochemical validation of LiFePO_4 powder from Hanwha was completed using lithium metal half cells. The electrode consisted of 84% LiFePO_4 , 4% SFG-6, 4% carbon black, and 8% PVDF binder. The loading was 9.3 mg/cm^2 . The electrode porosity was calculated to be 30% after calendaring. The electrolyte used in the half cell was 1.2 M LiPF_6 in EC/EMC without any additive. According to the formation cycle at a C/10 rate between 2.9 V and 3.8 V, the specific capacity during the 3rd formation cycle was determined to be 150 mAh/g. The irreversible capacity loss was about 4% during the 1st cycle. The rate performance test was also conducted on the half cells. The capacity delivered at the 2C rate was still more than 82% of the C/10 capacity.

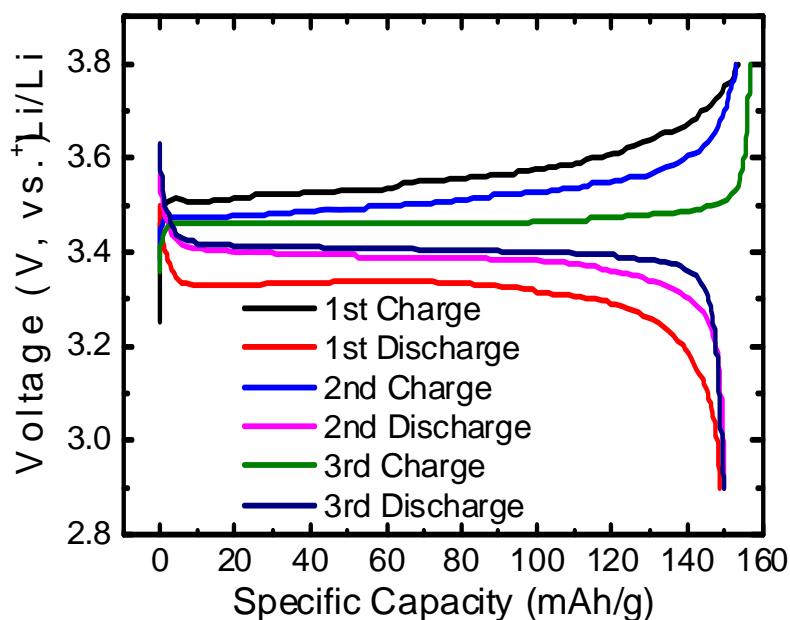


Figure 3. Voltage profile of Li/LiFePO₄ half cell during formation cycles.

(e) Summary of work in the past quarter related to milestone (e)

No significant activities on this milestone due to building shutdown.

(f) Summary of work in the past quarter related to milestone (f)

Each pouch cell build has consisted of multiple cells, for each variable tested, to provide statistically relevant data. Providing the statics of multiple cells being tested under the same variables is important. The data is simple to collect, but data processing can quickly become complex and time consuming. Effort has gone into utilizing Excel software to improve the data processing procedure. Excel macros and templates have been created in order to rapidly perform a significant number of consistently accurate automatic calculations for any size cell (i.e. coin cell, pouch cell, 18650, etc.), averaging of multiple data sets with sample standard deviation error bars, and creation of standard tables and plots for simplified data comparison. An Excel macro/template has been created for each of the main characterization tests used by the CFF, including: formation, rate study, HPPC, and cycle life testing. All the Excel macros/templates are accompanied with detailed work instructions.

The formation macro/template automatically plots the voltage profiles, capacity curves, and dQ/dV plots for up to 8 cells, along with a table of the first cycle efficiency and reversible capacity values (Table 1 and Figure 4). Both the individual cells and average processed data are available in the output.

Table 1. Capacity and efficiency values automatically calculated for formation testing (data provided from 8 pouch cells; CFF-B9A, “HE5050 LMR-NMC vs. A12 Graphite”).

	Cell #									
mAh/g	1	2	3	4	5	6	7	8	Average	Standard Deviation
1st C cap (mAh/g)	299	298	297	297	297	303	294	297	298	2.5
1st D Cap (mAh/g)	268	267	266	266	267	265	263	267	266	1.4
1st Cycle Eff (%)	90	90	90	89	90	87	90	90	89	0.8
Reversible C Cap (mAh/g)	268	267	268	267	268	273	264	268	268	2.1
Reversible D Cap (mAh/g)	266	265	266	266	266	267	262	266	265	1.2
Irreversible Cap Loss (mAh/g)	33	32	31	31	32	36	31	31	32	1.7
Irreversible Cap Loss (%)	11	11	10	10	11	12	11	11	11	0.5

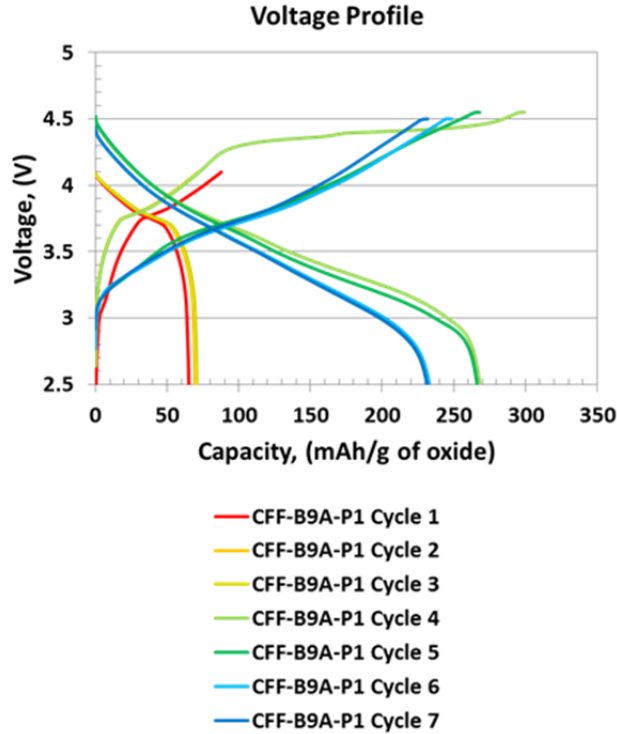


Figure 4. Typical voltage profile plot for an individual cell showing values for each cycle during the formation testing (“HE5050 LMR-NMC vs. A12 Graphite” pouch cell).

The rate study is an initial characterization test to determine a cell’s rate capability. The rate study macro/template automatically plots the voltage profiles, capacity vs. current, capacity vs. cycle number, averaging plots with trend lines for reasonable forecasting, a table of C-rates based on trend lines, and tables of capacities each cell obtained for each cycle. The macro can process (and average) up to 12 cells at one time. Both the individual cells and average processed data are available in the output. (Table 2 and Figure 5).

Table 2. Expected Discharge C-rates determined by the averaging of all the data with corresponding capacity values based on the rate study test results (data provided from 8 pouch cells; CFF-B9A, “HE5050 LMR-NMC vs. A12 Graphite”).

C-rate	mAh	mAh/g	mAh/cm ²
2C	409	196	2.42
1C	436	209	2.58
C/2	463	222	2.74
C/5	498	239	2.95
C/10	525	252	3.11

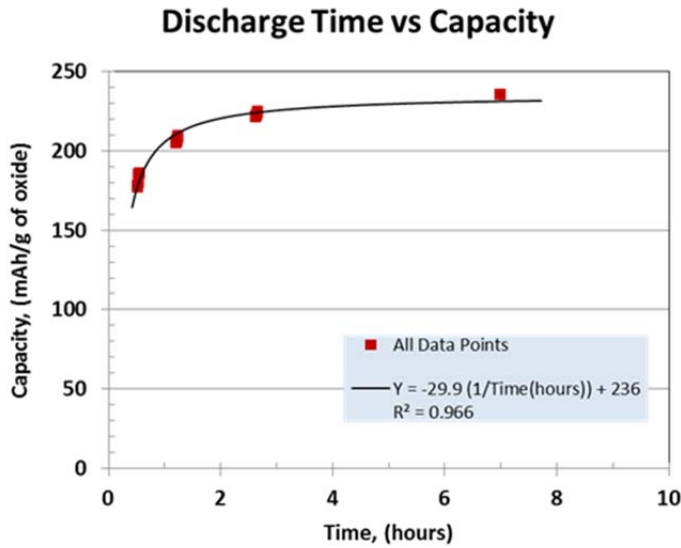


Figure 5. Typical discharge capacity plot of data from multiple cells showing an averaged trend line generated to predict an expected C-rate from the rate study test results (data provided from 8 pouch cells; CFF-B9A, “HE5050 LMR-NMC vs. A12 Graphite”).

The HPPC (hybrid pulse-power characterization) test is intended to determine dynamic power capability over the device’s usable voltage range using a test profile that incorporates both discharge and Regen (charge) pulses. The HPPC macro/template automatically plots the voltage profiles, area specific impedance (ASI) vs. open circuit voltage (OCV), ASI vs. depth of discharge (DoD) or as a function of pulse number, and ASI vs. time during pulse. The macro can process up to 8 cells at one time. Both the individual cells and average processed data are available in the output tab (Figure 6).

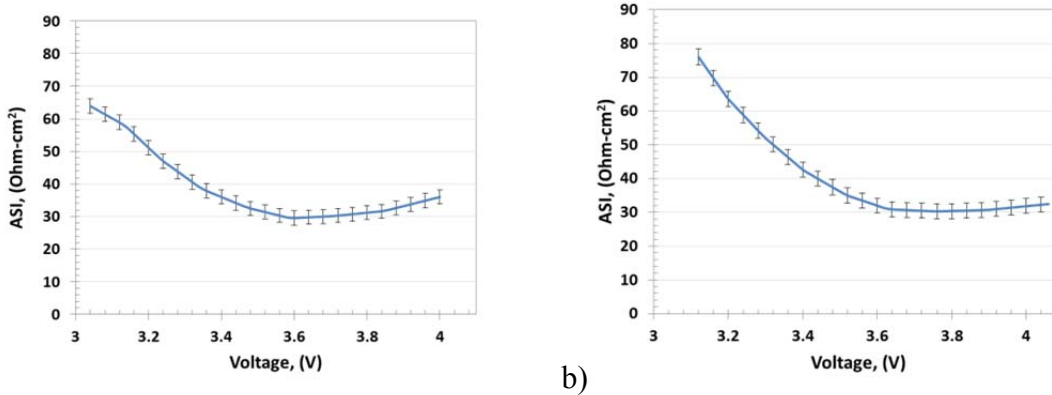


Figure 6. Typical HPPC ASI vs. OCV plots of average data with sample standard deviation error bars from multiple cells (data provided from 8 pouch cells; CFF-B9A “HE5050 LMR-NMC vs. A12 Graphite”) for a) charge and b) discharge.

The cycle life test is used to accelerate the aging of the cells by cycling at a C/2 rate while monitoring the capacity fade and impedance rise via scheduled HPPCs and

C/24 rates during cycling. The cycle life macro/template automatically creates multiple plots, including: capacity vs. cycle #, efficiency vs. cycle #, capacity retention vs. cycle #, energy and energy density vs. cycle #, energy retention vs. cycle #, ASI vs. depth of discharge (DoD) and voltage as a function of HPPC's performed throughout the cycle life, ASI vs. cycle # as a function of DoD, voltage vs. state of charge (SOC) as a function of cycle #, and dQ/dV vs. voltage as a function of cycle #. The macro processes only one cell at a time due to the large number of data points to be processed, and averaging of multiple cells takes place in a separate macro/template. The individual cell's processed data is available in the output tab (Figures 7 & 8). The cycle life macro/template processes the data in a matter of a couple minutes.

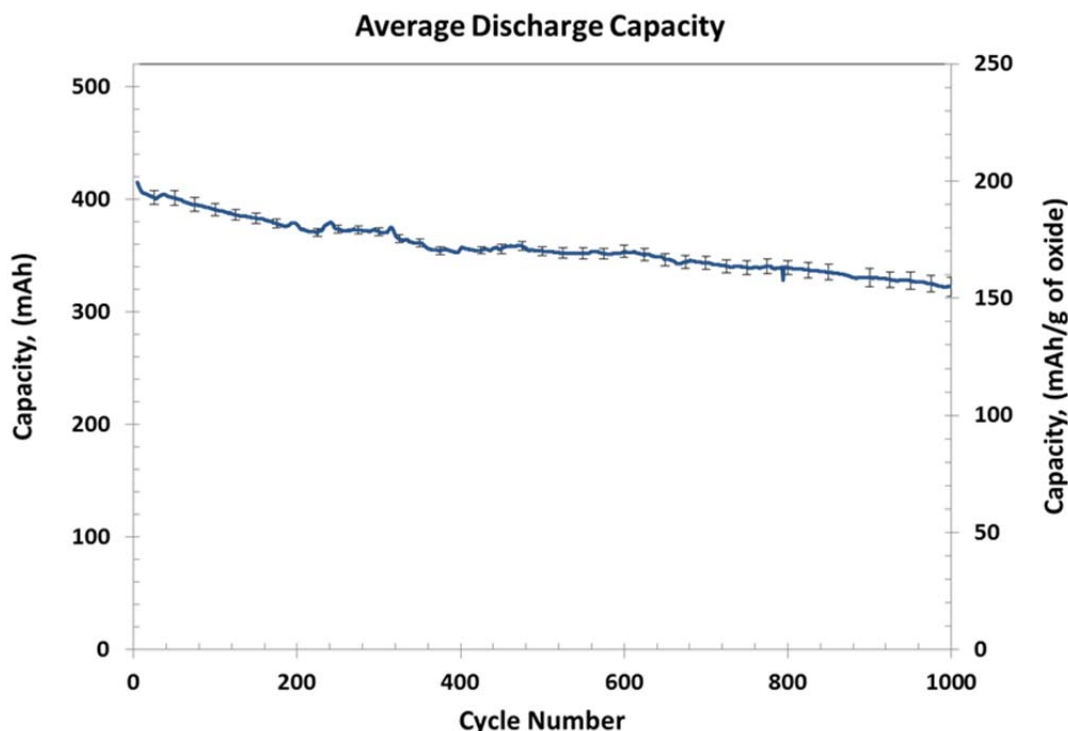


Figure 7. Typical discharge capacity vs. cycle number plot of average data with sample standard deviation error bars from multiple cells (data provided from 2 pouch cells; CFF-B9A, “HE5050 LMR-NMC vs. A12 Graphite”).

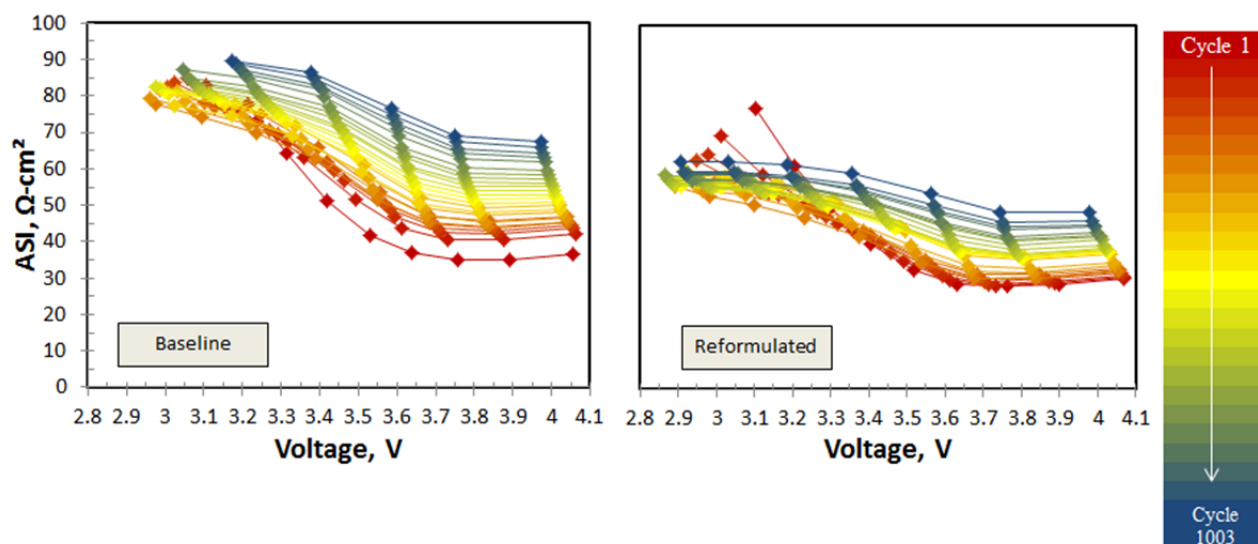


Figure 8. Example comparison plots exhibiting the powerful capabilities of the cycle life excel macro/template. The plots show the HPPC area specific impedance versus OCV, as a function of cycle life (color gradient) for “Baseline Cells” and “Reformulated Cells”. Note that the impedance is higher at lower voltages for both sets of cells. The impedance rise for the Reformulated cells is lower than that of the Baseline cells for the entire life of the cell (data provided from 1 Baseline pouch cell; CFF-B4A, “HE5050 LMR-NMC vs. A12 Graphite” and from 1 Reformulated pouch cell; CFF-B9A, “HE5050 LMR-NMC vs. A12 Graphite”).

(g) Summary of work in the past quarter related to milestone (g)

The ABR-1 positive electrodes contain 86 wt% $\text{Li}_{1.2}\text{Mn}_{0.55}\text{Ni}_{0.15}\text{Co}_{0.1}\text{O}_2$ (HE5050), 4 wt% SFG-6 graphite (Timcal), 2 wt% SuperP (Timcal) and 8 wt% PVdF (Solvay 5130). The ABR-1 negative electrodes contain ~90 wt% graphite (Conoco Philips A12), 6 wt% PVdF (Kureha KF-9300) and 4 wt% SuperP (Timcal). In previous reports we have shown that cell impedance rise is mainly governed by the positive electrode; impedance rise at the negative electrode is relatively small. Furthermore, cell capacity fade is believed to result from lithium trapping in the solid electrolyte interphase (SEI) of the negative electrode.

In order to elucidate the contribution of the negative electrode to full cell capacity loss, the cycling characteristics of cells containing $\text{Li}_{1.2}\text{Ni}_{0.15}\text{Mn}_{0.55}\text{Co}_{0.1}\text{O}_2$ -based positive and $\text{Li}_4\text{Ti}_5\text{O}_{12}$ -based negative electrodes were investigated. SEI formation and Li trapping is not expected in the $\text{Li}_4\text{Ti}_5\text{O}_{12}$ electrodes because the material shows a flat voltage profile about 1.55V vs. Li, much higher than the voltage at which electrolyte reduction occurs ($\leq 0.8\text{V}$ vs. Li/Li^+). These cells contain the ABR-1 positive electrodes described above; the negative electrode comprises a coating of 87 wt% $\text{Li}_4\text{Ti}_5\text{O}_{12}$, 5 wt% Timcal C45 carbon, and 8 wt% PVdF (Kureha 9300) binder on a 20 μm thick Al foil.

Representative data from a cell cycled in the 0.75–3.15V (2.3–4.7V for the positive vs. Li/Li^+) voltage window are shown in Figure 9. This cycling window is wider

than our typical cycling window for graphite-based full cells and was selected to accelerate performance degradation. The cycling is mainly conducted at a $\sim C/2$ rate, with periodic capacity measurements at a $\sim C/10$ rate. It is apparent from Figure 9 that the cell shows negligible capacity loss even after 600 cycles. Moreover, the measured coulombic efficiency is greater than 99.9%, which also indicates negligible Li loss during cell cycling. These data confirm that capacity loss arises at the negative electrode in the graphite-based cells. The plan is to continue cycling these $\text{Li}_{1.2}\text{Ni}_{0.15}\text{Mn}_{0.55}\text{Co}_{0.1}\text{O}_2//\text{Li}_4\text{Ti}_5\text{O}_{12}$ cells up to 1000 cycles – diagnostic data from the harvested electrodes, including results from microscopy and spectroscopy experiments, will be included in future reports.

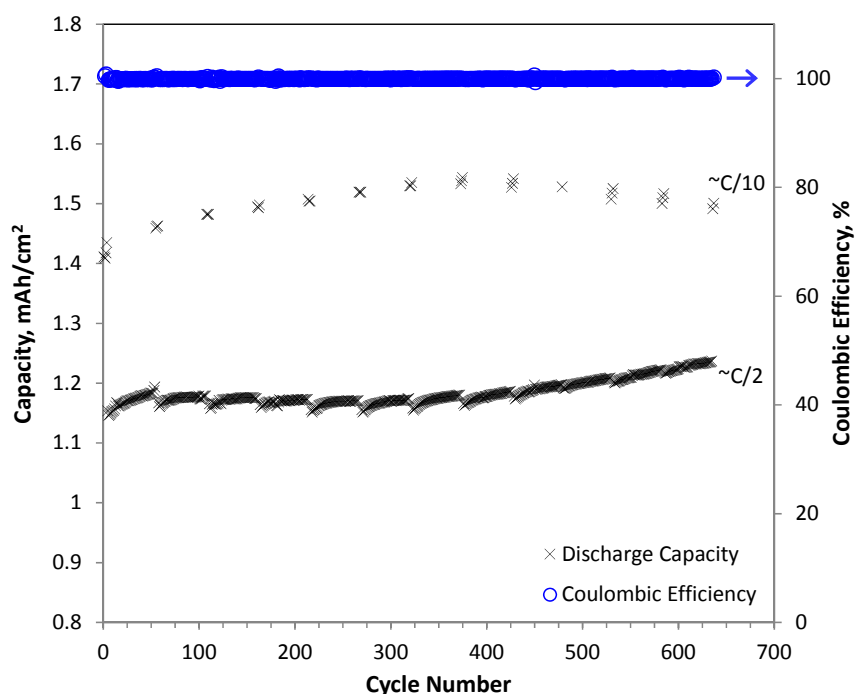


Figure 9. Capacity vs. cycle number plot for a full cell containing a $\text{Li}_4\text{Ti}_5\text{O}_{12}$ -based negative electrode. The data were acquired at 30°C , with $0.1 \text{ mA}/\text{cm}^2$ ($\sim C/10$) and $0.5 \text{ mA}/\text{cm}^2$ ($\sim C/2$) currents, in the $0.75\text{--}3.15\text{V}$ cycling window; the corresponding positive electrode cycling window is $\sim 2.3\text{--}4.7\text{V}$ vs. Li/Li^+ . A $1 \text{ mAh}/\text{cm}^2$ full cell capacity value roughly equals $150 \text{ mAh}/\text{g}$ -oxide in the positive electrode.

(h) Summary of work in the past quarter related to milestone (h)

Electrolyte additives are known to be an effective and economic approach to improving the stability of electrode surface films. In the past two decades, many organic and inorganic compounds have been identified as effective electrolyte additives: examples include vinylene carbonate (VC), ethylene sulfite (ES), [ENREF_11](#) vinyl ethylene carbonate (VEC), and fluoroethylene carbonate (FEC). In recent years, with the emergence of many high-voltage cathode materials, the anodic stability of common electrolytes is recognized as the main bottleneck limiting the calendar- and cycle- life of high-energy lithium-ion cells. Therefore, more attention has been devoted to improving stability of the cathode–electrolyte interface. Ways are being examined to mitigate

performance degradation of cells containing $\text{Li}_{1.2}\text{Ni}_{0.15}\text{Mn}_{0.55}\text{Co}_{0.1}\text{O}_2$ -based positive electrodes that are cycled at voltages beyond 4.5 V versus Li. Studies indicate that common electrolyte additives such as VC, VEC, and FEC are not effective at enhancing long-term cycling performance of these cells, *i.e.*, stable electrode passivation is not achieved with traditional SEI-forming additives. This observation underscores the need for new electrolyte additives that effectively form stable electrode passivation films in high-energy and high-voltage lithium-ion cells.

Polyfluoroalkyl (PFA) compounds are well known for their high chemical stabilities, and exhibit both hydrophobic and lipophobic behaviors. Upon dispersing in organic solvents, solvophobic PFAs tend to aggregate and form micelles in solution. These types of compounds have been extensively used as fluorosurfactants, and are especially valuable as additives in stain repellents. In light of these facts, it can be envisioned that compounds containing PFAs could serve as a new type of electrolyte additive, forming double-layered passivating layers that reduce both electrode surface degradation and electrolyte decomposition. In our design, the PFA additive has two components: (i) a reactive headgroup for attachment onto electrode surfaces via either reductive or oxidative decomposition, so that it becomes an integral part of the surface layer (inner layer); (ii) a polyfluoroalkyl chain that self-assembles on this inner layer as a solvophobic layer (outer layer) that is highly stable and impermeable to the electrolyte solvent. To explore this novel idea, we synthesized a series of PFA-substituted ethylene carbonates (PFA-EC) and studied them as electrolyte additives in our lithium-ion cells. Herein, we report the electrochemical behavior of ABR-1 cells containing the perfluorooctyl-substituted ethylene carbonate (PFO-EC) additive in the baseline Gen2 electrolyte.

Figure 10 shows capacity-voltage data from $\text{Li}_{1.2}\text{Ni}_{0.15}\text{Mn}_{0.55}\text{Co}_{0.1}\text{O}_2$ //graphite full cells containing the Gen2 electrolyte and Gen2+0.5wt% PFO-EC electrolyte. The initial cycling data, for cells with and without the additive, are very similar. After 200 cycles, the discharge capacity of cells with 0.5 wt% PFO-EC is 172 mAh/g, which is 66% of its initial discharge capacity (260 mAh/g). In contrast, the discharge capacity of the baseline (Gen2 only) cells is 70 mAh/g, which is 27% of its initial discharge capacity (258 mAh/g). These data indicate that the 0.5 wt% PFO-EC additive enhances capacity retention of the ABR-1 cells.

The PFO-EC additive is also effective at inhibiting cell impedance rise during long-term cycling. Figure 11a shows that cells with 0.5 wt% PFO-EC have similar impedances as baseline cells after the initial cycling. However, after 200 cycles between 2.2 and 4.6 V (Figure 11b), the impedance of the PFO-EC bearing cell is much smaller than that of the Gen2 baseline cell. Our previous studies have indicated that cell impedance rise in $\text{Li}_{1.2}\text{Ni}_{0.15}\text{Mn}_{0.55}\text{Co}_{0.1}\text{O}_2$ //graphite full cells occurs primarily at the positive electrode. The reduced full cell impedance for the PFO-EC containing cells suggests that the additive forms effective surface films at this electrode.

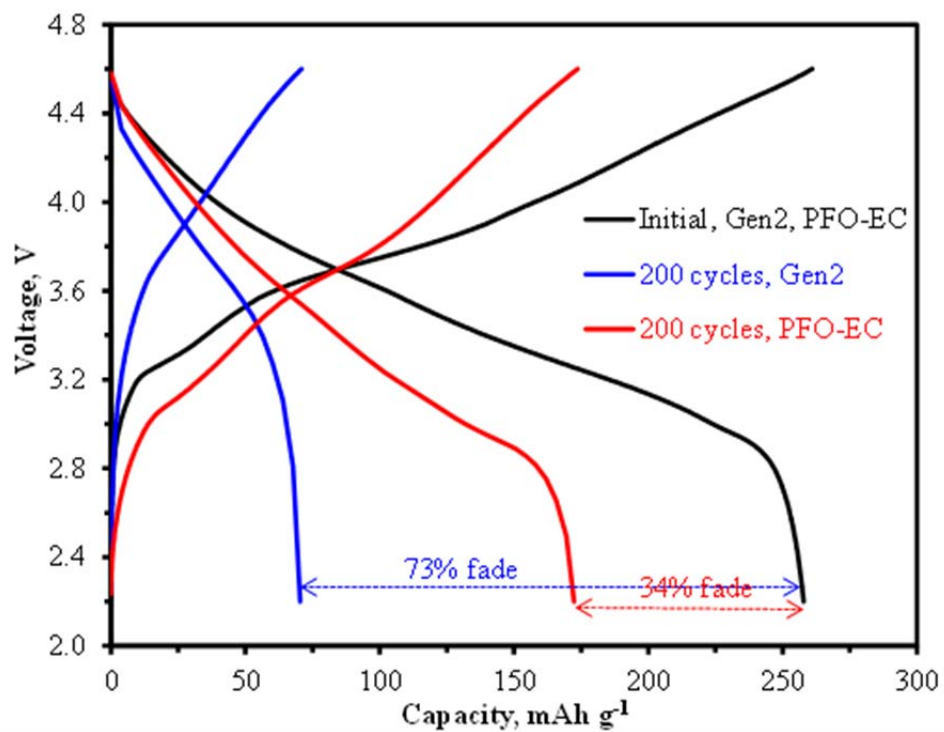


Figure 10. Capacity-voltage plots for full cells containing the Gen2 electrolyte and Gen2+0.5wt% PFO-EC electrolyte. The data were acquired with a 15 mA/g(oxide) current in the 2.2-4.6 V voltage window at 30°C. The initial data are similar for cells with and without the additive.

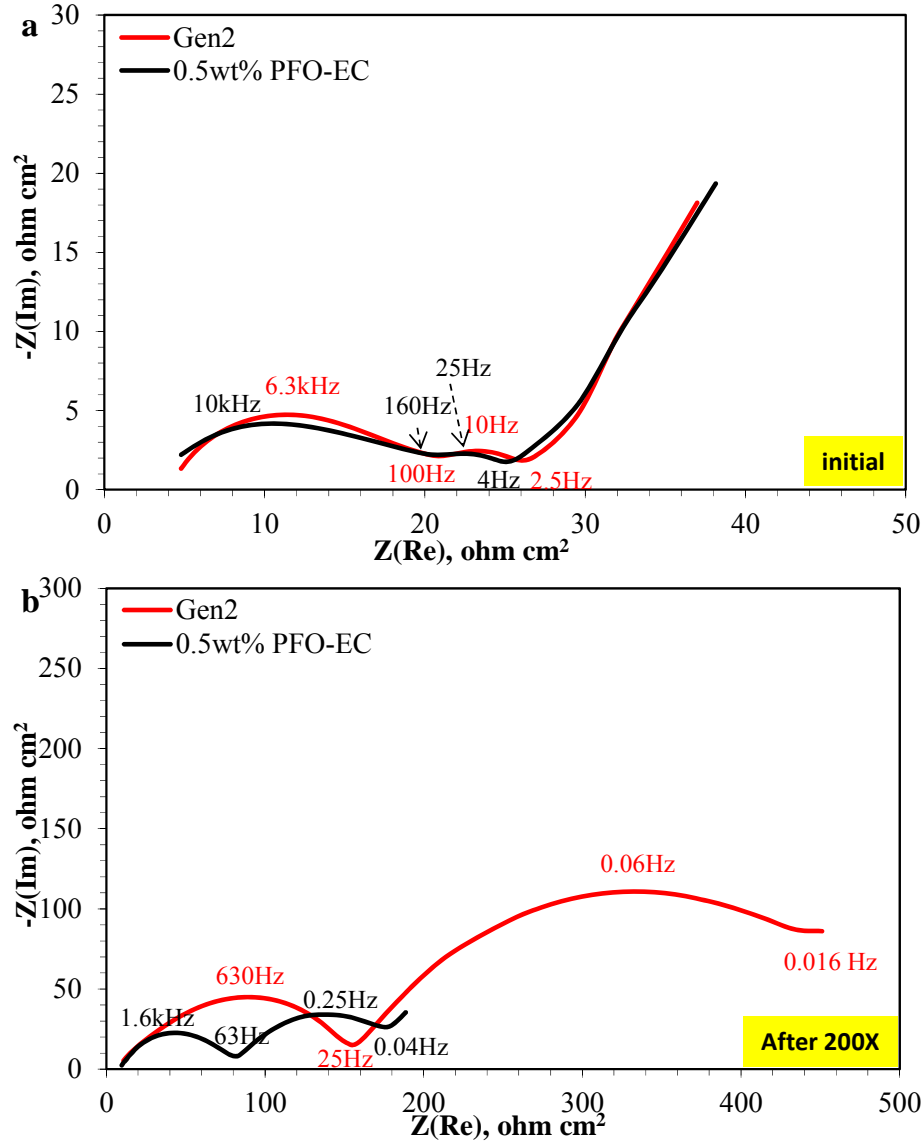


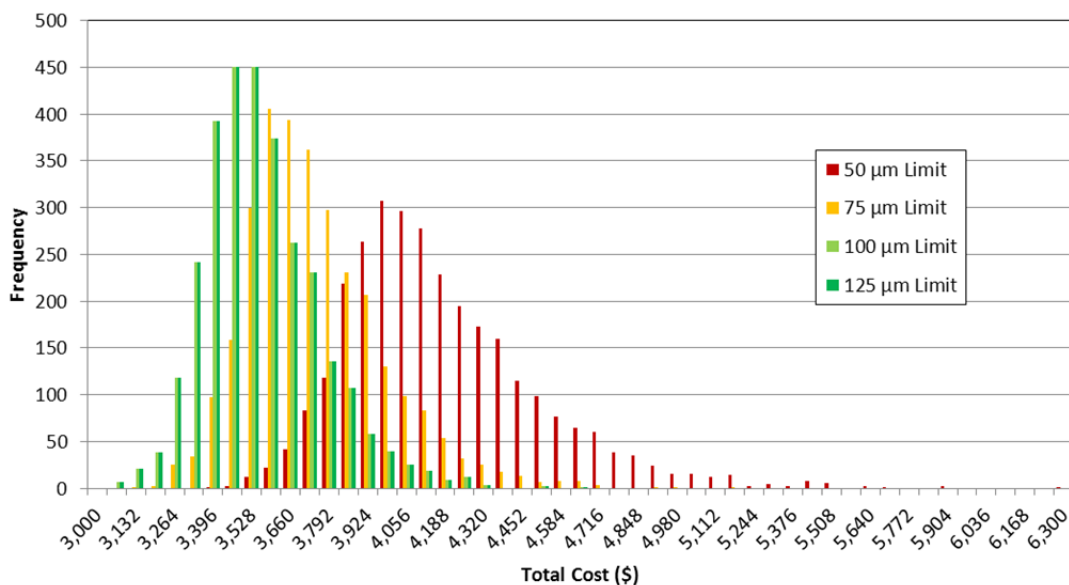
Figure 11. AC impedance spectra of $\text{Li}_{1.2}\text{Ni}_{0.15}\text{Mn}_{0.55}\text{Co}_{0.1}\text{O}_2$ //graphite full cell after (a) formation cycles, (b) 200 cycles at 30°C with and without 0.5 wt% PFO-EC.

(i) Summary of work in the past quarter related to milestone (i)

A new update of the BatPac model is currently being modified to yield a range of battery costs via a Monte Carlo simulation. While this version is not currently available to the public, the module has been made easy for a user to adjust the input and output parameters. In the simulation, the user can decide to vary up to 100 design parameters (*e.g.*, maximum electrode thickness, capacities) and/or input costs (*e.g.*, cathode costs, labor costs, capital costs) simultaneously. For each of the variables desired to be varied in the simulation, the user only needs to input a low, medium and high approximate value for the variable (a common approach used by industry) and then chose a desired distribution. Currently, the user can select one of four distributions for each variable: normal, log-normal, triangular, or uniform. In addition, up to 15 different output

parameters can be measured for up to 15 different battery configurations. This allows for quick calculations of average total costs, profit margins, and battery weight or volume, all of which are crucial in the battery design.

With this add on to the BatPac model, various plots can quickly be plotted to help in the optimization of battery parameters. Figure 12 shows the chosen input parameters and output for an example run, varying the maximum allowable electrode thicknesses for both the cathode and anode.



Parameter Varied	Distribution Type	Number of Iterations	Battery Size
Anode Material Costs	Normal	3000	14 kWh
Cathode Material Costs	Normal	Output Parameter	Electrode Couple
Labor Costs	Normal	Total Battery Cost	LMR-LMC / Graphite
Separator Costs	Log-Normal	Battery Parameter	Number of Battery Configurations
Electrolyte Costs	Normal	Maximum Allowable Thickness	7

Figure 12. A sample Monte Carlo simulation output for a LMR-NMC and Graphite couple. This data indicates that for this system there is no significant cost benefit to coating thicker than ~80 microns. However, thinner coatings can cost substantially more.

(j) Summary of work in the past quarter related to milestone (j)

As described in the previous report, the Electrochemical Impedance Spectroscopy (EIS) electrochemical cell model is being used to examine the impedance characteristics of the hysteresis between charge and discharge in LMR-NMC positive electrodes. Diagnostic micro-reference electrode lab cell EIS studies have been conducted on the

baseline HE5050 LMR-NMC electrode at several states-of-charge (between 3.0 and 4.5 volts vs. lithium) during charge and discharge half cycles. Detailed EIS data has been collected during formation and early in cycle life. Also, significant EIS aging studies have been conducted. Parameter fitting of EIS data to the electrochemical model is continuing, focusing on the characteristics and changes of the solid electrolyte interphase (SEI) as the material is formed and cycled.

As described in the previous report, the EIS electrochemical cell model was developed strictly for intercalation active materials. However, the hysteresis and other characteristics indicate that the LMR-NMC material is obviously more complex. It is applied here to obtain a “snapshot” of the electrode at each SOC. To accurately model the bulk transport characteristics of the LMR-NMC active materials the EIS electrochemical cell model will need to be modified. The bulk transport electrochemical model is being developed under the Voltage Fade effort (see report on Voltage Fade in the LMR-NMC Materials). Because this model development is lagging behind the EIS SEI modeling studies in this effort, work under this effort this past quarter was redirected to advance the electrochemical bulk transport model. As confidence in the bulk transport model improves, it will be integrated into the EIS electrochemical model.

Additional activities this past quarter include modifying the open circuit voltage expressions for phase change active materials (*i.e.*, in this case the graphite negative) in the DC electrochemical cell model. This corrects a nagging issue with the model that tended to occasionally drive one of the local lithium active material concentrations negative at high discharge rates. This model has been used extensively to examine performance changes with electrode thickness. Further electrode thickness studies are planned in support of the prototype cell fabrication effort and BatPaC development.

Publications, Reports, Intellectual property or patent application filed this quarter. (Please be rigorous, include internal reports--invention records, etc.)

"A Volume Averaged Approach to the Numerical Modeling of Phase-Transition Intercalation Electrodes Presented for Li_xC_6 ", by Kevin G. Gallagher, Dennis W. Dees, Andrew Jansen, Daniel Abraham, and Sun-Ho Kang, *Journal of The Electrochemical Society* **159**(12), A2029-A2037 (2012).

"Electrochemical Modeling the Impedance of a Lithium-Ion Positive Electrode Single Particle", by Dennis W. Dees, Kevin G. Gallagher, Daniel P. Abraham, and Andrew N. Jansen, *Journal of The Electrochemical Society* **160**(3), A478-A486 (2013).

“Positive Electrode Passivation by LiDFOB Electrolyte Additive in High-capacity Lithium-ion Cells”, by Ye Zhu, Yan Li, Martin Bettge, and Daniel P. Abraham, *Journal of The Electrochemical Society* **159**, A2109-2117 (2012).

"Overcharge Effect on Morphology and Structure of Carbon Electrodes for Lithium-ion Batteries", Wenquan Lu, Carmen M. Lopez, Nathan Liu, John T. Vaughey, Andrew Jansen, and Dennis W. Dees, *Journal of The Electrochemical Society* **159**(5), A566-A570 (2012).

"Electrolyte Additive Combinations that Enhance Performance of $\text{Li}_{1.2}\text{Ni}_{0.15}\text{Mn}_{0.55}\text{Co}_{0.1}\text{O}_2$ -Graphite Lithium-ion Cells" by Y. Zhu, Y. Li, M. Bettge, and D.P. Abraham, *Electrochimica Acta* in press; 10.1016/j.electacta.2013.03.102 (2013).

"Examining Hysteresis in Composite $x\text{Li}_2\text{MnO}_3 \cdot (1-x)\text{LiMO}_2$ Cathode Structures", by J. R. Croy, K. G. Gallagher, M. Balasubramanian, Z. Chen, Y. Ren, D. Kim, S.-H. Kang, D. W. Dees, and M. M. Thackeray, *Journal of Physical Chemistry C* **117**, 6525–6536 (2013).

"Structure Evolution of $\text{Li}_{1-x}\text{VPO}_4\text{F}$ Studied by In situ Synchrotron Probes", by Ying Piao, Yan Qin, Chengjun Sun, Yang Ren, Steve M. Heald, Dehua Zhou, Bryant J. Polzin, Steve E. Trask, Khalil Amine, Yinjin Wei, Gang Chen, Ira Bloom, and Zonghai Chen, under review by *Energy & Environmental Science*.

"Understanding Long-Term Cycling Performance of $\text{Li}_{1.2}\text{Ni}_{0.15}\text{Mn}_{0.55}\text{Co}_{0.1}\text{O}_2$ – Graphite Lithium-Ion Cells", by Y. Li, M. Bettge, B. Polzin, Y. Zhu, M. Balasubramanian and D.P. Abraham, *Journal of The Electrochemical Society* **160**(5), A3006-A3019 (2013).

"Perfluoroalkyl-substituted ethylene carbonates: novel electrolyte additives for high-voltage lithium-ion batteries", by Y. Zhu, M.D. Casselman, Y. Li, A. Wei, D.P. Abraham, *J. Power Sources* 246 (2013) 184 –191. 10.1016/j.jpowsour.2013.07.070

TASK 2

Calendar & Cycle Life Studies

Project Numbers: 1.1.1 and 2.4 (ES033)

Project Title: Strategies to Enable the Use of High-Voltage Cathodes (1.1.1) and Diagnostic Evaluation of ABRT Program Lithium Battery Chemistries (2.4)

Project PI, Institution: Robert Kostecki, Lawrence Berkeley National Laboratory

Collaborators (include industry): None

Project Start/End Dates: LBNL carried out diagnostics in the ATD Program since its 1999 inception, and the ABRT Program began October 2008

Objectives: Task 1.1.1: To enable increased energy density by addressing the impact of high-voltage cathodes on the conducting carbon matrix. Task 2.4: (i) Determine the key factors that contribute to the degradation mechanism in the PHEV test cells and individual cell components. (ii) Characterize SEI formation on model electrode surfaces to improve understanding of key interfacial phenomena in PHEV cells.

Approach: Task 1.1.1: (i) determine the mechanisms for carbon damage and retreat at high potentials. (ii) Investigate mitigating treatments, additives, and procedures. Task 2.4: Use in situ and ex situ advanced spectroscopic and microscopic techniques in conjunction with standard electrochemical methods to characterize components harvested from fresh and tested PHEV cells, model thin-film cells, and special cells used to evaluate SEI formation processes.

Milestones: (i) Determine degradation mechanism in high-voltage cathodes (August 2013), (ii) synthesize a new type of CB with improved interfacial properties (September 2013), (iii) attend review meetings and present diagnostic results obtained in collaboration with ABRT Program participants.

Financial data: FY 2013 funding \$600K

PROGRESS TOWARD MILESTONES

The focus of our work in the third quarter was on (i) investigations of the long-time effect of the CO₂ heat-treated carbon black in NMC composite electrodes, and (ii) determination of the mechanism the chemical cross-talk in ABR baseline electrodes.

In collaboration with V. Battaglia group in LBNL, LiNi_{0.33}Co_{0.33}Mn_{0.33}O₂ composite electrodes (NMC, Umicore) with the baseline carbon black or the CO₂ heat-treated carbon black, have been manufactured and cycled between 2.5 and 4.6 V vs Li/Li⁺ in coin cells with metallic lithium as counter and reference electrode (Figure 1). The cells with baseline and modified cathodes perform very similar during the initial cycles.

Interestingly, the cell with the modified CB cathode displays better capacity retention over the first 60 cycles and the cell sudden decline in capacity occurs 30 cycles later than for the cell with the standard carbon black additive.

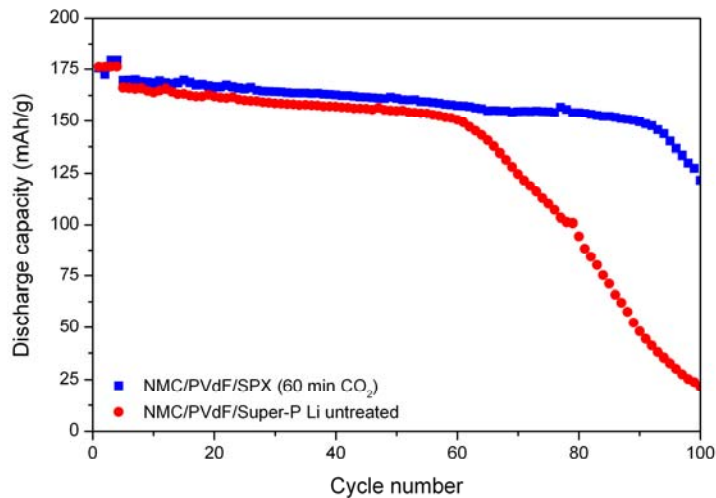


Figure 1: Discharge capacity vs cycle number of coin cells utilizing $\text{LiNi}_{0.33}\text{Co}_{0.33}\text{Mn}_{0.33}\text{O}_2$ (NMC) and pristine (red) or heat treated (blue) carbon black in EC:DEC 1:2 1M LiPF_6

This clearly indicates the beneficial effect the CO_2 heat-treatment on the interfacial stability of the carbon black and composite electrode, and on lifetime of the entire Li-ion cell. $\text{LiNi}_{0.5}\text{Mn}_{1.5}\text{O}_4$ composite electrodes with standard and modified CB additive were also manufactured. Coin cells utilizing these electrodes are currently undergoing long-term cycling tests.

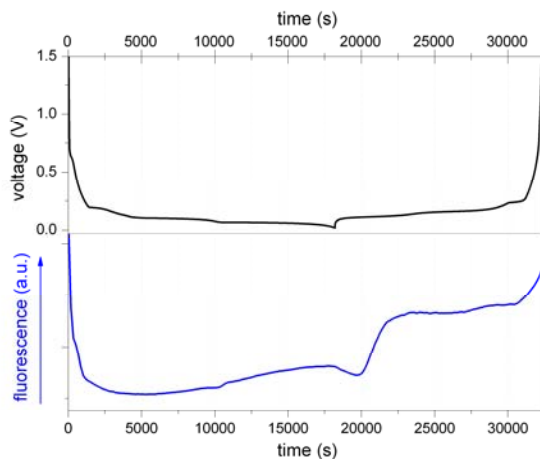


Figure 2. Electrochemical data (top), corresponding integrated fluorescence intensity (bottom-blue) of a CPG-A12/PVdF composite electrode cycled galvanostatically (0.1 mA/cm^2) in EC:DEC 1:2 1M LiPF_6

To determine the mechanism of the chemical cross-talk in Li-ion cells, *in situ* fluorescence spectro-electrochemical cell were designed and constructed. In this new cell, the investigation the laser beam is solely focused on the electrode/liquid electrolyte interface. Figure 2 depicts the fluorescence response of an ABR baseline anode, a CPG A12 graphite composite electrode that was cycled galvanostatically against metallic lithium counterelectrode. The electrode was polarized with a current of 0.1 mA/cm² with cut-off potential limits at 0.02 and 1.5 V vs. Li/Li⁺ for lithiation and delithiation processes, respectively. The black line depicts the voltage response of the cell, whereas in the blue plot shows the integrated fluorescence intensity. Interestingly, the fluorescence on the electrode-electrolyte interface decreases strongly from the electrolyte background intensity level during the SEI formation. However, upon Li⁺ intercalation in graphite the photoluminescent intensity at the interface begins to rise with distinctive changes in the slope of the fluorescence intensity, which corresponds to formation of different GICs. This indicates that the fluorescence species (and the primary components of the electrolyte) from the electrolyte get consumed at the electrode surface at different rates, which depends on the Li_xC composition and polarization. This effect seems to represent the dynamics of the SEI layer formation during the first formation cycle.

TASK 2 Calendar & Cycle Life Studies

Project Number: 1.1, 2.4, and 3.3 (ES034)

Project Title: Life and abuse tolerance diagnostic studies and new electrolytes development for high energy density PHEV batteries

Task 1.1: Develop/Engineer PHEV Electrode Materials, Electrolytes, & Additives

Task 2.4: Life Diagnostics

Task 3.3: Abuse Behavior Modeling and Diagnostics

PI, Institution: Xiao-Qing Yang and Kyung-Wan Nam, Brookhaven National Laboratory

Barrier: Calendar and cycling life, Abuse tolerance

Project Start/End Dates: October 2012 / September 2013

Objects: The primary objectives of the efforts at BNL are: to determine the contributions of electrode structural changes, interfacial phenomena, and electrolyte decomposition to lithium-ion cell capacity and power decline, and abuse tolerance; to develop new diagnostic techniques (in situ and ex situ) for lithium-ion batteries; to collaborate with other ABR teams and the battery developers to understand the technical barriers, especially the voltage fading mechanism of high energy density Li and Mn rich NCM cathode materials during cycling; to explore new approaches to improve the abuse tolerance. The other objective is to design, synthesize and characterize new electrolyte for PHEV oriented lithium-ion batteries with better performance and safety characteristics. Special attention will be given to the new electrolytes for high voltage cathode materials.

Approach: Our approach is to use a combination of *in situ*, *ex situ* and time-resolved synchrotron based x-ray techniques to characterize electrode materials and electrodes taken from baseline ABR Program cells. *Ex situ* soft X-ray absorption spectroscopy (XAS) will be used to distinguish the structural differences between surface and bulk of electrodes using both electron yield (EY) and fluorescence yield (FY) detectors. Time-resolved X-ray diffraction (TR-XRD) technique will also be used to understand the reactions that occur in charged cathodes at elevated temperatures in the presence of electrolyte. In situ x-ray diffraction will be used to monitor the structural changes of the electrode materials during charge-discharge cycling at different conditions. A combination of TR-XRD, in situ soft and hard X-ray absorption (XAS), in situ transmission electron microscopy (TEM) techniques during heating will be applied to study the thermal stability of the electrode materials. These approaches developed at BNL will be utilized to study various cathode-anode chemistry pair systems of ABR projects through extended collaboration with other ABR members, such as Dr. Khalil

Amine, Dr. Daniel Abraham, Dr. Chris Johnson, and Dr. Zhengcheng Zhang at ANL. We will continue to develop new synchrotron based x-ray techniques such as combined in situ x-ray diffraction and mass spectroscopy during heating for the thermal stability of cathode material studies. We will continue to develop TEM based in situ diagnostic tools to study the structural changes at both surface and bulk of the electrode particles with high spatial resolution.

Milestones:

(a) By April 2013, complete the studies of thermal decomposition of charged $\text{Li}_{1.2}\text{Ni}_{0.15}\text{Mn}_{0.55}\text{Co}_{0.1}\text{O}_2$ (Toda HE5050) cathode materials during heating using combined Time-Resolved XRD and Mass Spectroscopy, **Completed.** (b) By April 2013, complete the ex situ soft x-ray XAS studies of $\text{Li}_{1.2}\text{Ni}_{0.15}\text{Mn}_{0.55}\text{Co}_{0.1}\text{O}_2$ (Toda HE5050) cathode material during charge-discharge cycling to distinguish the structural change differences between the surface and the bulk, **Completed.** (c) By September 2013, complete the in situ hard x-ray XAS studies of $\text{Li}_{1.2}\text{Ni}_{0.15}\text{Mn}_{0.55}\text{Co}_{0.1}\text{O}_2$ (Toda HE5050) cathode material for the voltage fading mechanism and structural instability during extended cycling, **Completed.** (d) By September 2013, complete the studies of thermal decomposition of charged $\text{Li}_{1.2}\text{Ni}_{0.17}\text{Mn}_{0.53}\text{Co}_{0.1}\text{O}_2$ (ANL-HE) cathode materials with and without AlF_3 coating during heating using combined Time-Resolved XRD and Mass spectroscopy, **on schedule.**

Progress toward milestones for the 3rd quarter of FY2013:

Summary of work in this quarter related to milestone (c)

In the third quarter of FY2013, the mile stone (c) has been completed. Using in situ x-ray absorption spectroscopy (XAS) at transition metal K-edges, the local crystal and electronic structure changes of $\text{Li}_{1.2}\text{Ni}_{0.15}\text{Mn}_{0.55}\text{Co}_{0.1}\text{O}_2$ (Toda HE5050) cathode material during charge-discharge cycling have been identified.

The in situ XAS spectra have been collected during 1st, 2nd, 25th and 46th cycles. Unlike the Ni K-edge results, the XANES spectra at Mn and Co K-edges during charge-discharge do not show clear edge shifts thus making difficult to correlate their contributions to the charge capacity. Therefore, changes of the first bond length between transition metals (Ni, Co, and Mn) and oxygen have been determined by the EXAFS fitting analysis and used to track the average oxidation state changes of each element during extend cyclings (Figure 1). Clear bond length contraction/expansion changes during charge and discharge were observed for the Ni-O bond revealing the reversible redox reaction between Ni^{2+} and Ni^{4+} in the $\text{Li}_{1.2}\text{Ni}_{0.15}\text{Mn}_{0.55}\text{Co}_{0.1}\text{O}_2$. The bond length changes of the Ni-O ($\sim 0.16\text{\AA}$) during charge-discharge was preserved during the extended cyclings suggesting the excellent reversibility of $\text{Ni}^{2+/4+}$ redox reactions. In contrast to the Ni case, oscillation amplitude of the Co-O bond length decreased from ~ 0.05 for the 1st charge to $\sim 0.03\text{\AA}$ for the 25th charge showing a decreasing capacity contribution from the Co redox reactions (likely the partial $\text{Co}^{3+/4+}$ redox reaction) with increasing cycle number. This result suggests the capacity fading might be attributed to the increased numbers of inactive Co sites during extended cycling in this material. The Mn-O bond length oscillation showed a reversible behavior during cycling except for the

1st charge in which the activation process of Li_2MnO_3 species in $\text{Li}_{1.2}\text{Ni}_{0.15}\text{Mn}_{0.55}\text{Co}_{0.1}\text{O}_2$ took place. One thing to be worth mentioning is the continuous expansion of the Co-O and Mn-O bond lengths at fully discharged states as the cycle number increases. This continued bond length expansion of Mn-O and Co-O strongly suggests the continued structural changes of $\text{Li}_{1.2}\text{Ni}_{0.15}\text{Mn}_{0.55}\text{Co}_{0.1}\text{O}_2$ from the pristine layered phase to the one with lower average oxidation states of transition metals (likely spinel-like phase) caused by cycling. This structural transition is mainly related to the Co and Mn sites and might be closely related to the voltage fading behavior of this class of materials during cycling.

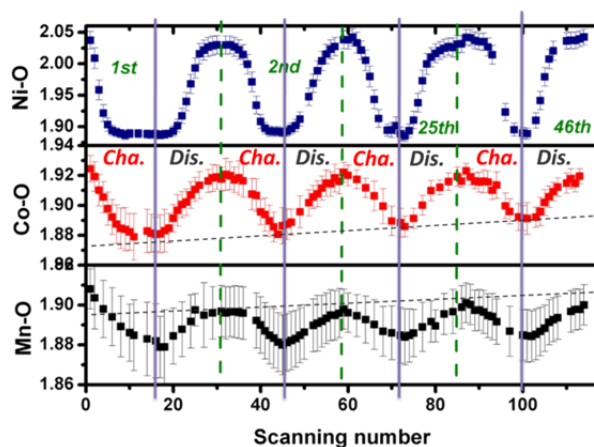


Fig. 1. Changes of transition metal (Ni, Co, and Mn) and oxygen bond length obtained from EXAFS analysis of $\text{Li}_{1.2}\text{Ni}_{0.15}\text{Mn}_{0.55}\text{Co}_{0.1}\text{O}_2$ during extended cyclings.

Summary of work toward the completion of milestone (d) in the 4th quarter of 2013

Thermal stability studies of charged $\text{Li}_{1.2}\text{Ni}_{0.17}\text{Mn}_{0.53}\text{Co}_{0.1}\text{O}_2$ (ANL-HE) cathode materials with and without AlF_3 coating during heating are underway using combined Time-Resolved XRD and mass spectroscopy.

TASK 2

Calendar & Cycle Life Studies

Project Number: CSP Project 18502, CSP Agreement 23060, ORNL FWP CEVT110 (ES165)

Project Title: Roll-to-Roll Electrode Processing NDE and Materials Characterization for Advanced Lithium Secondary Batteries

Project PI, Institution: David Wood, Oak Ridge National Laboratory

Collaborators:

- **Equipment Suppliers: Ceres Technologies, Keyence, FLIR**
- **Battery Manufacturers: Dow Kokam, A123 Systems**
- **Materials Suppliers: TODA America**
- **National Laboratories: Argonne National Laboratory, National Renewable Energy Laboratory**

Project Start/End Dates: 10/1/11 to 9/30/14

Objectives: Due to high scrap rates of 10-20% or more associated with lithium secondary cell production, new methods of quality control (QC) must be implemented. Often flaws in the electrodes are not detected until the formation cycling when the entire series of manufacturing steps has been completed, and the associated scrap rates drive the costs of lithium secondary cells to an unacceptable level. If electrode flaws and contaminants could be detected in line near the particular processing steps that generate them, then the electrode material could be marked as unusable and the processing equipment could be adjusted to eliminate the defects more quickly. ORNL is considering in line analysis methods such as X-ray fluorescence spectroscopy (XRF) for electrode component uniformity and metal particle detection and laser thickness sensing of the electrode wet thickness measurement. In addition, on-line laser thickness measurement and IR imaging of wet and dry electrode coatings are being implemented for thickness uniformity and coating flaw detection. These methods have been effectively utilized in other industries such as photovoltaic, flexible electronics, and semiconductor manufacturing, but the equipment and measurement methods must still be tailored for lithium secondary cell production. The object of this project is to raise the production yield of lithium secondary battery electrodes from 80- 90% to 99% and reduce the associated system cost by implementing in line XRF and laser thickness control. In addition, ORNL is providing its diagnostics capabilities and expertise to address materials issues with ABR cathode materials.

Approach: Ceres Technologies has been identified as a top manufacturer of in line XRF instruments for roll-to-roll applications and has a great deal of experience with the photovoltaics industry. ORNL will work closely with them to establish this technology for the lithium secondary battery industry by producing tape casted and slot-die coated electrode rolls (anodes and cathodes) with deliberately introduced flaws to test the

appropriateness of the method and the equipment modifications to the standard model. All key process parameters, such as line speed, coating thickness range, metal particle density, elemental homogeneity, etc., will be examined. In-line XRF data will also be correlated with ex-situ XCT data to gain a complete chemical and structural picture of the electrode as it is coated and dried.

Keyence has been selected as the partner for developing a set of laser thickness sensors for lithium secondary battery electrode production. ORNL has purchased sensors with point scanning capability from Keyence and integrated them directly into the slot-die coating line for the proof-of-concept experiments. The next step is to implement sensors with the capability of scanning multiple points or a full line scan across the web.

The output data from the wet layer thickness measurements using the laser sensors will be used to mark regions that are out of specification during the coating process. The coated electrode rolls with markings will be fed into the in line XRF equipment to determine if wet regions out of specification match with dry regions that are determined to be out of specification. Ultimately a feedback mechanism will be designed that considers whether the wet or dry thickness is a better input for adjusting the dispersion flow rate into the slot-die coater. The IR imaging QC will be correlated with thickness variation data to determine any further systematic flaw formation mechanisms such as pinholes, divots, and large agglomerates.

ORNL characterization capabilities and offline diagnostics consisting of acoustic emission detection, in-situ and ex-situ X-ray diffraction, neutron scattering, magnetic property determination, and high-resolution microscopy will be utilized to investigate cathode materials issues with ABR developed materials (specifically TODA HE5050).

FY13 Milestones:

- 1) Determine feasibility of measurement of deliberately introduced metal contaminants into cathodes with in-line XRF using ORNL tape caster line (January 2013 – delayed to July 2013).
- 2) Correlation of wet and dry thickness using laser line-scan thickness measurement (wet thickness) and in line XRF (dry thickness) to within $\pm 10\%$ (July 2013).
- 3) Ceres Technologies to complete final design of in-line XRF system for secondary lithium battery electrode production (July 2013).
- 4) Transfer technology associated with each of the three techniques (in-line laser thickness, XRF, and IR imaging) to industry partner (TBD) pilot/production line (September 2013).

Financial data: \$300k/year (FY12-FY13)

PROGRESS TOWARD MILESTONES

Summary of work in the past quarter related to milestones (1) and (3): XRF for measurement of electrode component uniformity, metal contaminant position, and transition-metal composition at different points.

1. Measuring the composition of transition metal ions:

XRF was used to measure the transition metal (TM) ion composition at different points (four regions) of a TODA NMC 532 cathode coating. In figure 1a, we show the Mn to Co ratio and Ni to Co ratio, which was found to be ~ 2.5 and 1.5 respectively. These results demonstrate excellent compositional homogeneity across the electrode. Compositional analysis was also completed using a LMR-NMC (TODA HE5050) cathode, and the ratio between Mn to Co and Ni to Co within four different regions of the coating was found to be 1.5 and 5.5, respectively.

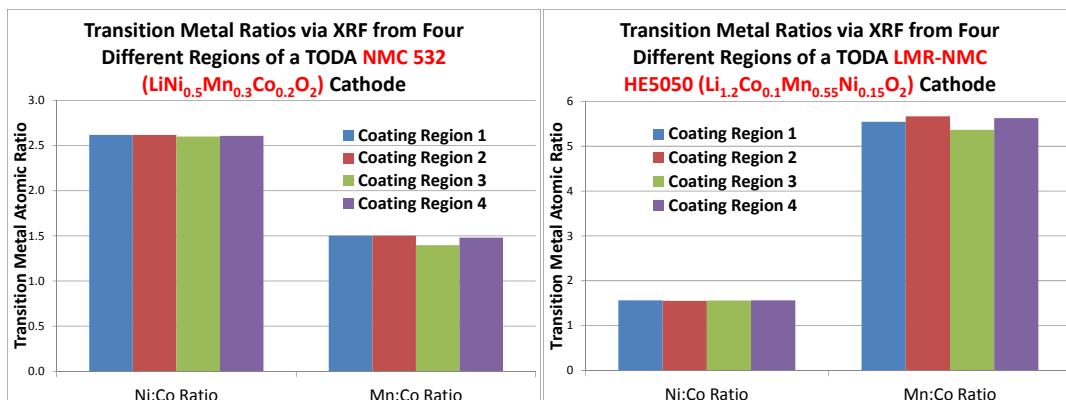


Figure 1: Transition metal ratios of (a) TODA NMC 532 and (b) lithium-manganese-rich (LMR)-NMC cathodes. Four different regions from the same electrode were sampled.

2. Examining deliberately introduced metal-particle contamination in cathodes:

To detect contamination present in the cathodes, two samples were prepared:

- Sample 1: Co and Cu metal powder were mixed into a TODA NMC 532 slurry, and then the electrode was prepared by tape casting (designated as NMC532-Co-Cu).
- Sample 2: Cu metal powder was sprinkled over the wet electrode after tape casting (NMC532-Cu).
- Sample 3: Co metal powder was sprinkled over the wet electrode after tape casting (NMC532-Co).

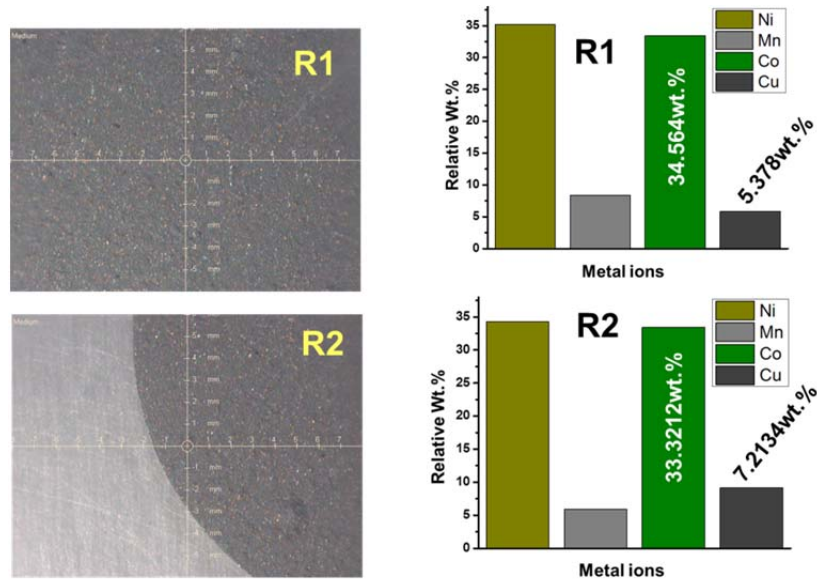


Figure 2: XRF data from Sample 1 (NMC532-Co-Cu). Optical image (left), and relative wt% of transition-metal composition with Co and Cu impurity (right) from region R1 and R2.

Figure 2 shows the relative transition metal ion composition collected from Sample 1 (NMC532-Co-Cu) in region R1 and R2. From the XRF data it is evident that the Co concentration is higher because excess Co was added in the slurry before preparing the cathode. It was also observed that the wt% of Cu in the region R1 is 5.378% and R2 is 7.213%, which demonstrates the ability of XRF technique for detecting metal-particle contamination that might be present in the cathode slurry while mixing. Figure 3 shows the composition spectrum acquired from region R1, confirming the presence of Co and Cu impurities in the electrode.

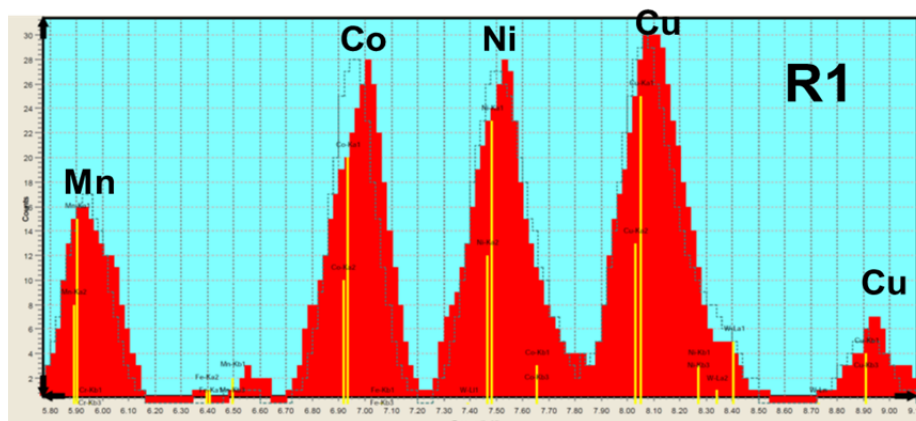


Figure 3: Composition spectrum collected from Sample 1 (NMC532-Co-Cu) showing the presence of Cu contamination and excess Co in region R1.

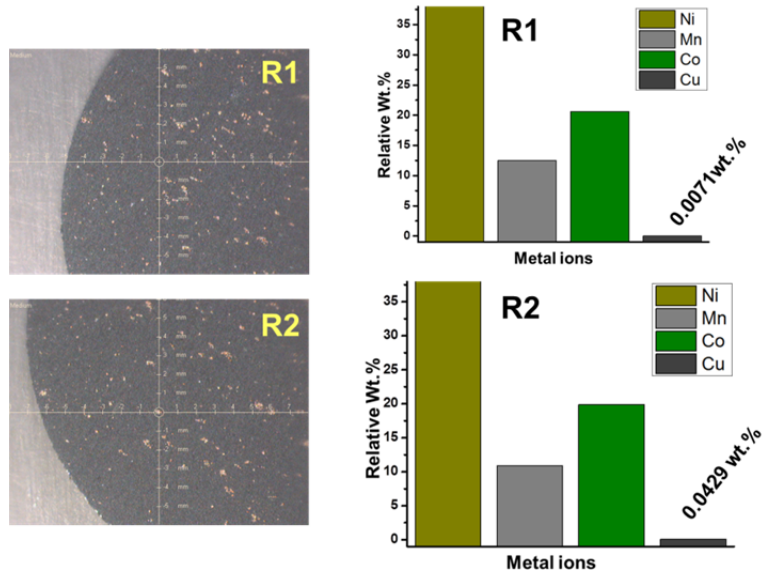


Figure 4: XRF data from Sample 2 (NMC532-Cu). Optical image (left), and relative wt% of transition metal composition with Cu impurity (right) from region R1 and R2.

Figure 4 shows the relative transition metal ion composition collected from Sample 2 (NMC532-Cu) in region R1 and R2. It was observed that the wt% of Cu in region R1 was 0.0071% and R2 was 0.0429%, showing that the XRF technique can also detect trace amounts of metal contamination from the Cu foil slitting process. The optical images also show a higher amount of Cu in region R2 compared to R1.

Figure 5 shows the relative transition metal ion composition collected from Sample 3 (NMC532-Co) in region R1 and R2. It was observed that the wt% of Co in region R1 was 22.77% and R2 was 29.45%, demonstrating that the R2 region had more Co contamination than R1 and that both regions had an excess of Co. In this electrode, a negligible amount of Cu (~0.003%) was detected.

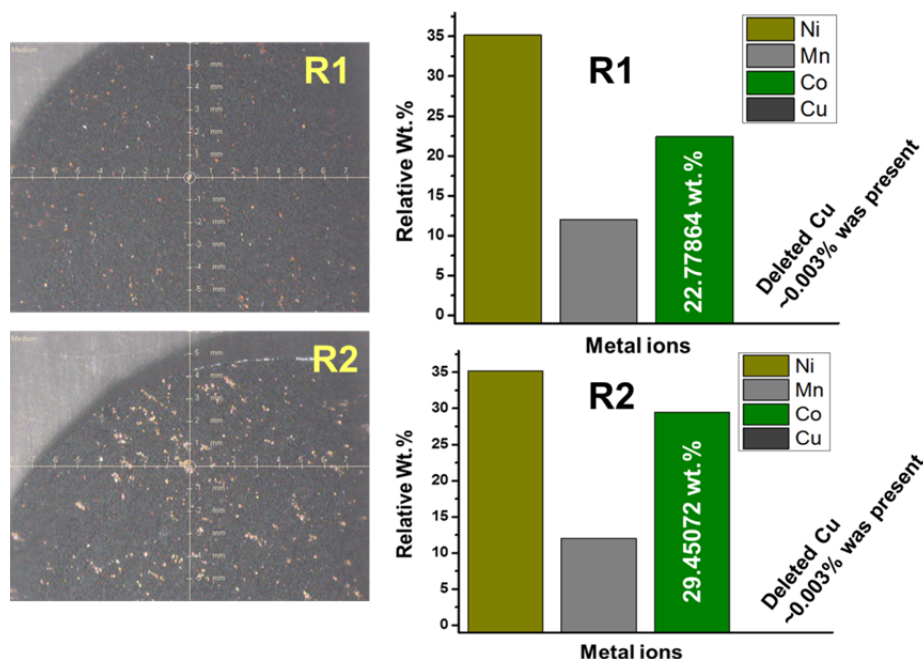


Figure 5: XRF data from Sample 3 (NMC532-Co). Optical image (left), and relative wt% of transition metal composition with Co impurity (right) from region R1 and R2.

Publications, Reports, Intellectual Property or Patent Applications filed this quarter.

1. D. Mohanty, L.C. Maxey, R.B. Dinwiddie, J. Li, and D.L. Wood, “Improved QC of Slot-Die Coated Lithium Ion Battery Electrodes by IR Thermography and Laser Thickness Techniques,” *Analytical Methods*, Under Review, 2013.
2. D. Mohanty, A. Safa-Sefat, J. Li, R.A. Meisner, A. J. Rondinone, D. P. Abraham, D.L. Wood, and C. Daniel, “Correlating Cation Ordering and Voltage Fade in a Lithium- Manganese-Rich Lithium-Ion Battery Cathode Oxide: a Joint Magnetic Susceptibility and TEM Study” *Chemistry of Materials*, Under Review, 2013.
3. D. Mohanty, A. Huq, E. Andrew Payzant, A. S. Sefat, J. Li, D. P. Abraham, D. L. Wood, and C. Daniel, “Neutron Diffraction and Magnetic Susceptibility Studies on a High-Voltage $\text{Li}_{1.2}\text{Mn}_{0.55}\text{Ni}_{0.15}\text{Co}_{0.10}\text{O}_2$ Lithium-Ion Battery Cathode; an Insight to the Crystal Structure” *Chemistry of Materials*, Under Review, 2013

TASK 3

Abuse Tolerance Studies

Project Number: 3.2 (ES036)

Project Title: Abuse Tolerance Improvements

Project PI, Institution: Chris Orendorff, Sandia National Laboratories

Collaborators (include industry): ANL, INL, BNL, ORNL, NREL, Physical Sciences Inc.

Project Start/End Dates: 10/1/2012-9/30/2013

Objectives: The objective of this work is to develop inherently abuse tolerant lithium-ion cell chemistries. This involves understanding the mechanisms of cell degradation and failure, determining the effects of new materials & additives on abuse response, and cell level abuse testing and cell characterization to quantify improvements

Approach: Materials to full cell characterization to determine inherent safety and reliability of the most advanced lithium-ion chemistries. Approaches include a suite of battery calorimetry techniques (microcal, DSC, TGA/TDA, isothermal, ARC), abuse tests (electrical, mechanical, thermal), and analytical diagnostics (electrochemical characterization, optical spectroscopy, mass spectrometry, computed tomography, electron microscopy, etc.)

Milestones:

- (a) Evaluation of coated materials (ON GOING, on schedule)
- (b) Abuse testing and characterization of FRION electrolytes (starting Q3)
- (c) Abuse tolerance of high energy materials (ON GOING, on schedule)

Financial data: Total budgeted \$1.0M; received \$500K

PROGRESS TOWARD MILESTONES

(a) Coated materials. Q3 focused on Al₂O₃ ALD on NMC cathode materials to determine a coating thickness that would begin to influence safety performance. Work in Q2 showed that at 2 ALD cycles, coatings on NMC were not thick enough to positively affect any safety performance characteristics. Figure 1 shows DSC data for coated NMC from 2 to 12 ALD cycles of Al₂O₃. Results show an inflection in the DSC data at 6 ALD cycles (~ 1 nm thick Al₂O₃ coating). Cell specific capacity is shown for each of these materials in Figure 1 during formation. Results show no significant change in performance (at least during the initial formation process) up to 6 ALD cycles, with a decrease in specific capacity at 8, 10 and 12 ALD cycles. With this information, we will down select to 6 Al₂O₃ ALD cycles as the next candidate for 18650 electrode coating, cell building, and ARC measurements in Q4.

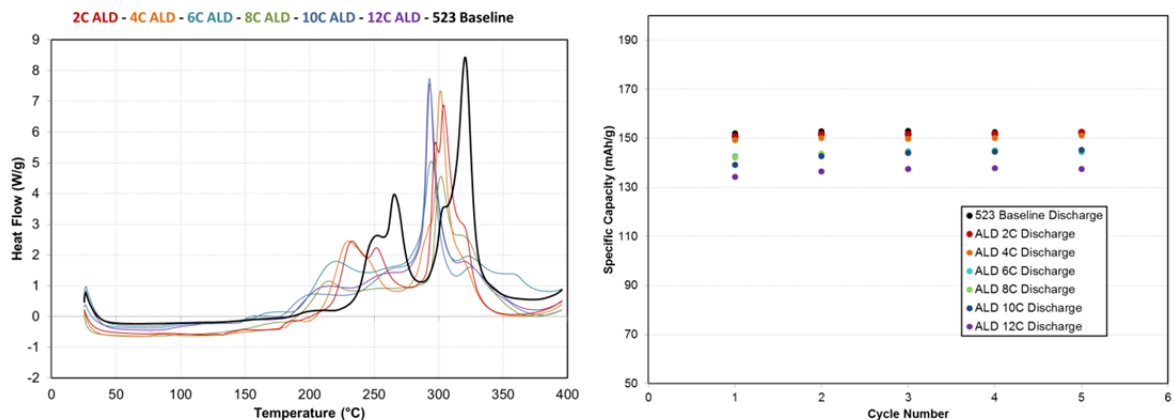


Figure 1. DSC of Al₂O₃ ALD coated NMC and specific capacity of ALD coated NMC cathodes in cells.

(b) FRION electrolyte development. A candidate FRION (flame retardant ion) electrolyte (developed at Case Western under the BATT program) was sent to ANL in Q2 for screening and electrolyte formulation. This electrolyte will be sent to Sandia for 18650 cell building and safety performance testing. ARC and flammability measurements will be performed on the FRION and control cells to determine the impact of the FRION on cell thermal stability during runaway and the efficacy of the flame retardant electrolyte in cells during ignition testing.

(c) High Energy Materials. One objective for FY13 is to determine baseline safety performance and thermal stability of high energy lithium-ion materials (lithium-rich LMO, Si-composites, and high voltage LMNO). The largest barrier to the success of this effort to date has been the availability and access to these high energy materials. In Q2 we received a small quantity of lithium-rich LMO positive material from Toda (HE5050). Initial work has focused on baseline materials characterization. Figure 5 shows DSC data for HE5050 at 4.6 V. Results show a relatively high onset temperature for decomposition and specific heat release of 1860 J/g (comparable to NMC 523 at 4.2 V). In Q3 we received an appreciable quantity of Si-composite anode for coating and evaluation. As with any new material, coating the Si anode for 18650s proves to be a challenge because of slurry heterogeneity, defining coating parameters, loadings, etc. The first electrodes were heavily streaked and gave poor electrochemical performance (Figure 3). We are working with the supplier to improve the coatings and plan to evaluate these materials in 18650 cells in Q4.

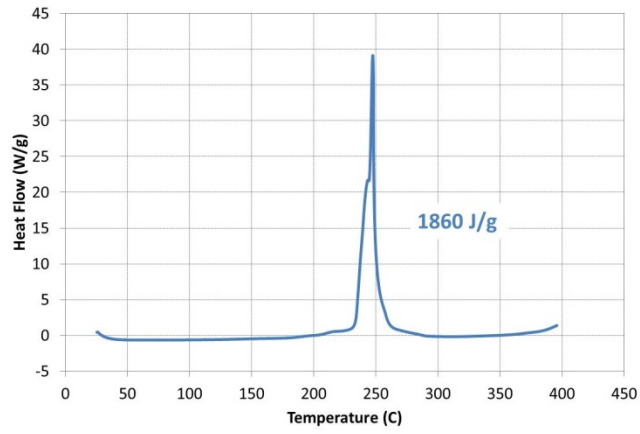


Figure 2. Representative DSC data for HE5050 cathode electrode at 4.6 V.

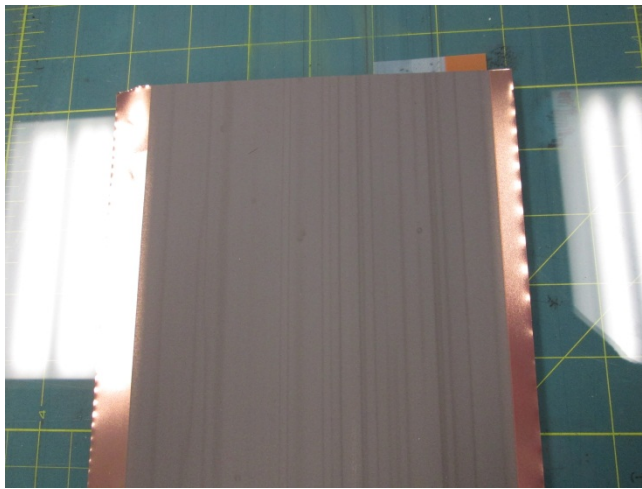


Figure 3. Heterogeneous streaked negative electrode (Si-composite).

TASK 3

Abuse Tolerance Studies

Project Number: 3.3 (ES037)

Project Title: Overcharge Protection for PHEV Batteries

Project PI, Institution: Guoying Chen, Lawrence Berkeley National Laboratory

Collaborators: Robert Kostecki, John Kerr, Vince Battaglia, Marca Doeff, Gao Liu, Quy Ta and Brian Nguyen (American Dye Source, Inc.).

Project Start Date: March 2009

Objectives: Develop a reliable, inexpensive overcharge protection system. Use electroactive polymers for internal, self-actuating protection. Minimize cost, maximize rate capability and cycle life of overcharge protection for high-energy Li-ion batteries for PHEV applications.

Approach: Our approach is to use electroactive polymers as self-actuating and reversible overcharge protection agents. The redox window and electronic conductivity of the polymer will be tuned to match the battery chemistry for non-interfering cell operation. Rate capability and cycle life of the protection will be maximized through the optimization of polymer composite morphology and cell configuration.

Milestones:

- a) Investigate rate performance and cycle life of Li-ion cells protected by electrospun electroactive-fiber-composite separators (January 2013). **Complete**
- b) Evaluate alternative placements of the fiber-composite membranes in battery cells (March 2013). **Complete**

Financial data: \$240K/FY2012

PROGRESS TOWARD MILESTONES

In this quarter, we evaluated the long-term cycling stability of rechargeable lithium batteries overcharge protected by an electroactive-polymer-fiber separator. The composite separator with a bilayer structure was prepared by electrospinning a chloroform solution of poly[(9,9-dioctylfluorenyl-2,7-diyl)] end-capped with dimethylphenyl groups (PFO-DMP) on an aluminum substrate and then a poly(3-butylthiophene) (P3BT) solution on top of the PFO-DMP layer. A small amount of polyethylene oxide (PEO) was added to both solutions to achieve the desired viscosity for fiber formation. The thickness of each polymer fiber layer was controlled by the duration of the electrospinning process. After removing from the substrate, the PEO polymer was

removed by sonication in water and the membrane was assembled into a cell with the high-voltage PFO-DMP side facing the cathode and the low-voltage P3BT side facing the anode. Fig. 1 shows the room temperature cycling profiles and the specific capacities of a spinel $\text{Li}_{1.05}\text{Mn}_{1.95}\text{O}_4$ half-cell overcharge protected by the fiber separator with a PFO-DMP: P3BT weight ratio of 3:1 and a thickness of 50 μm . When cycled at C/1.5 rate and 125% overcharge, the cell repeatedly reached and maintained at a steady state of 4.2 V, suggesting reversible and stable overcharge protection (Fig. 1a). The cell was able to maintain its discharge capacity under these severe overcharge abuse conditions for well over 800 cycles in the duration of over 4000 h (Fig. 1b). This is by far the most stable overcharge protection reported on rechargeable lithium batteries, clearly demonstrating the unique capability of electroactive-polymer fiber separators in providing prolonged high-rate protection. The electrospinning process is low-cost and easily scalable, both of which are attractive for commercialization.

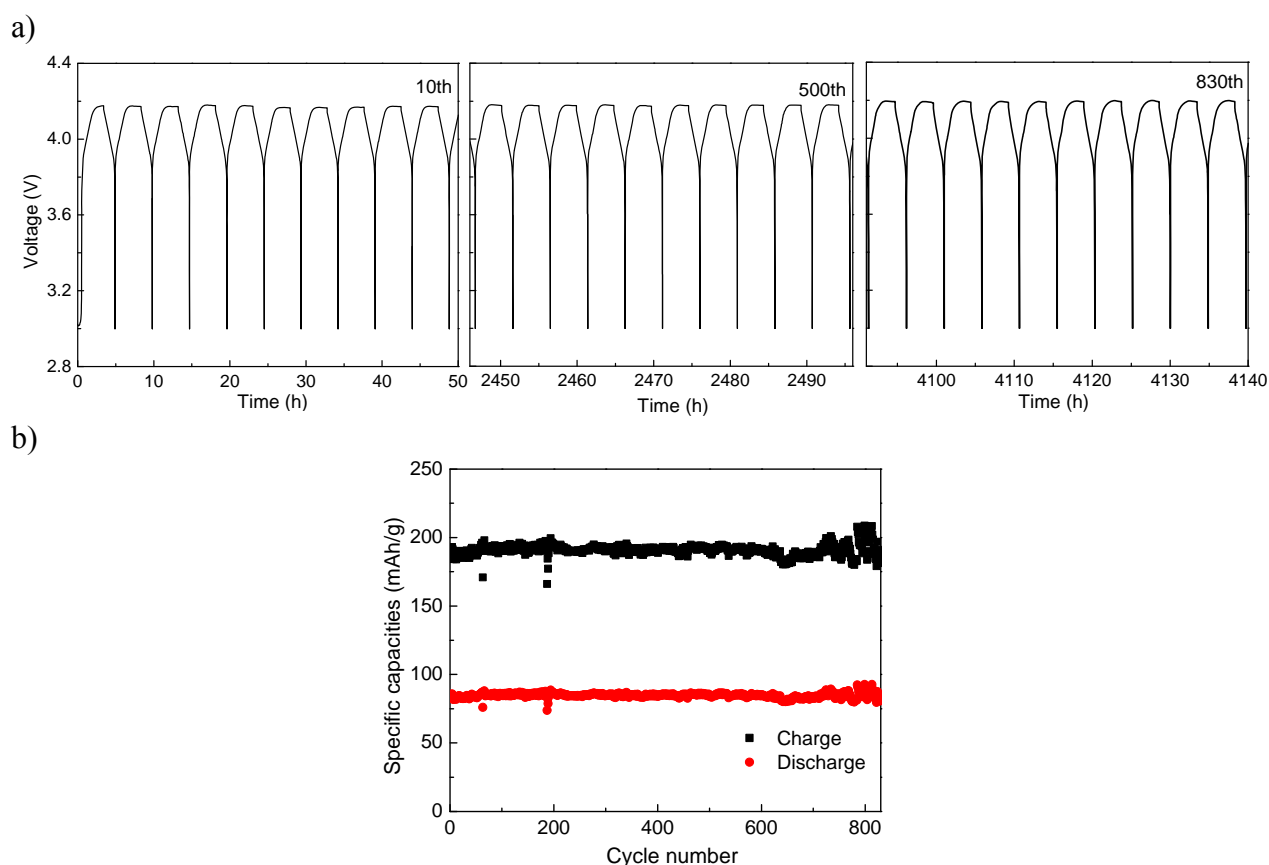


Figure 1. a) Charge-discharge cycling profiles and b) specific capacities as a function of the cycle number of a $\text{Li}_{1.05}\text{Mn}_{1.95}\text{O}_4$ half-cell overcharge protected by the electrospun PFO-DMP/P3BT composite separator.